The Thesis Committee for Thomas Brandt Christiansen
Certifies that this is the approved version of the following thesis:

Explicitly linking field- and satellite- derived measurements for improved vegetation quantification and disturbance detection

APPROVED BY
SUPERVISING COMMITTEE:

Supervisor:

Kelley A. Crews

Jennifer A. Miller

Kenneth R. Young

Explicitly linking field- and satellite- derived measurements for improved vegetation quantification and disturbance detection

by

Thomas Brandt Christiansen, BA

Thesis

Presented to the Faculty of the Graduate School of

The University of Texas at Austin

in Partial Fulfillment

of the Requirements

for the Degree of

Master of Arts

The University of Texas at Austin

December 2014

Acknowledgements

First and foremost I would like to thank the people of the Etshas, Seronga, and Mababe for letting us walk through their settlements to do our field work and for being kind and welcoming. I am also greatly appreciative of countless Maun residents, particularly the Okavango River Lodge family, who helped immensely by providing accommodation, support, and friendship. I would like to thank project leaders Kelley A. Crews, Brian King, Kenneth R. Young, and Thoralf Meyer for their leadership, guidance, feedback, and support in the field and while writing this thesis. I am also greatly thankful for the continued support and feedback from committee member Jennifer A. Miller. Thank you Jamie Shinn, fellow research assistant, for all the great times in the field and for the support on political ecology and livelihood literature. I would also like to thank all of our wonderful field assistants and translators for all their help on this work. Thank you to my great friends in the lab (Molly, Niti, and Paul) for the moral support and technical advice. This material is based upon work which was partially supported by the National Science Foundation Graduate Research Fellowship under Grant No. BCS 0964596. This work would not have been possible without your support.

Abstract

Explicitly linking field- and satellite- derived measurements for improved vegetation quantification and disturbance detection

Thomas Brandt Christiansen, MA

The University of Texas at Austin, 2014

Supervisor: Kelley A. Crews

Arid and semi-arid ecosystems have been recognized as critical in supporting over one-third of the world's populations, notably those more dependent on the natural resource base for their livelihoods. These systems, and especially savannas within them, are highly vulnerable to predicted fluctuations in climatic change, disturbances, and management regimes. This research posits these areas in a social-ecological system (SES) framework that encompasses human, governance, and recourse units. A challenge in both SES and CHANS (coupled human and natural systems) research is how to explicitly and empirically link the social and the ecological, and further how to extrapolate from sets of case studies to the greater region, supra-system, or SES / CHANS theory and practice. This work leverages Landsat and IKONOS imagery as well as field-based vegetation sampling (structure and species) through the use of IDL (interactive data language) visualizations, both pixel- and object-based classifications, and CART (classification and regression tree) analysis. The longer term goal of this work is to produce a protocol and

classification scheme modified from the 1976 Anderson scheme to include both structure and disturbance explicitly in processing, mapping, monitoring, and management. In creating SVCs (Structural Vegetation Categories) built from field data there is strong potential for extracting 3-D data from 2-D imagery once the protocol produces robust results with high enough accuracies. As hypothesized, the object-based classifications produced higher overall accuracy (70.83%), though the pixel-based classification performed better in the detection of woodlands (90.91%). Given the spatial scales of the imagery as compared to the size of the field plots and transect spacing, it is important to remember that when extrapolating to other areas a critical part of spatial scale is extent (not just grain). That is, the inherent clumping of trees versus shrubs may be driving the better performance of pixel-based for woodlands but not so for shrublands. Sensitivity to placement of plots and especially plot sizes across future sites will help explore this question and move SES research into a realm whereby remote sensing and vegetation sampling can provide improved empirical linkages among the subsystems and their feedbacks.

Table of Contents

List of Tables

List of Figures

List of Illustrations

Chapter 1: Introduction

Arid and semi-arid ecosystems cover approximately 40% of the Earth's land surface and are home to more than one third of the world's human population (MEA 2005). They are important food-production regions worldwide and are highly vulnerable to climatic fluctuations such as drought, climate change and changes in land-use patterns (Archer, Schimel and Holland 1995). Research suggests that under current climatic developments, arid and semi-arid regions will experience an increase in aridity due to higher temperatures and wider variability in precipitation patterns (Tucker and Nicholson 1999, IPCC 2013). Such changes will directly affect the availability of natural resources, influencing the complex interactions between social and ecological systems. Apart from the United States and Australia, these regions are situated in developing countries where a significant part of the population depends directly or indirectly on the use of naturally available resources to sustain their livelihoods (Ellis 2000, Kgathi et al. 2004).

The natural resources required by a population vary by geographic location due to cultural adaptations (including migration) over time based upon shifting available resources. It is important to note that these needs may also vary between two villages even in the same general area, whether due to microsite environmental or climatic heterogeneity or differences between villages in terms of differential structural and/or negotiated access rules (Shinn et al. 2014). The interactions between and among humans and environments can be placed within frameworks called social-ecological systems (SESs). As articulated in Ostrom (2007), each social-ecological system has a particular geographic extent in which subsystems exist, including resource systems (e.g. vegetation), resource units (e.g. berries, timber, and building materials), users (human extractors), and governance systems (organization, culture, and rules shaping patterns of resource extraction) (Ostrom 2007). These subsystems exist for an array of resources within each social-ecological system and their linkages are often complex. Understanding these interwoven and dynamic interactions is vital for management purposes as well as ensuring the sustainability of individual systems for both ecological functioning and local livelihoods.

Typically, "wall-to-wall" (complete spatial) coverage of land-cover changes in the landscapes are monitored by remote sensing systems (e.g., satellite or airborne systems) given their synoptic coverage, multi-temporal or repeat capabilities, and ability to detect spectral and spatial information beyond that visible by humans (Jensen 2009). Land-uses are associated with particular land-covers or land-cover combinations in a given area, culture (Liverman et al. 1998) or here, SES and may be tracked over time to assess, in particular, their sustainability. The majority of current land-cover classifications for arid and semi-arid ecosystems, however, are based on broad land-cover classes limited by the characteristics of passive optical remote sensing technologies. While passive remote sensing systems can be used to distinguish between trees and shrubs, they are not designed to penetrate land surface features (e.g., vegetation canopies) and are therefore not appropriate for measuring vegetation structure directly. Active systems, including RADAR and LIDAR, can detect vegetation structure but do so at the loss of spectral information (Jensen 2009). In addition, these systems are extremely expensive and lack the historical archives traditionally needed for land-cover change analysis.

Vegetation structure is important for local livelihoods and the sustainability of individual social-ecological systems. The first objective of this research is therefore to assess the structural heterogeneity within pixel- and object-based land-cover classifications using field data and three-dimensional vegetation visualizations. I hypothesize that the structural heterogeneity within land-cover classes will be high for pixel-based classifications and lower for object-based classifications. The second objective of this research is to generate structural vegetation categories (SVCs) by leveraging field data, IDL (Interactive Data Language) visualizations (three-dimensional representations of vegetation structure), and CART (classification and regression tree) results. Structural vegetation categories, defined as vegetation units with similar structure and therefore likely subject to similar disturbances such as fire or human disturbance, will inform beyond traditional land-cover classes by explicitly quantifying vegetation structure. SVCs however will be based on structural measurements of vegetation from field plots. The last objective of this research is to extrapolate SVCs, through both pixel- and object-based land-cover classifications, to broader areas. This information can facilitate the assessment of the extent and sustainability of land-uses necessary to sustain local livelihoods. In addition, by classifying past satellite imagery and comparing it to present imagery this work can potentially help explain not only how land-cover and structural vegetation disturbance classes have changed over time but also how land available for individual land-uses has changed both spatially and temporally. Such work could ultimately aid in making predictions regarding how future increase in climate variability or changes in land-cover could influence local livelihoods by facilitating changes in land practices and, reciprocally, resource availability.

This research frames such questions for the region encompassing a series of villages, Etsha-1 to Etsha-13, along the western edge of the Okavango Delta (see Section 2.3). Data were collected through vegetation field sampling as well as household interviews regarding livelihood practices, land management, and resource use in order to understand the complexity of this particular social-ecological system. The high environmental variability of this system, particularly flooding levels, makes this system additionally interesting. Environmental uncertainly was hypothesized to differ in perception by local users and to directly influence livelihood strategies, such as creating new fields, planting crops, or focusing on alternative strategies (Shinn et al. 2014). These actions affect the environment, potentially further adding to the environmental uncertainty of the region. Finally, this work asks whether current land-cover classification schemes are adequate within the framework of social-ecological systems with high environmental variability and uncertainty.

1.2 Savanna Ecology

Savannas are defined as tropical and sub-tropical ecosystems characterized by a continuous herbaceous layer (absent disturbance such as recent fire or over-grazing) and a discontinuous layer of trees and shrubs. The herbaceous layer consists mainly of heliophilous C4 grasses but also includes scattered forbs. Savannas are the most common type of ecosystem throughout the tropics and subtropics and cover an eighth of the global terrestrial surface while containing one fifth of the world's human population (Solbrig 1996, Beerling and Osborne 2006). These regions exhibit well defined wet and dry seasons with a mean annual rainfall that ranges from 300 mm to 1600 mm (Frost, Medina and Menaut 1986).

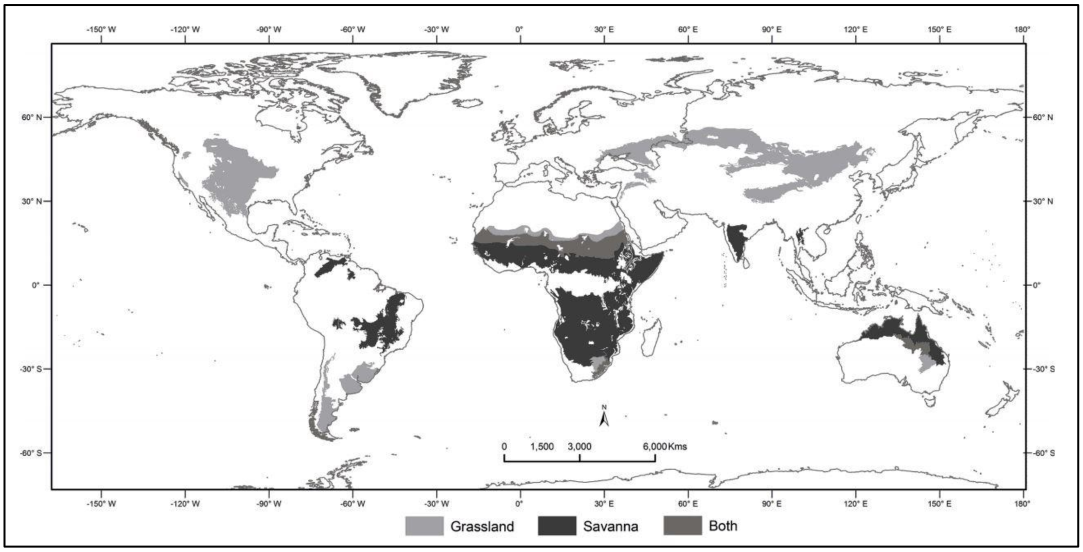

Figure 1: World-wide distribution of savannas and grasslands (Mishra and Young 2014).

The spatial configuration and ratio of woody plants to grasses within savanna ecosystems are a function of poorly understood complex factors (Archer et al. 1995, Scholes and Archer 1997, Tedder et al. 2014). An understanding of which factors determine tree-grass ratios is important, as woody cover affects savanna function by influencing rates of transpiration and production, nutrient cycling, soil erosion, hydrological cycles, and as a result, local and regional biogeochemical cycles (Joffre and Rambal 1993, Schlesinger et al. 1996, Reid et al. 1999, Rietkerk and Van de Koppel 1997). Interactions between plant available moisture (PAM), plant available nutrients (PAN), fire, and herbivory influence savanna structure and function (Cole 1986, Skarpe 1992, Scholes and Walker 1993, Higgins, Bond and Trollope 2000).

At regional and continental scales, woody plant dominance increases as plant available moisture produced through annual precipitation increases. Sankaran et al. (2005) analyzed determinants (mean annual precipitation or MAP, temperature, soil characteristics, and fire occurrence) of woody and herbaceous cover for sub-Saharan Africa and found that MAP was the driving factor for woody cover in arid and semi-arid savannas. In these areas, maximum tree cover occurs at MAP levels of 650 ± 134 mm, while 101 mm is required for woody cover occurrence. At finer scales, however, the spatial and temporal distribution of rainfall varies greatly within each wet season through intense localized thunderstorms (Thomas and Shaw 1991). Soil nutrient levels also influence savanna structure and function over local scales through the quality of soil parent material and the timing of rainfall as it controls mineralization events and thus nutrient release (Sankaran et al. 2005). Fire plays an important additional role in determining vegetation structure and composition by hindering woody plant dominance in savanna ecosystems (Bond and van Wilgen 1996). Fire disturbances control woody cover distribution in areas below the MAP-determined boundary (Sankaran et al. 2005). Several recent studies on the effects of different fire regimes (season, frequency, and intensity) have shown that decreased fire frequencies can result in woody plant encroachment while high fire frequencies can lead to the transition of savannas to grasslands (Trollope et al. 1998, D'Odorico et al. 2007, D'Odorico and Porporato 2006). Fires within savannas are primarily surface fires which spread quickly during the dry, hot, and windy condition during the latter stages of the dry season. Fires commonly occur in savannas every one to three years but such frequencies are dependent on climatic conditions, fuel load, and land-uses (Van Wilgen et al. 2004). Fires are mainly caused by anthropogenic ignition sources, both deliberate and accidental, although lightning does ignite fires in less populated areas (Roy et al. 2011). Fires predominately burn grasses and forbs which are able to regrow quickly post-fire, while mortality is generally low for established trees. Herbivory, through both grazing and browsing by wild and domesticated mammals, affects savanna structure by the trampling of soils (and subsequent root damage) and damaging shrubs and trees (Hopcraft, Olff and Sinclair 2010, Pringle et al. 2007). Large herbivores can damage trees which increases mortality (through debarking for example) while many herbivores eat the foliage of seedlings and increase recruitment (Sinclair 1995). Areas of high herbivory often experience woody plant encroachment as a result in savanna ecosystems (Trodd and Dougill 1998, Lambin et al. 2001, Augustine, McNaughton and Frank 2003). Human disturbances also have significant impacts on savanna structure and function. The overuse of natural resources in arid and semi-arid ecosystems often leads to land degradation. The clearing of land for agricultural purposes resets the successional stage of the habitat as fields are often later abandoned. Intentional burning (for purposes such as for clearing fields, improving soil nutrients and improving grasses for grazing) also changes ecosystem dynamics. Resource extraction, e.g., for building materials and firewood, directly changes savanna structure and species composition.

1.3 MODELS OF TREE-GRASS COEXISTENCE

Several different models have been proposed to explain the mechanisms that permit trees and grasses to coexist without one displacing the other. This tree-grass coexistence is posed as fundamental for savanna ecology. Conceptual models for tree-grass coexistence fall within two main categories: those that focus on competitive interactions between trees and grasses (competition-based models), and those that emphasize climatic variability and disturbances as bottlenecks to hinder tree dispersal and establishment (demographic-bottle neck models).

Early models of savanna dynamics focused on the competitive dynamics between trees and grasses. These models explain tree-grass coexistence based on niche differences, both spatial and temporal, in the way trees and grasses acquire resources. The root niche separation model, proposed by Walter (1971), assumes that water is the limiting factor, since trees and grasses have different assess to water through their unique rooting profiles. Grass roots typically dominate the topsoil layer while tree roots dominate sub-soils (Walter and Mueller-Dombois 1971). Water availability was therefore seen as the limiting factor of tree-grass coexistence through root niche separation in water uptake (Walker and Noy-Meir 1982). The vertical distribution of water in the soil profile thus dictates the ratio of trees to grasses with all other environmental conditions held constant (Walker et al. 1981, Walker and Noy-Meir 1982, Van Langevelde et al. 2003).

The phenological niche separation model explains tree-grass coexistence through differences in seasonal growth potential between trees and grasses. The growth period is limited in savanna ecosystems due to the nature of distinct wet and dry seasons. Savanna trees are capable of storing nutrients and water through the dry season and are therefore able to achieve full leaf expansion quickly as the wet season begins (Scholes and Archer 1997). Peak leaf area of savanna grasses, however, is achieved later in the wet season. Trees therefore potentially have exclusive access to resources in the early and late stages of the growing season while grasses are believed to outcompete trees in periods of growth overlap (Sala, Lauenroth and Golluscio 1997). The balanced competition model stresses trees as superior competitors for both light and soil resources. Tree density, however, is limited by competition between trees for water above a precipitation threshold. Grasses dominate the system below this threshold (Scholes and Archer 1997, House et al. 2003). Within the context of this model, savannas represent non-equilibrium states, with wooded savannas as the exception, which are maintained by grazing pressure and fire (Scholes and Archer 1997). The hydrologically driven competition-colonization model incorporates the balance between the competitive ability and colonization potential of trees and grasses in a disequilibrium framework. The superior competitor changes over time due to inter-annual rainfall variability that determines soil water stress (Fernandez-Illescas and Rodriguez-Iturbe 2003).

As opposed to competition-based models, demographic-bottleneck models focus on the role of disturbances (e.g. fire and grazing pressure) and climatic variability in limiting tree seedling germination, establishment, and demographic transition towards mature size classes (Hochberg, Menaut and Gignoux 1994, Higgins et al. 2000, van Wijk and Rodriguez-Iturbe 2002). Within this model, two main frameworks exist with respect to the degree of control of savanna structure and functioning. The disequilibrium framework views disturbances (e.g. fire and herbivory) as forms which maintain, not only modify, savanna structure by restricting the system to transition into pure woodland or grassland (Jeltsch et al. 1996, Jeltsch, Weber and Grimm 2000). The alternate framework interprets savanna structure based on non-equilibrium dynamics in xeric areas while disequilibrium dynamics, driving by fire intensity, dominate in mesic areas. Tree recruitment in xeric areas, such as arid to semi-arid systems, thrives through localized thunderstorms. Trees are able to dominate the canopy cover in mesic savannas, while frequent high intensity fires (due to high fuel loads) and browsing hinder complete tree dominance over grasses (Jeltsch et al. 1996).

1.4 SOCIAL-ECOLOGICAL SYSTEMS

Humans have interacted with and altered the environment since the beginning of human history. Such impacts include the use of fire to change / clear flora in addition for hunting strategies, the cutting / clearing of forests for building materials and firewood, and the creating of irrigation systems in arid regions (Pearce and Turner 1990). These impacts were restricted to local and regional scales until the past 300 years. The human population has increased exponentially, in addition to becoming a fossil fuel based society; these shifts have increased the impact on the environment. Global impacts of human activity are now apparent through changes in biogeochemical cycles and severe alterations in climate and its variability (IPCC 2013). Understanding of such changes with respect to local, regional, and global resources for an expanding global population is becoming increasingly important. While many disciplines focus upon either anthropogenic or natural components, the complex interactions among society and nature have been studied in fields such as sustainability science and coupled human and natural systems (CHANS) (Kates et al. 2001, Cash and Moser 2000, Gibson, Ostrom and Ahn 2000). These fields employ interdisciplinary approaches by the integration of both ecological and social sciences in order to understand the "interaction of global processes with the ecological and social characteristics of particular places and sectors" (Kates et al. 2001). Research framed within CHANS focuses on three individual aspects of socio-ecological interaction: the patterns and processes that link human and natural systems; the reciprocal interactions and feedbacks within these systems; and the human-environment interactions within and across scales of analysis (Liu et al. 2007).

The social-ecological (SES) framework presented by Ostrom (2007, 2008, 2009) offers a functional approach to study CHANS by addressing the interconnection between the social and natural spheres while stressing feedbacks between subsystems and their anthropogenic and ecological significance. Each SES under study has a specified geographic extent in which subsystems exist, including a resource system (e.g., vegetation), resource units (e.g., berries, timber, and building materials), users (e.g., human extractors), and governance systems (e.g., organization, culture, and rules shaping patterns of resource extraction) (Figure 2) (Ostrom 2009).

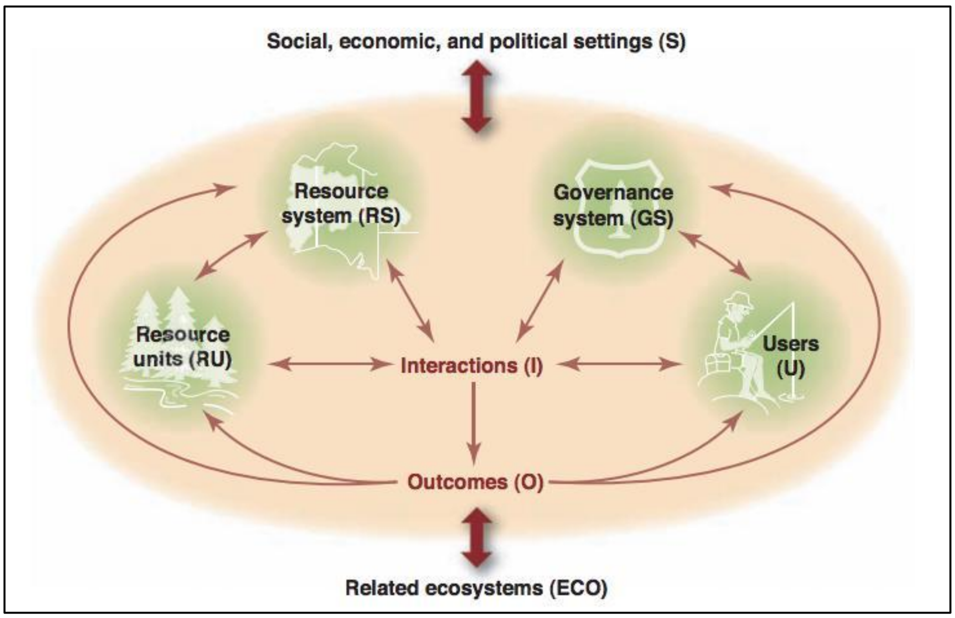

Figure 2: The first-level core subsystems in a framework for analyzing social-ecological systems (Ostrom 2009).

These first-level core subsystems exist for an array of resources within each social-ecological system and links among them are often complex and stretch across multiple scales. Each core system consists of multiple second-level variables (e.g., the productivity of a resource system, the social or economic value of resource units, the operational rules, and the number of users in the system), which each are then composed of deeper-level variables (Ostrom 2009).

The environment guides human activities such as settlement, resource use and extraction, and livelihoods. Environmental uncertainty, such as that surrounding precipitation or flooding levels, can have a large effect in SESs and influences local livelihoods and resources. Locals make livelihood decisions based on their perception of the environmental variability (or lack thereof). This facet is particularly important in systems with high inter-annual environmental uncertainty. Livelihood decision making, such as the creating of new fields or abandoning fields in favor of other livelihood activities, directly influences the environment and particularly vegetation communities. Such activities compound environmental variability, further adding to the system's overall environmental uncertainty. The sustainability of each SES and the resource systems within it thus depend directly upon users and governance systems, each of which may vary widely even within a single SES (Shinn et al 2014).

Chapter 2: Site & Situation

2.1 THE KALAHARI ENVIRONMENT

The Kalahari Desert and its sand deposits cover approximately 2.5 million square kilometers of the interior of southern and central Africa (Scholes et al. 2002). The Kalahari Beds extend from the Orange River in the south to as far north as the equator. These sands have been deposited and worked by aeolian processes during the Eocene to Pliocene period (two to seven million years ago) and accumulated within the Kalahari Basin (Thomas and Shaw 1991).

Figure 3: Spatial extent of the Kalahari sand deposits (Meyer 2014).

Despite its name, the Kalahari Desert is in fact not a desert but a semi-desert based upon the definition of deserts as hot regions with annual rainfall not exceeding 250 mm. The Kalahari Desert is located within the southern hemisphere subtropical high pressure belt that along with the Southern Atlantic Oscillation (SAO) controls the climate of the region. The seasonal fluctuations of this belt and the Inter-tropical Convergence Zone (ITCZ) result in a strong delineation between the wet and dry seasons of the Kalahari region. The wet season lasts from November to March while the dry season dominates the remainder of the year. The annual rainfall within the Kalahari Desert varies from 250 mm in the extreme south to more than 1000 mm in the north (Shugart et al. 2004). The Kalahari Desert is therefore a semi-arid region in its central and southern parts while it is a dry sub-humid region to the north. The majority of rainfall comes from convective thunderstorm systems that contribute to high year-to-year rainfall variations for a given location and high variability among sites of close proximity.

The soils of the Kalahari are often described as homogenous and low in organic materials and nutrients (D'Odorico et al. 2007). Although this description is accurate, especially with respect to particle size, variability does exist across finer scales (Meyer 2014). This variability results in relatively high spatial heterogeneity in vegetation composition. Most of the vegetation within the Kalahari is described as savanna, defined as tropical and near-tropical ecosystems characterized by a continuous herbaceous layer and a discontinuous layer of trees and shrubs. Vegetation cover, diversity, and biomass are heavily correlated to the climatic north-south gradient, resulting in closed tropical forests in the north to typical savannas to open grasslands in the south. Disturbances, soil types, and geomorphological effects, however, create inter-regional exceptions to this general trend.

2.2 THE OKAVANGO DELTA

The Cubango and Cuito Rivers come together in Southern Angola to form the Okavango River. The Okavango River runs through Namibia, where it is referred to as the Kavango River, until it enters the Okavango Delta in northwestern Botswana. The Okavango Delta is a large, inland alluvial fan (22,000 km^2, though the actual area covered changes with flooding fluctuations) that is formed by the Okavango River. That river, constrained on either side by faults, travels southeast from the panhandle in the Namibian Caprivi Strip and northwestern Botswana until it reaches a major fault line (the Gumare fault) where the water disperses into the fan and distal regions. The distal regions are bounded by two fault lines, the Kunyere and Thamalakane faults, with waters then lost primarily to evapotranspiration, though in extremely wet periods, such as recently, the water does spill over into the Boteti River.

Figure 4: The Okavango Delta and its headwaters in the Angolan highlands (Mendelsohn et al. 2010).

The Delta extends a total of 250 km and covers an area over 22,000 km^2 (Smith et al. 1997). The Okavango system falls within the semi-arid climate of the surrounding Kalahari region with annual rainfall ranging from 450mm in the distal south to 650mm in the north / panhandle. The rainy season occurs between November and March while minor precipitation may occur sporadically in the dry season the remainder of the year. Precipitation, however, only provides roughly half of water inflow to the system (though this proportion varies from year to year). The other portion comes from upstream rains in the catchment area (over 325,000km^2) of the Angolan highlands that eventually feed the Okavango system (McCarthy et al. 2003). The peak flooding in the Delta thus occurs in the dry season as a result of it taking several months for the Angolan sourcewaters to move downstream. Water stages are highest in March to April at the panhandle of the Delta while highest in August at the Delta's most distal reaches. Flooding patterns in the Delta often change both spatially and temporally given the high spatio-temporal variability of both precipitation and channel movement. Flooding levels are also cyclical and have gone through high flooding years to low flooding years on a quasi-decadal scale from the 1950s to the 1990s. Since 2000, however, peak flooding levels have been increasing steadily. The majority of surface water is lost to evapotranspiration (~2172 mm/year), while the remainder runs out of the Delta to the southeast into the Boteti River (McCarthy et al. 2003).

The entire active catchment area of the Okavango Delta spans three countries (Angola, Namibia, and Botswana) and was designated by international treaty in 1997 to be a Ramsar wetland of importance. The majority of the Delta is further protected as part of the Moremi Game Reserve or Wildlife Management Areas, although village communal lands do exist where grazing and wetland floodplain farming ("*molapo*" in

Setswana) occurs. The Delta and its dynamic channels, swamps, seasonal floodplains, riparian woodlands, and dry woodlands contain a much higher level of biodiversity, both flora and fauna, than the surrounding Kalahari savanna ecosystem (Ramberg et al. 2006), though the combination of its multi-national nature and high number of migratory species do produce relatively low rates of endemism. Wildlife populations, however, have been declining since the 1960s, primarily due to a series of veterinary fences that were erected to control the spread of livestock diseases (Perkins and Ringrose 1996, Mbaiwa and Mbaiwa 2006).

The resources associated with the Delta have enabled a larger human population to reside around its periphery than farther into the Kalahari. The complex nature of the Delta as a system, however, also increases the variability and uncertainty of the quantity and quality of available resources from year to year largely due to [primarily] cyclical climate fluctuations. Roughly 125,000 people live in or around the Okavango Delta and almost all (over 95%) directly or indirectly depend on natural resources from the area to sustain their livelihoods (NWDC 2003). Veld products locally collected and sometimes sold include palm leaves (*Hyphaene petersiana*) for basket weaving, thatching grass (e.g., *Eragrostis pallens, Aristida stipitata,* and *Cymbopogon excavatus*) and river reeds for building materials, medicinal plants, fruits, and *mopane* worms, as well as other fencing, building, canoe ("*mokoro"* in Setswana), and fuel wood materials (*Colophospermum mopane, Dichrostachys cinerea, Diospyros mespiliformis* and others). However, many of these materials are decreasing in availability due to an increase in their demand (ADRC 2001).

Both dryland and flood recession (*molapo*) agriculture is practiced in the Okavango region. 48,900 hectares have been cleared for crops in Okavango Delta region, of which 75% were dryland fields and 25% were *molapo* fields. This number is deceivingly high as only about 10,000 hectares are used in a given year (Mendelsohn et al. 2010). Dryland farming is practiced on the sandy soils of the uplands away from the floodplain. Fields are cleared through manual labor by removing all woody vegetation, although some trees may be left to provide shade. Several different crops are grown including maize, sorghum, millet, and watermelons. Fields are fenced in wire covered with thorn-bushes to keep cattle and wildlife out. Crop yields are generally low due to the poor fertility of the soil and low rainfall. *Molapo* farming takes advantage of seasonal swamps on the fringes of the Delta that are much more fertile than the sandy soils in the backcountry as well as having close proximity to crops needing greater water. Crops are thus planted in the floodplains, taking advantage of the moisture in the soil. These areas flood during the high flood season (that is, the dry season) and water then slowly infiltrates or evaporates. These areas are ideal for seasonal farming as they are able to take advantage of greater soil moisture as the floods recede. The main crops planted in *molapo* areas are maize, while beans and other vegetables are also planted. Being able to predict flooding levels, therefore, is vital for crop planning as the success of *molapo* farming is primarily determined by flooding, both from the previous season and of that coming season. Crops can be ruined in years of too little or too much flooding. The recent trend of increasing flood levels has therefore been troublesome for many households' local livelihoods (Shinn et al. 2014), though some have benefitted from the situation. In addition, precipitation in the Delta can cause early floods that can damage standing crops. Livestock, mainly cattle and goats, is also widely kept by families to sustain their livelihoods in years of low crop yields. Livestock is either based at cattle posts or roam the village where they graze outwards from communal or tribal lands. Livestock may be kept for commercial purposes (more common in areas away from the Delta, though this trend is changing) but is usually kept for subsistence use, security assets, and occasional ceremonies such as wedding gifts. The relative contribution of individual livelihood strategies may differ from year to year and even within the year based on the perception of environmental conditions (Shinn et al. 2014).

2.3 THE ETSHA SETTLEMENTS

The Etsha region[1] is comprised of thirteen settlements situated along the western boundary of the Okavango Delta. These villages were created when 3,300 members of the Hambukushu tribe in southern Angola fled into Botswana during Angola's war of independence in 1967. The Hambukushu were adopted as part of the Batswana tribe and were allocated the land that is now the Etsha settlements or villages[1]. The Delta and its banks were already inhabited by the Bayei, resulting in the Etsha communities being a mix of Hambukushu and Bayei. The Hambukushu are resourceful people whose livelihoods depend on dryland farming, cattle, and basket-making of palm leaves. The Bayei are more people of the water and utilize flood cycles through *molapo* farming and fishing. Livelihood strategies do, however, overlap between the two groups and no strategy is exclusive to one group (Meyer et al. 2011).

[1] For the purpose of clarity, the following naming convention is used to refer to the components and reaches of the Etsha area: E_xS refers to all Etsha settlements (Estha 1 - Etsha 13) in the settled zone (see Figure 6), with $E_{13}S$ for instance representing the Etsha 13 settlement only. Similarly, E_xR represents the entire Etshas region with, for example, $E_{13}R$ referring only to the Etsha 13 village and usage / backcountry area. This naming convention recognizes 1) the different "zones" in the Etshas area of dense settlement versus sparse settlement and veld collection / dryland farming and 2) the heterogeneity among the 13 Etsha settlements.

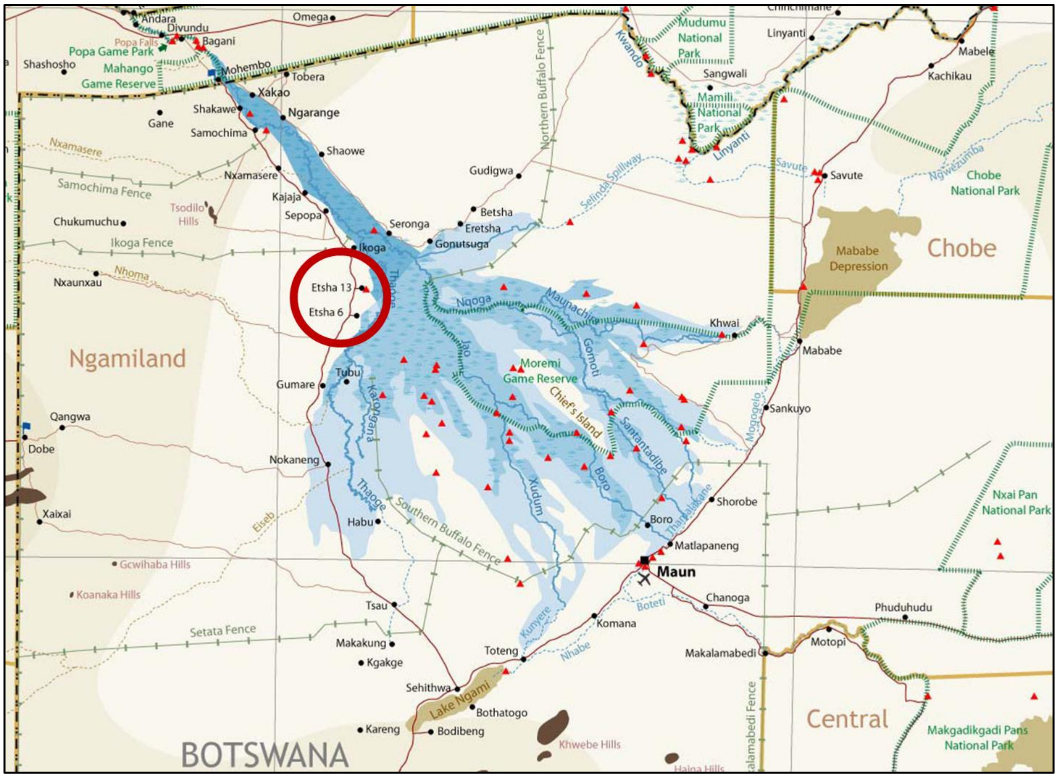

Figure 5: The Etsha region (imagery from National Geography / ESRI).

Four main land-use zones exist: the Delta, the floodplain, the village and fields area (here, called settlements), and the backcountry, collectively referred to in this work as the Etshas region. The Delta is a wetland ecosystem and is used for fishing and collected natural materials. The high seasonal and inter-annual flooding variability influences land-uses in the floodplain used for *molapo* farming and grazing areas on rich soils. The village and backcountry areas are typically savanna ecosystems with low annual precipitation (~450 mm). The sandy soils are used for dryland farming despite low yields due to low nutrient levels. Mainly maize, sorghum and millet are grown although many fields are abandoned.

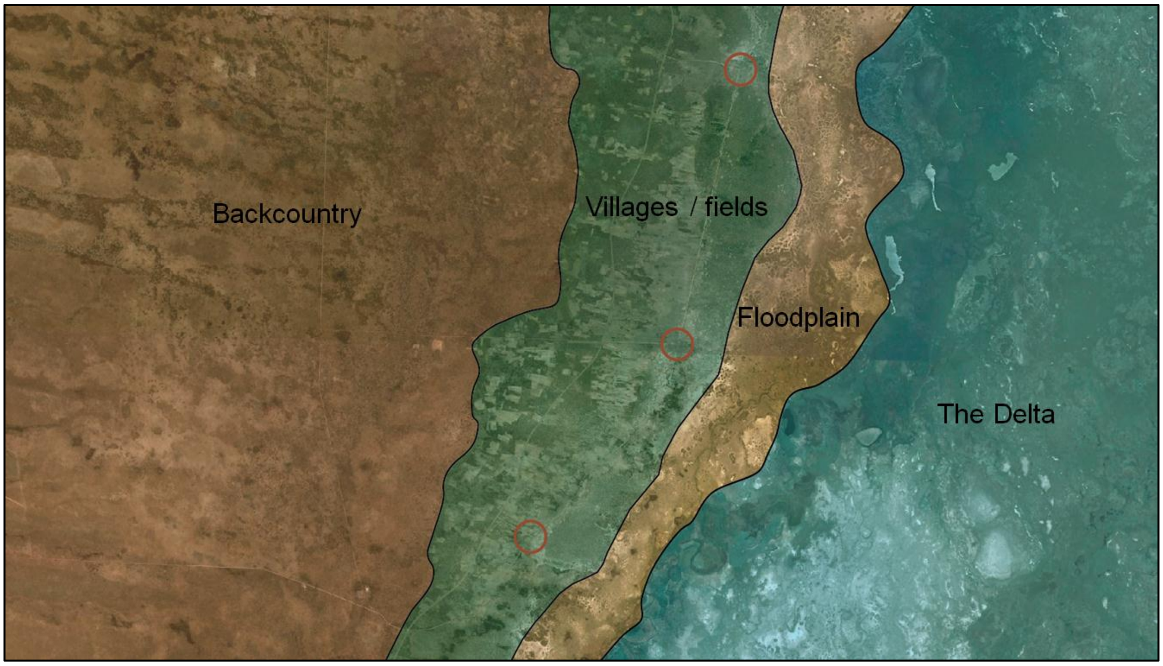

Figure 6: Land-use zones in the Etsha region.

Chapter 3: Research Objectives and Methodology

3.1 RESEARCH OBJECTIVES

In order to assess whether current land-cover classification schemes are adequate within the context of social-ecological systems, this research addresses three main objectives:

Objective 1: Assess the structural heterogeneity within pixel- and object-based land-cover classifications using three-dimensional vegetation visualizations.

Objective 2: Generate quantifiable structural vegetation categories by leveraging field data, IDL visualizations (three-dimensional representations of vegetation structure), and CART (classification and regression tree) results.

Objective 3: Assess the ability of detecting SVCs through land-cover classifications, both pixel- and object-based, for broader areas.

For the first objective, Landsat TM imagery was used for both pixel- and object based land-cover classifications. The structural heterogeneity was then assessed within each land-cover classification, for both methods, through the use of three-dimensional vegetation visualizations created using plot structural measurements and Interactive Data Language (IDL). I hypothesized that the structural heterogeneity would be high within pixel-based land-cover classes, while it would be lower within object-based land-cover classes.

For the second objective, structural variables (e.g., number of trees, height and clustering classes, diversity, etc.) were calculated for all sampled plots and then used to create quantifiable structural vegetation categories (SVCs) by using a classification and regression tree (CART). CART analysis is a statistical tree-building technique which ranks and splits data by determining which variables explain trends in the data. Accuracy assessment was performed using IDL visualizations to inspect the spatial heterogeneity within each structural vegetation category. I hypothesized that the structural heterogeneity within SVCs would be much lower than within land-cover classes from the first objective. In addition, I hypothesized the distribution of SVCs would be spatially related to the proximity of major roads, the Delta, and central village areas, with backcountry dominant SVCs being different than village SVCs due to pressures from land-use and closer proximity to denser populations in the latter.

For the third objective, the ability of detecting SVCs through land-cover pixel- and object-based classifications for broader (i.e., non field-sampled) areas was tested. Ideally, each SVC would fall within exclusive land-cover classes. I hypothesized that each SVC would fall within several land-cover classes and would not be mutually exclusive.

3.2 Remote Sensing of Savanna Landscapes

Earth observation satellites have greatly increased our ability to monitor landscapes by providing access to both visible and non-visible portions of the electromagnetic spectrum at multiple spatial, temporal, and spectral resolutions (Jensen 1996). The United States Landsat program launched Landsat 1 in 1972 and the availability of satellite imagery, along with derived products, has grown since. Additional satellites have further increased the spatial resolution (e.g., Quickbird and IKONOS), spatial extent ideal for monitoring landscapes at broader scales (e.g., MODIS and AVHRR), and spectral resolution (e.g., Landsat TM and Landsat 8) of available imagery. In combination with *in-situ* data, remotely sensed imagery enables the environmental assessment of landscapes through the observation of changes in land-cover. Anderson (1976) introduced a multi-level classification framework for national [US] land use and land cover (LULC) classifications with both exhaustive and mutually exclusive classes (e.g., deciduous forest land, evergreen forest land, and mixed forest land within the "forest land" level-one class). While effective at continental scales, such a classification scheme is less ideal for regional and local scales as they (1) describe multiple land surface types within the same class, and (2) include fuzzy class definitions.

Land-cover classifications are difficult in spatiotemporally dynamic landscapes (such as savannas) due to the heterogeneity of vegetation composition and structure (Thompson 1996, Jung et al. 2006). Land-cover classes for vegetation within savannas, and arid to semi-arid ecosystems, are identified based upon characteristics such as structure (height and/or cover), species composition, or other observable habitat properties. Structural and hierarchical classification schemes have been developed based upon principles of the Anderson framework but with more detail in terms of vegetation life form, height, cover, and composition. Such approaches, as presented by Edwards (1983) and Grunblatt et al. (1989), utilize lifeforms (such as woodland or shrubland) with modifiers to describe structure and composition. These classification schemes characterize land-cover in detail although class verbiage often overlap, making both classification and interpretation subjective (e.g. shrubbed woodland versus treed shrubland). Within the framework of SES, it is essential to apply land-cover classes to the landscape that are relatable not only to land use activities but also to how such activities disturb vegetation in terms of structure and spatial arrangement. In addition, there is a need for quantifiable structural land cover classes as opposed to current classification schemes based on descriptive variables such as lifeform and broad modifiers. Pixel-based land-cover classification is widely used although the patch-dynamic nature of savannas often makes the variability within classes higher than between classes. Object-based classifications can therefore be advantageous within savanna systems as they segment homogeneous pixels together into objects based on shape, compactness, and texture. These two methods are compared in this work in terms of creating accurate land-cover classifications in a savanna system.

3.3 FIELD METHODOLOGY

Vegetation data were collected along a series of villages (Etsha-1 to Etsha-13) and their usage back-country areas (together, E_xR) by the western edge of the Okavango Delta. Vegetation measurements were taken within 10 x 25 meters plots (58 in total) that were spaced every 500 meters along 9 transects laid perpendicular to the Delta, in each case starting at the edge of the current extent of the Delta's waters and moving due west. Within each plot, all woody species above 25 centimeters in height were measured with regards to the Cartesian location, stem and canopy dimensions, number of stems, diameter at breast height, cover estimates, and species identification of individual trees. Vegetation data were not recorded if the plot fell within agricultural fields or a house, compound, or village center. In such instances, however, a broad description of the vegetation was noted. Semi-structured interviews were also conducted with members of the Etsha settlements to gain insights into livelihood practices, land management, resource use and extraction, and perceptions of environmental uncertainties.

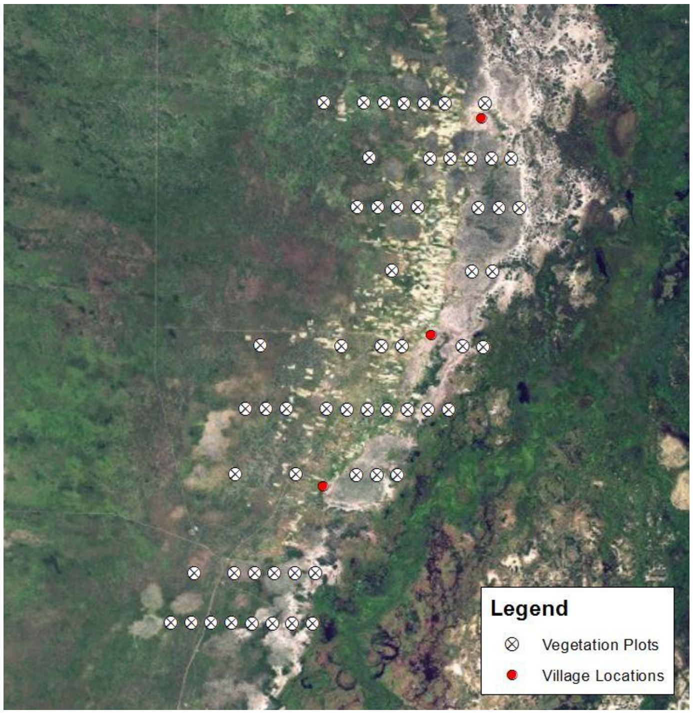

Figure 7: Transect layout & plot locations (imagery from GeoEye / ESRI).

3.4 THREE-DIMENSIONAL VISUALIZATIONS OF VEGETATION STRUCTURE

Field measurements were used to create three-dimensional visualizations of the vegetation structure of each plot with Interactive Data Language (IDL). IDL is a programming language that can be used for customized data analysis and graphical visualizations. Each tree was modeled with a stem and canopy component. The stem component uses x and y locational measurements, dbh (diameter at breast height), and height of the stem to create three-dimensional rectangular boxes to represent the stem for each tree. For multi-stemmed trees, the stems have been combined into one shape due to several factors including; (1) the extensive time required to note the Cartesian location of each individual stems for shrubs with up to 100+ stems, and (2) in order to avoid creating systematic error by introducing patterns in which to place stems in the model. The canopy component uses x and y measurements of canopy extent and the start and total height of the canopy to create an octahedron to represent the canopy. This shape was chosen to represent the canopy since no geometric shape could accurately represent complex tree canopy structures and it is purely based on field measurements (while an ellipsoid for example would imply a canopy structure which may not have been observed in the field). In combination, the stem and canopy components represent an individual tree. Each tree was modeled in this fashion and placed within a three-dimensional coordinate system.

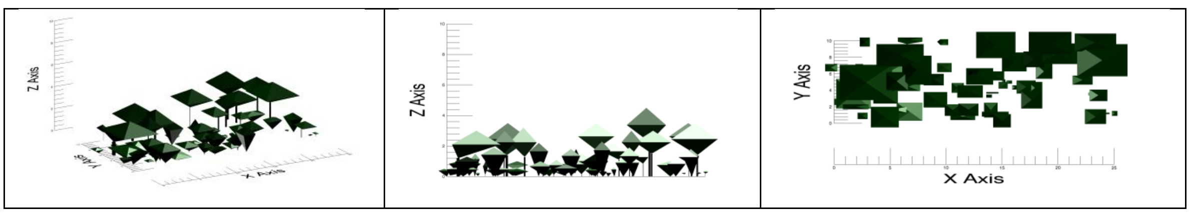

Illustration 1: Angled, side, and top view of a plot's vegetation structure.

3.5 CLASSIFICATION AND REGRESSION TREE (CART)

Classification and regression tree (CART) analysis in the R statistics package was used to assess vegetation structure among plots in order to create structural categories. Structural variables were calculated for each plot and used in the CART analysis. Variables included: number of individuals, number of species, percentages of all tree genera found in the area, biomass, Simpson's diversity index, densiometer readings of canopy closure (taken in field), total canopy cover, height categories (percent below 0.5

m, between 0.5 and 2 m, and above 2 m), stem area, and stem categories (percent single stem, 2 to 5 stems, 6 to 20 stems, and more than 20 stems per tree).

Several CART trees were produced and assessed in terms of similarity within and differences among structural categories and were compared to the IDL visualizations. The CART tree chosen (based on ecological and structural differences between categories) contained ten categories based on six variables: number of individuals, height category 1 (below 0.5 m), height category 2 (0.5 m to 2 m), height category 3 (above 2 m), stem category 3 (6 to 20 stems), and stem category 4 (20+ stems). The ANOVA method was used, which maximizes the sum of squares between groups through a regression tree. Other settings included the minimum split at 10, which requires that the minimum number of observations in a node to be 10 before attempting a split and a cost complexity factor at 0.001, which means a split must decrease the overall lack of fit by a factor of 0.001.

Chapter 4: Analysis & Results

4.1.1 Supervised Pixel-Based Land-cover Classification

A supervised land-cover classification was created with Landsat TM 5 imagery from the 27th of April 2009. A total of 31 classes were left after evaluating the separability of all 255 classes following the protocol described in Messina et al. (2000). These 31 classes were then attributed to a land-cover type based on lifeform and tree cover density using high resolution IKONOS imagery (from the 17th of October 2011) for accuracy assessment. The classification scheme presented by Grunblatt et al. (1989) was used, although modifiers such as height and species dominance were not used as they could not be assessed from a [remote] nadir perspective. In addition, the definition of trees was slightly altered to fit the ecosystem characteristics, as many trees are multi-stemmed (usually between two and five stems, but some species up to 100 or more stems) in the Botswana Kalahari. For example, a land-cover with 60% shrub cover and 20% tree cover is classified as "dense treed shrubland".

Level	Criteria	Terms	Description
1	Lifeform	Woodland	Land dominated by trees (woody, single stemmed plants)
		Shrubland	Land dominated by shrubs (woody, multi-stemmed plants)
		Grassland	Land dominated by herbaceous (non-woody) cover
		Bareland	Land with less than 2% of total vegetation cover
2	Cover	Closed	80-100% canopy cover
		Dense	50-79% canopy cover
		Open	20-49% canopy cover
		Sparse	2-19% canopy cover

Table 1: Land-cover classification scheme presented by Grunblatt et al. (1989).

The classification resulted in eight land-cover classes: dense woodland, dense shrubbed woodland, open shrubbed woodland, dense treed shrubland, open treed shrubland, open shrubland, sparse treed shrubland, and sparse shrubland (Figure 8). The variability within classes, however, was higher than among classes. This results in the inability of the classification to detect fields accurately as there was high overlap among vegetation land-cover classes and fields.

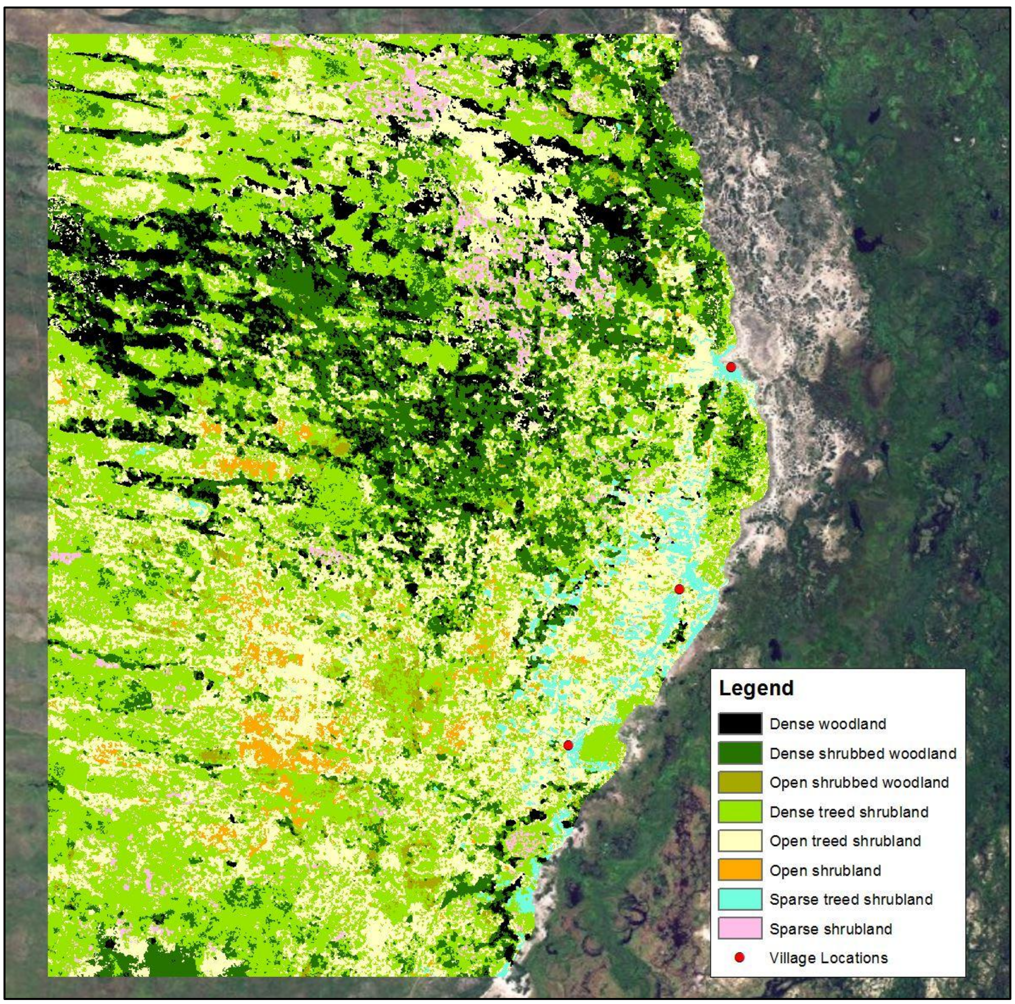

Figure 8: Land-cover classification with Landsat TM 5 (04/27/2009).

The E_sR (settlement region) was then classified on its own in order to detect fields more accurately (Figure 9). While the village classification performed better in identifying fields there was still high variability within classes, which resulted in a simplified land-cover depiction of the area. The original land-cover classification was thus used for SVCs since it covers the entire area of interest and classifying the E_BR (backcountry region) based on the E_sR would introduce error and bias.

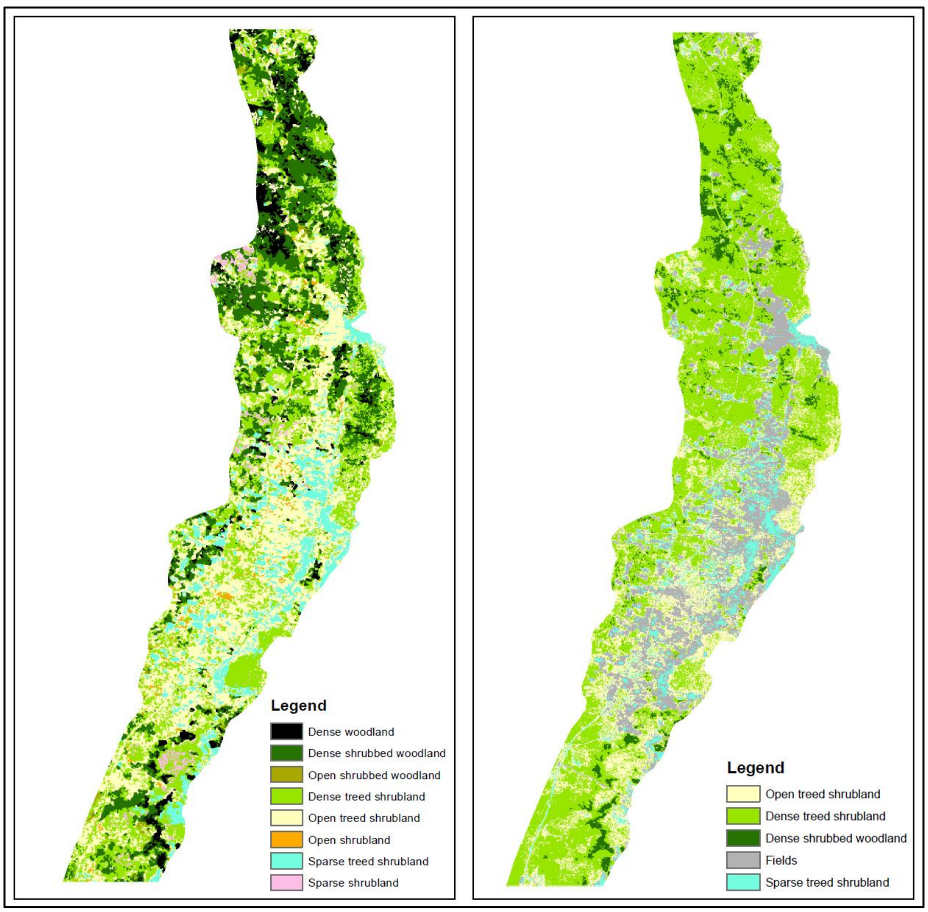

Figure 9: Side by side comparison of the areas land-cover classification (left) and the village area classification (right).

4.1.2 STRUCTURAL HETEROGENEITY WITHIN THE SUPERVISED PIXEL-BASED LAND-COVER CLASSIFICATION

Plots within each land-cover type (derived from the Landsat object-based land-cover classification) were compared in terms of vegetation structure using IDL visualizations. The structural variability within each structural category was high as shown in the illustration below (illustration 2). No plots fell within the open shrubland or sparse treed shrubland. Note the high structural heterogeneity within each pixel-based land-cover class.

Pixel-based land-cover class	Plots within each pixel-based land-cover class (side and top view)	
Dense woodland	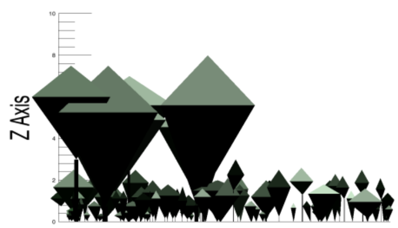	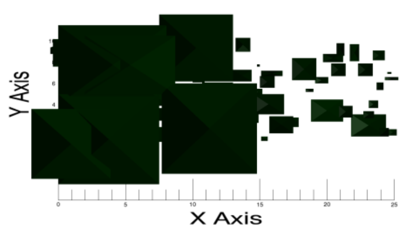
Dense shrubbed woodland	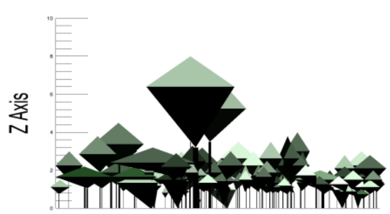	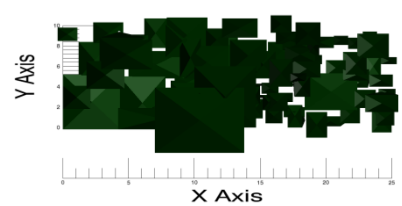
	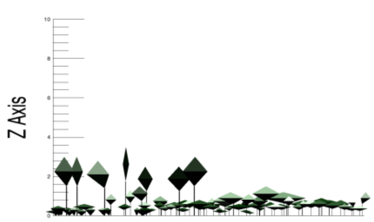	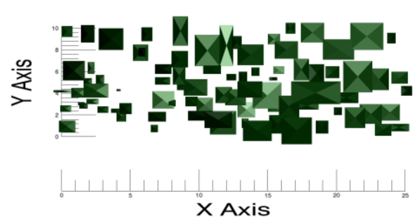

Illustration 2: Structural heterogeneity within pixel-based land-cover classes.

Dense shrubbed woodland (continued)	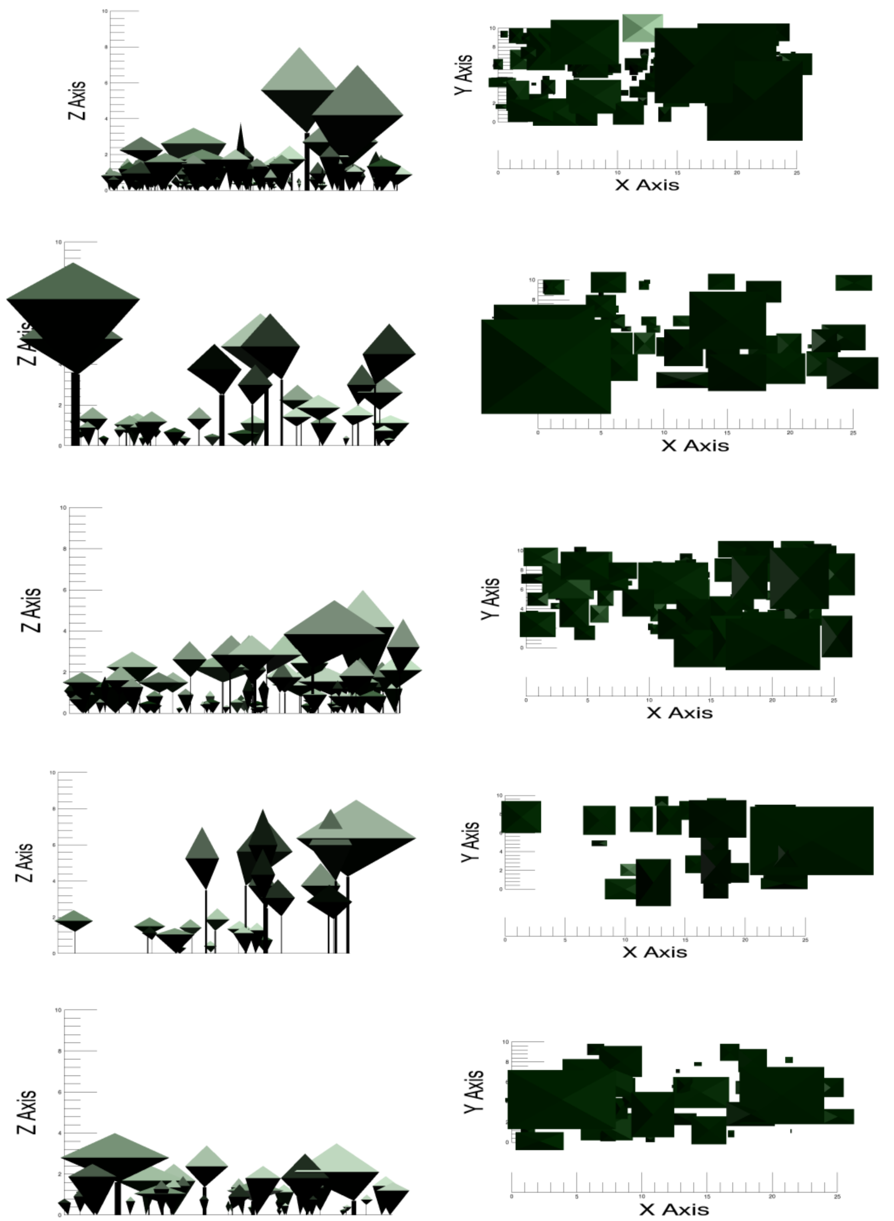

Illustration 2: Structural heterogeneity within pixel-based land-cover classes (continued).

Open shrubbed woodland	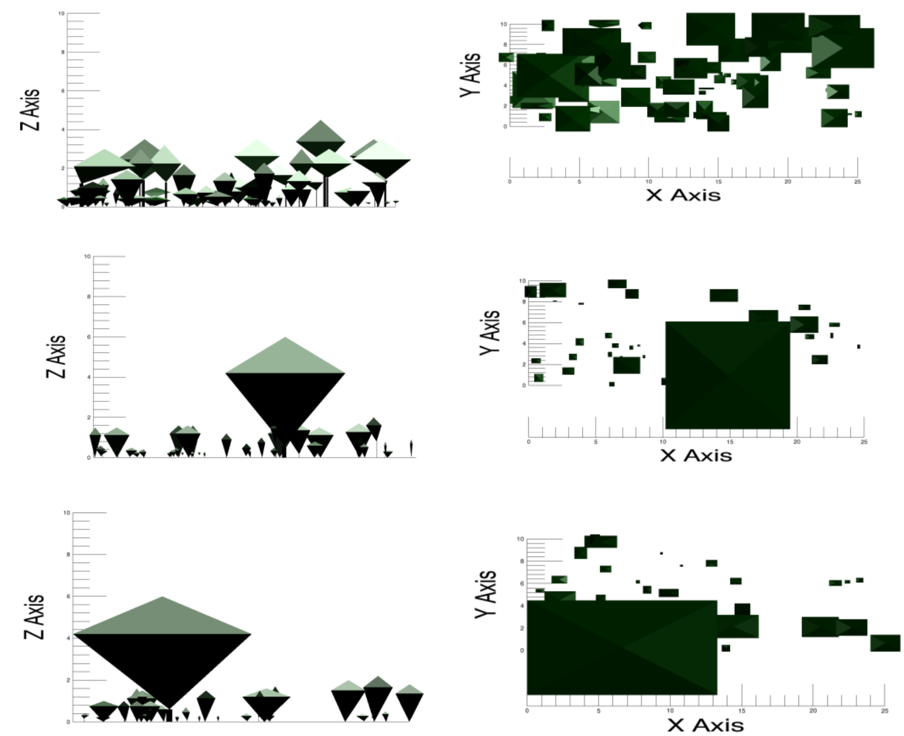
Dense treed shrubland	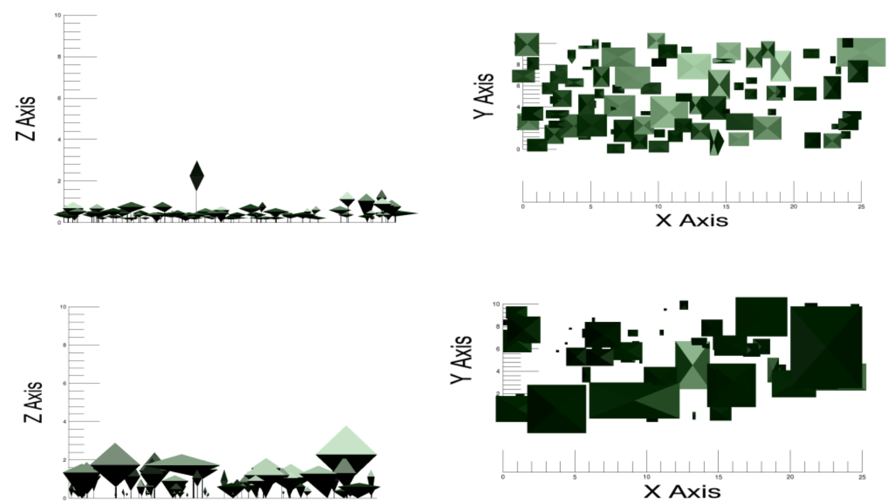

Illustration 2: Structural heterogeneity within pixel-based land-cover classes (continued).

Dense treed shrubland (continued)	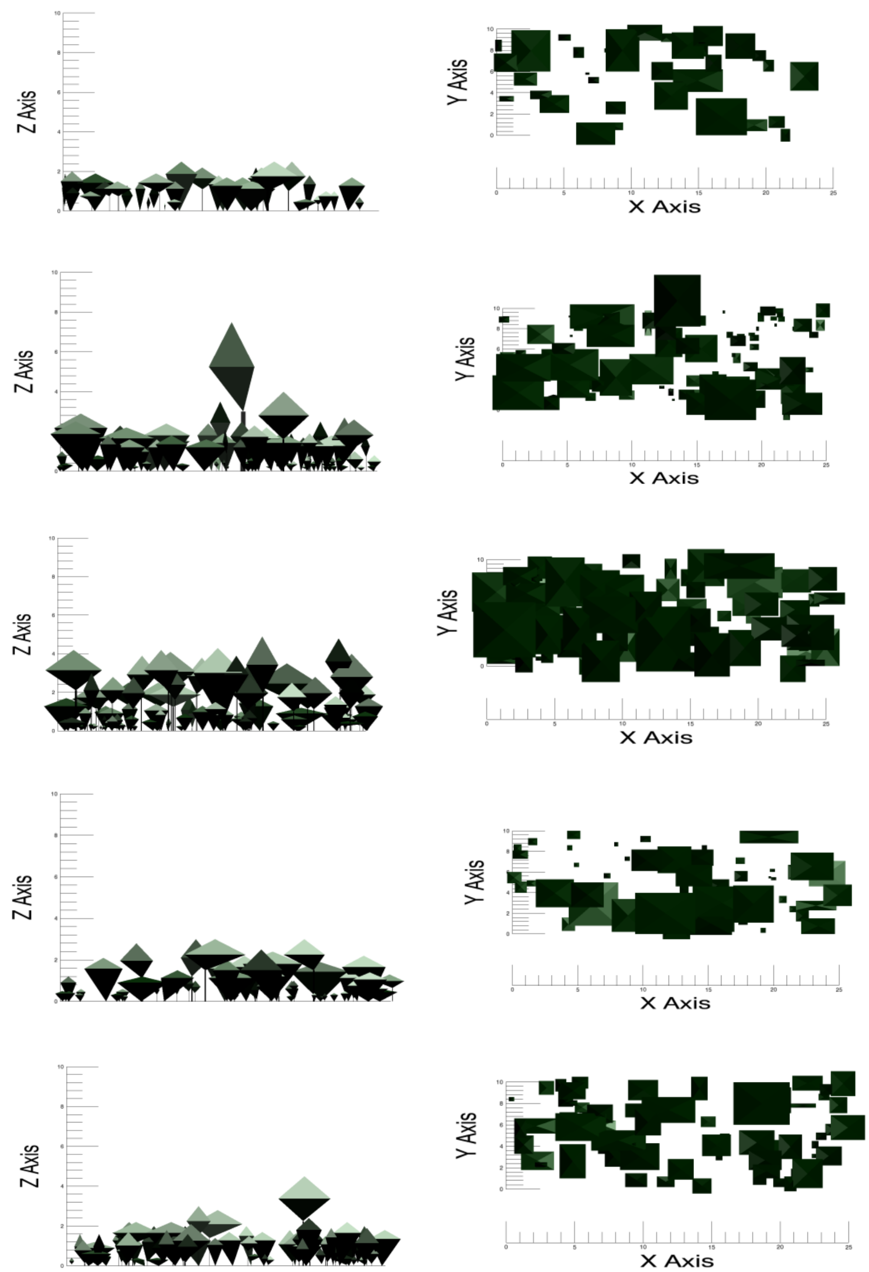

Illustration 2: Structural heterogeneity within pixel-based land-cover classes (continued).

Dense treed shrubland (continued)	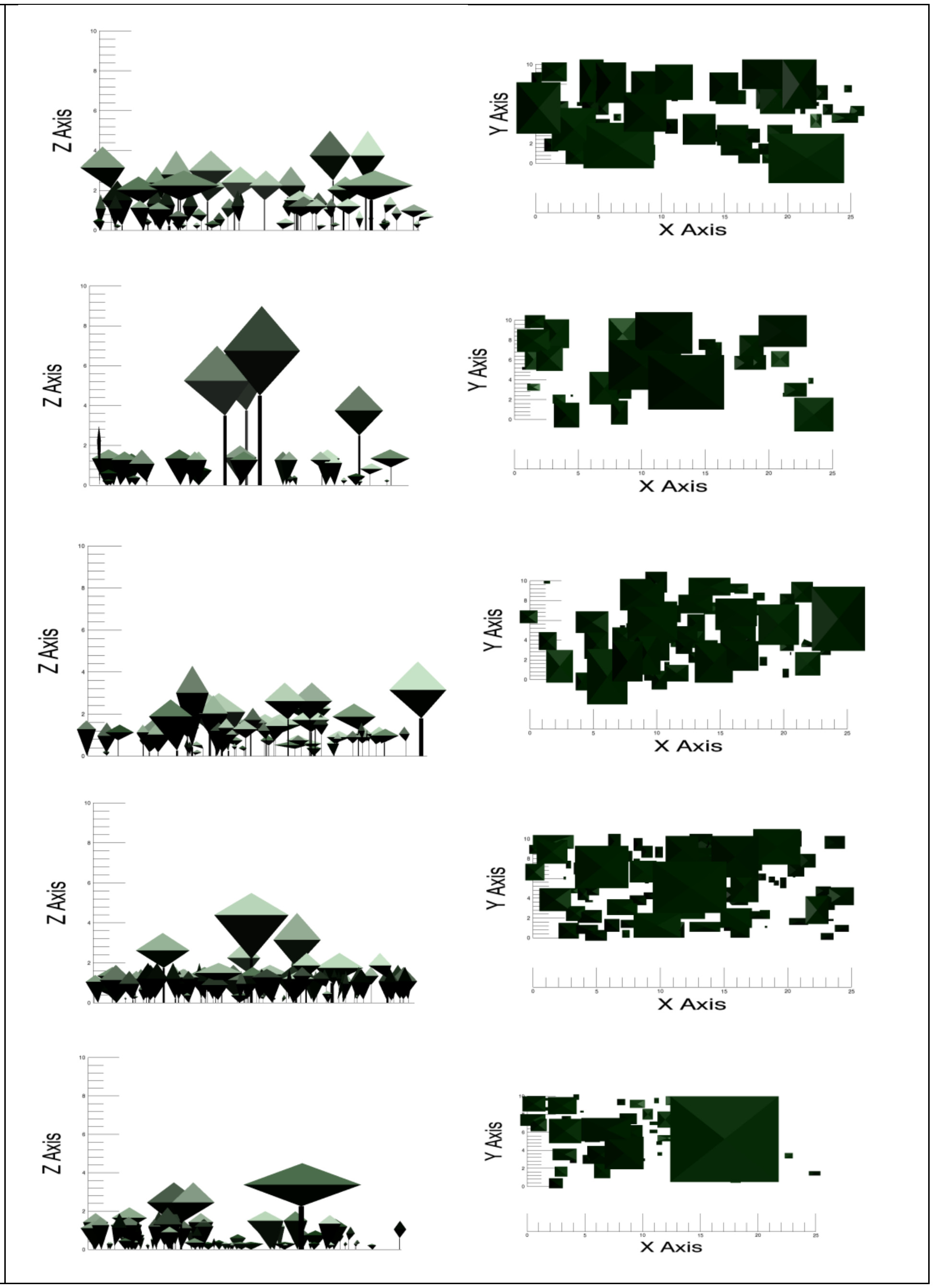

Illustration 2: Structural heterogeneity within pixel-based land-cover classes (continued).

Dense treed shrubland (continued)	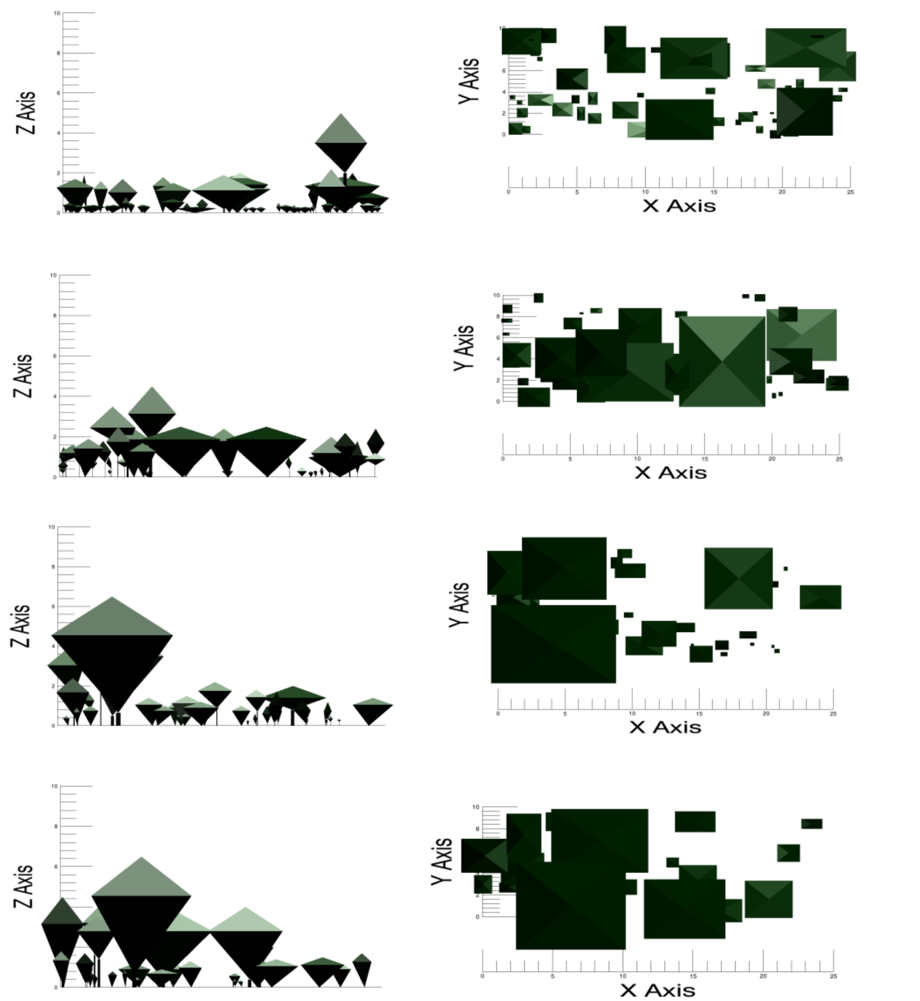
Open treed shrubland	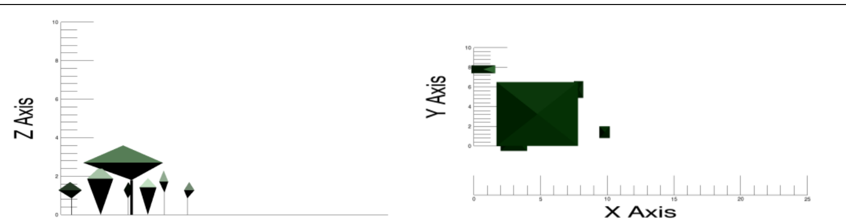

Illustration 2: Structural heterogeneity within pixel-based land-cover classes (continued).

Open treed shrubland (continued)	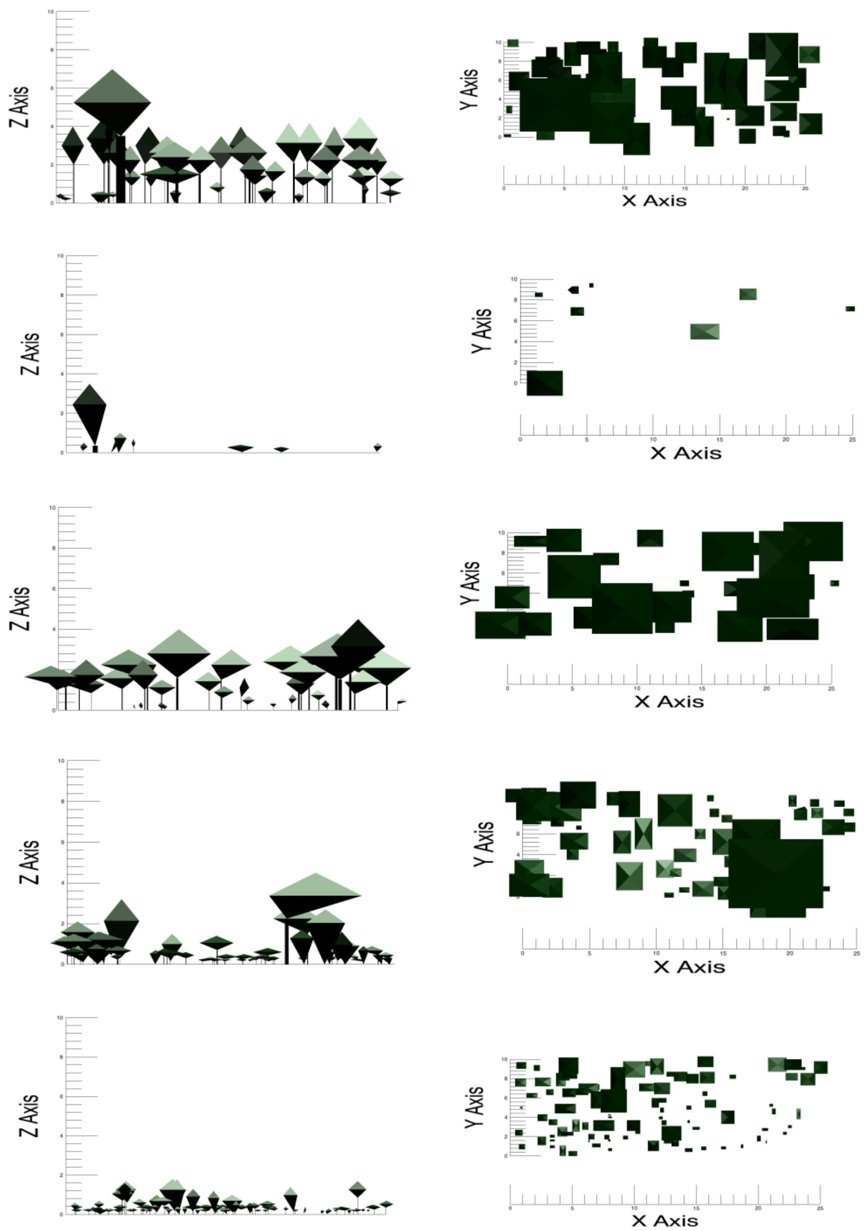

Illustration 2: Structural heterogeneity within pixel-based land-cover classes (continued).

Open treed shrubland (continued)	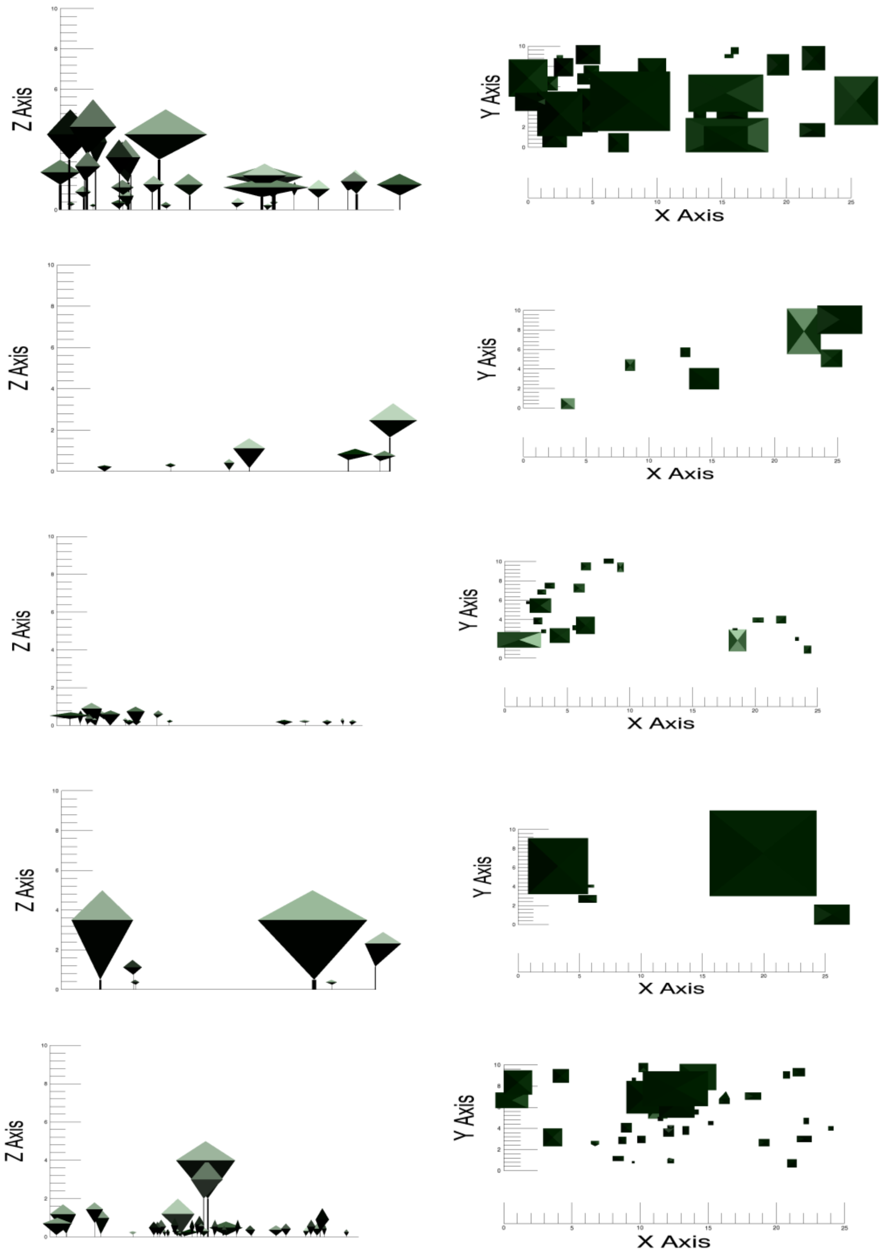

Illustration 2: Structural heterogeneity within pixel-based land-cover classes (continued).

Open treed shrubland

(continued)

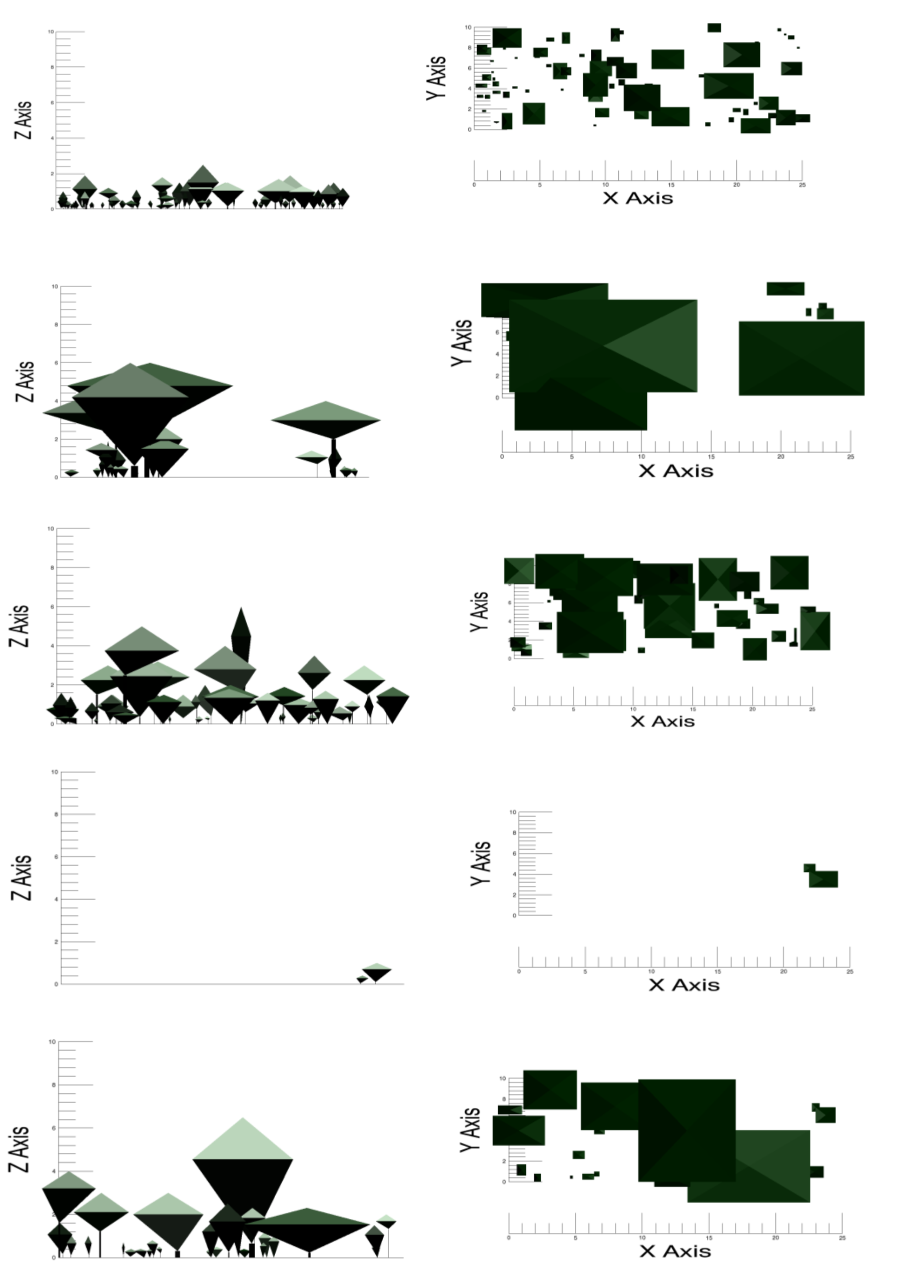

Illustration 2: Structural heterogeneity within pixel-based land-cover classes (continued).

<table>
<tr>
<td>Open treed shrubland

(continued)</td>
<td>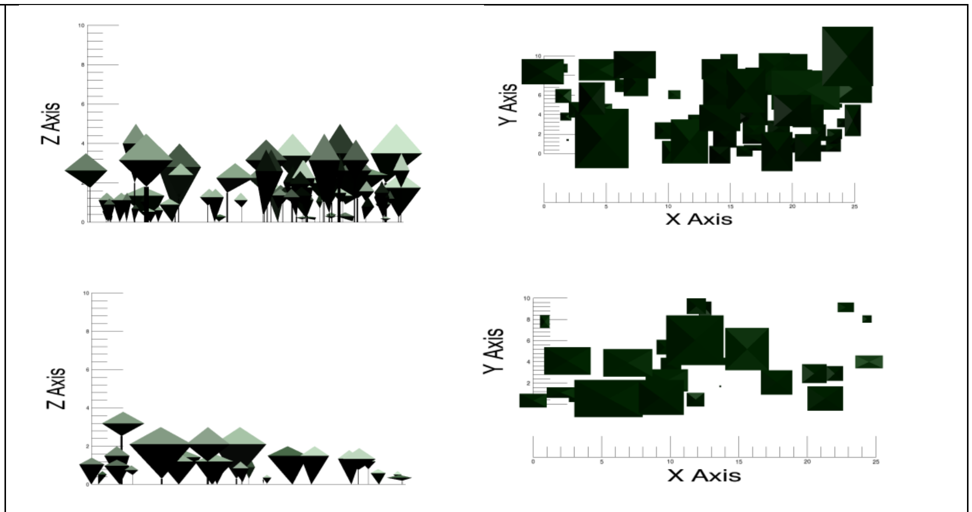
</td>
</tr>
<tr>
<td>Sparse shrubland</td>
<td>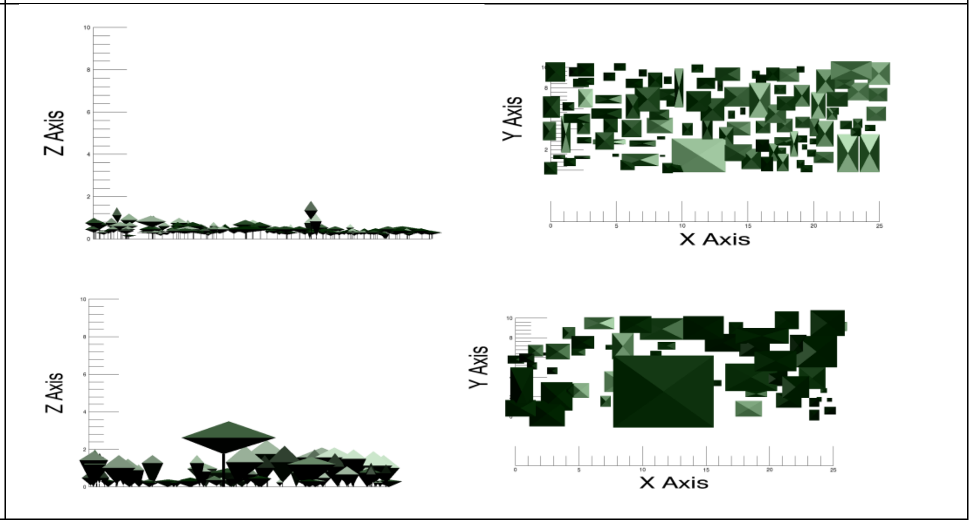
</td>
</tr>
</table>

Illustration 2: Structural heterogeneity within pixel-based land-cover classes (continued).

4.2.1 OBJECT-BASED LAND-COVER CLASSIFICATION

The classification scheme was slightly modified due to the nature of object-based classification and its ability to segment vegetation communities. Within each segment, at a segmentation level of 20, the dominant lifeform was first identified and then described in terms of its canopy cover. The second lifeform was then identified and described in terms of its cover. For example, if a community has 65% tree cover and 25% shrub cover it would be classified as Open Shrubbed Dense Woodland. If a community has 65% shrub cover and 25% tree cover it would be classified as Open Treed Dense Shrubland. This distinction from the original classification scheme does a better job of describing the vegetation structure and the balance between trees and shrubs.

TREE DOMINATED		
TREE COVER	SHRUB COVER	CLASSIFICATION
80 - 100 %	< 5 %	Closed woodland
	5 - 19 %	Sparsely shrubbed closed woodland
	20 - 49 %	Openly shrubbed closed woodland
	50+ %	Densely shrubbed closed woodland
50 - 79 %	< 5 %	Dense woodland
	5 - 19 %	Sparsely shrubbed dense woodland
	20 - 49 %	Openly shrubbed dense woodland
	50+ %	Densely shrubbed dense woodland
20 - 49 %	< 5 %	Open woodland
	5 - 19 %	Sparsely shrubbed open woodland
	20 - 49 %	Openly shrubbed open woodland
5 - 19 %	< 5 %	Sparsely treed grassland
	5 - 19 %	Sparsely shrubbed sparse woodland
SHRUB DOMINATED		
SHRUB COVER	TREE COVER	CLASSIFICATION
80 - 100 %	< 5 %	Closed shrubland
	5 - 19 %	Sparsely treed closed shrubland
	20 - 49 %	Openly treed closed shrubland
	50+ %	Densely treed closed shrubland
50 - 79 %	< 5 %	Dense shrubland
	5 - 19 %	Sparsely treed dense shrubland
	20 - 49 %	Openly treed dense shrubland
	50+ %	Densely treed dense shrubland
20 - 49 %	< 5 %	Open shrubland
	5 - 19 %	Sparsely treed open shrubland
	20 - 49 %	Openly treed open shrubland
5 - 19 %	< 5 %	Sparsely shrubbed grassland
	5 - 19 %	Sparsely treed sparse shrubland
GRASS DOMINATED		
TREE COVER	SHRUB COVER	CLASSIFICATION
< 5 %	< 5 %	Grassland
5 - 19 %	< 5 %	Sparsely treed grassland
< 5 %	5 - 19 %	Sparsely shrubbed grassland
BARELAND		
TREE COVER	SHRUB COVER	CLASSIFICATION
< 2 %	< 2 %	Bareland

Table 2: Land-cover classification scheme for modified object-based framework.

The software eCognition was used to run an object-based classification on the Landsat image (April 2009), although the image was cropped to the extent of available high resolution IKONOS imagery as opposed to the larger extent used for the pixel-based classification. This was done as the high resolution image was used to identify land cover types within the modified classification scheme. The object-based classification was not done with the high resolution imagery in order to maintain the ability to compare results with the pixel-based classification afterwards. All bands were given equal weight at a segmentation level of 10 with 0.5 weight for shape and 0.2 weight for compactness. This resulted in a total of 2658 segments classified into 13 land-cover types (openly shrubbed dense woodland, sparsely treed open shrubland, etc.) and 3 land-use types (village areas, fields, and roads). For Figure 10, segments have been dissolved into like cover types, thus not showing individual segments in most areas. It is important to note that the modified classification scheme is more detailed, which could lower the structural accuracy score when compared to the less detailed land-cover classification used for the pixel-based classification. Note the ability to classify village settlement areas and fields (which was problematic for the pixel-based classification).

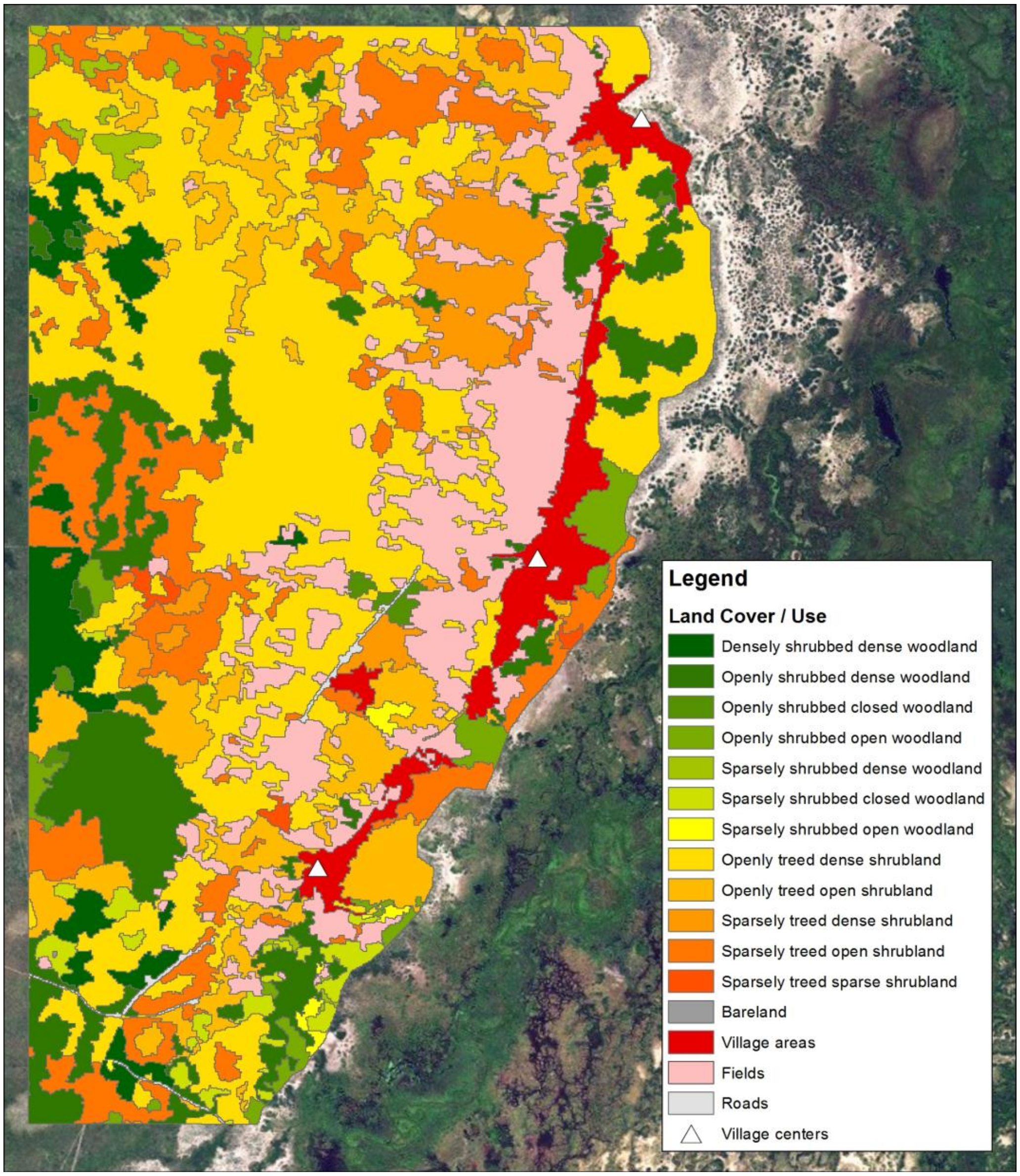

Figure 10: Object-based land-cover classification (base imagery from GeoEye / ESRI).

4.2.2 Structural Heterogeneity within the Object-based Land-cover Classification

Plots within each land-cover type (derived from the Landsat object-based land-cover classification) were visually compared in terms of vegetation structure using IDL visualizations (illustration 3). Note that although structural heterogeneity still exists within each object-based land-cover class, it is significantly less than within the pixel-based land-cover classes (reference illustration 2).

Object-based land-cover class	**Plots within each object-based land-cover class (top and side view)**
Openly shrubbed closed woodland	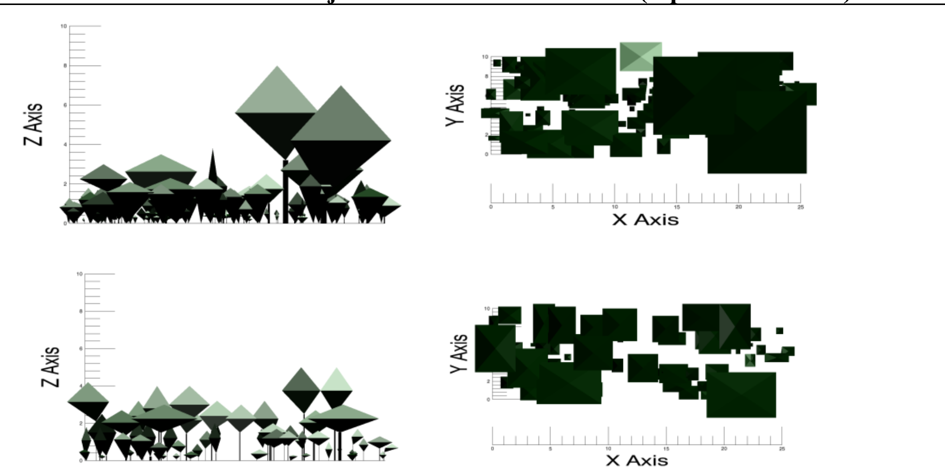
Openly shrubbed dense woodland	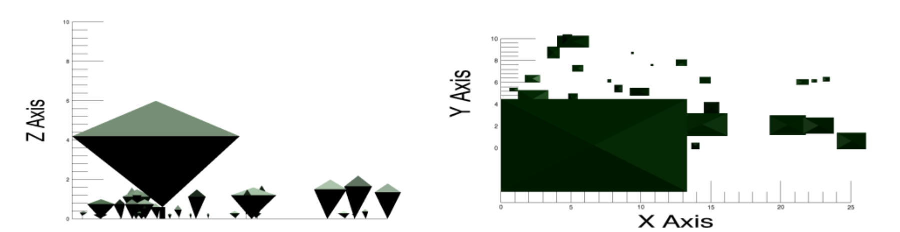

Illustration 3: Structural heterogeneity within object-based land-cover classes.

Openly shrubbed dense woodland (continued)	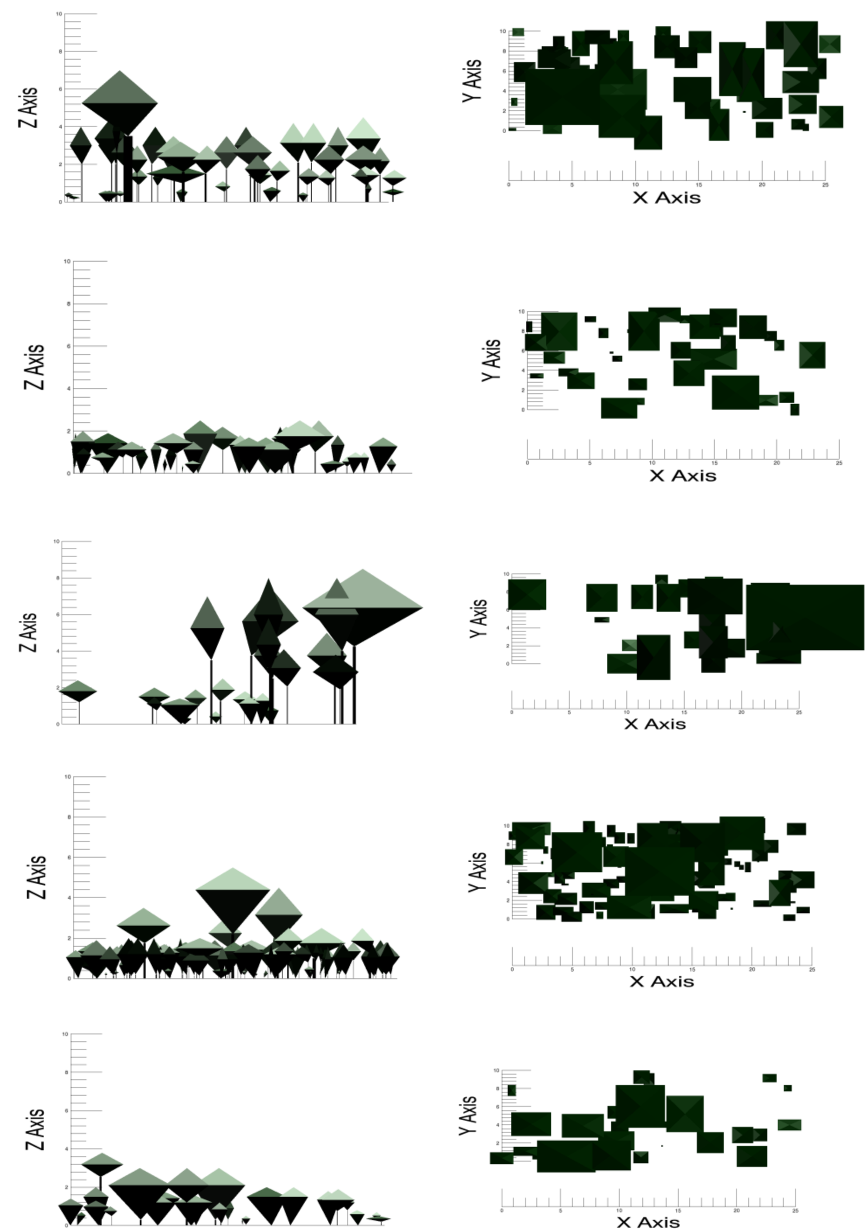

Illustration 3: Structural heterogeneity within object-based land-cover classes (continued).

Openly shrubbed dense woodland

(continued)

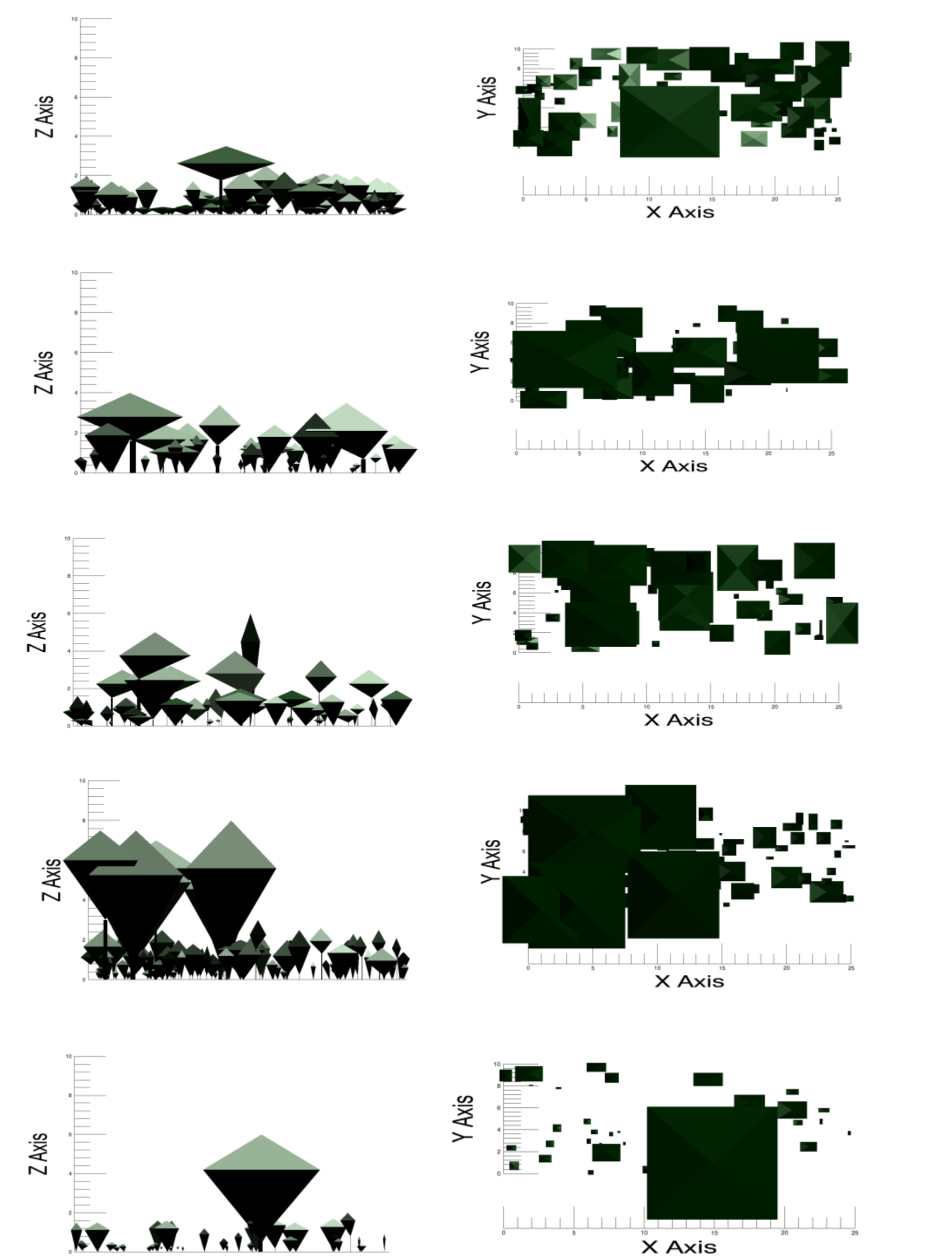

Illustration 3: Structural heterogeneity within object-based land-cover classes (continued).

Openly shrubbed open woodland	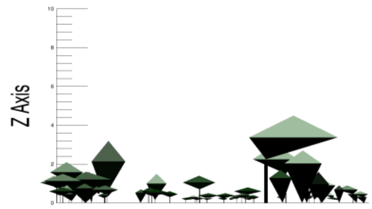	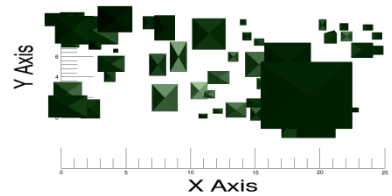
Sparsely shrubbed dense woodland		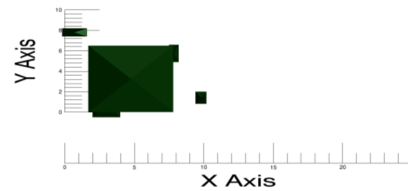
Sparsely shrubbed open woodland	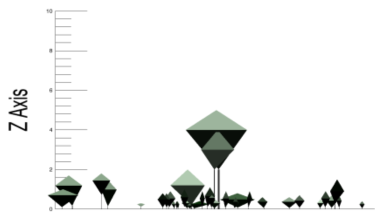	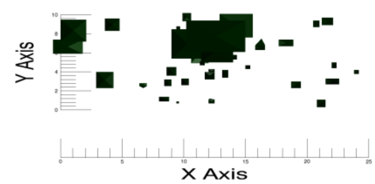
	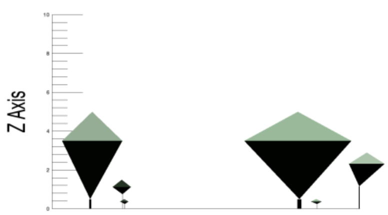	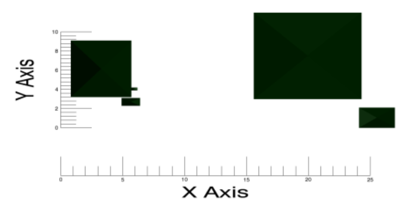
Openly treed dense shrubland	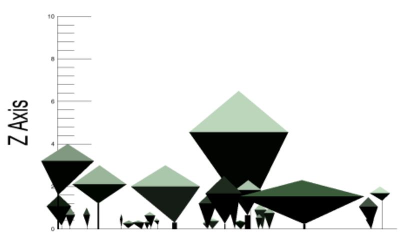	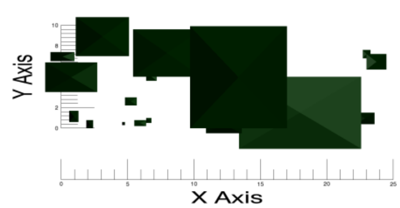

Illustration 3: Structural heterogeneity within object-based land-cover classes (continued).

Openly treed dense shrubland

(continued)

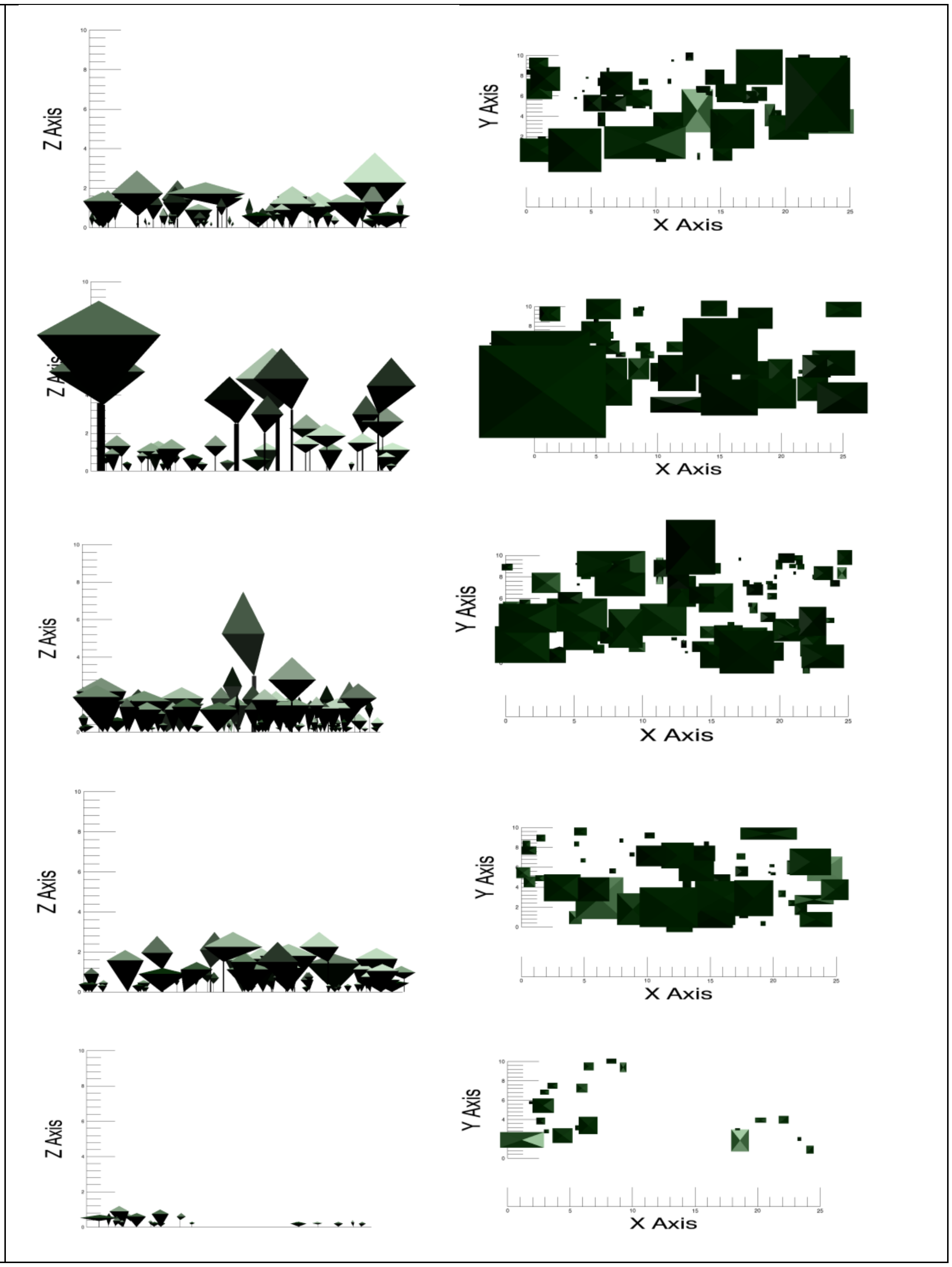

Illustration 3: Structural heterogeneity within object-based land-cover classes (continued).

Openly treed dense shrubland (continued)	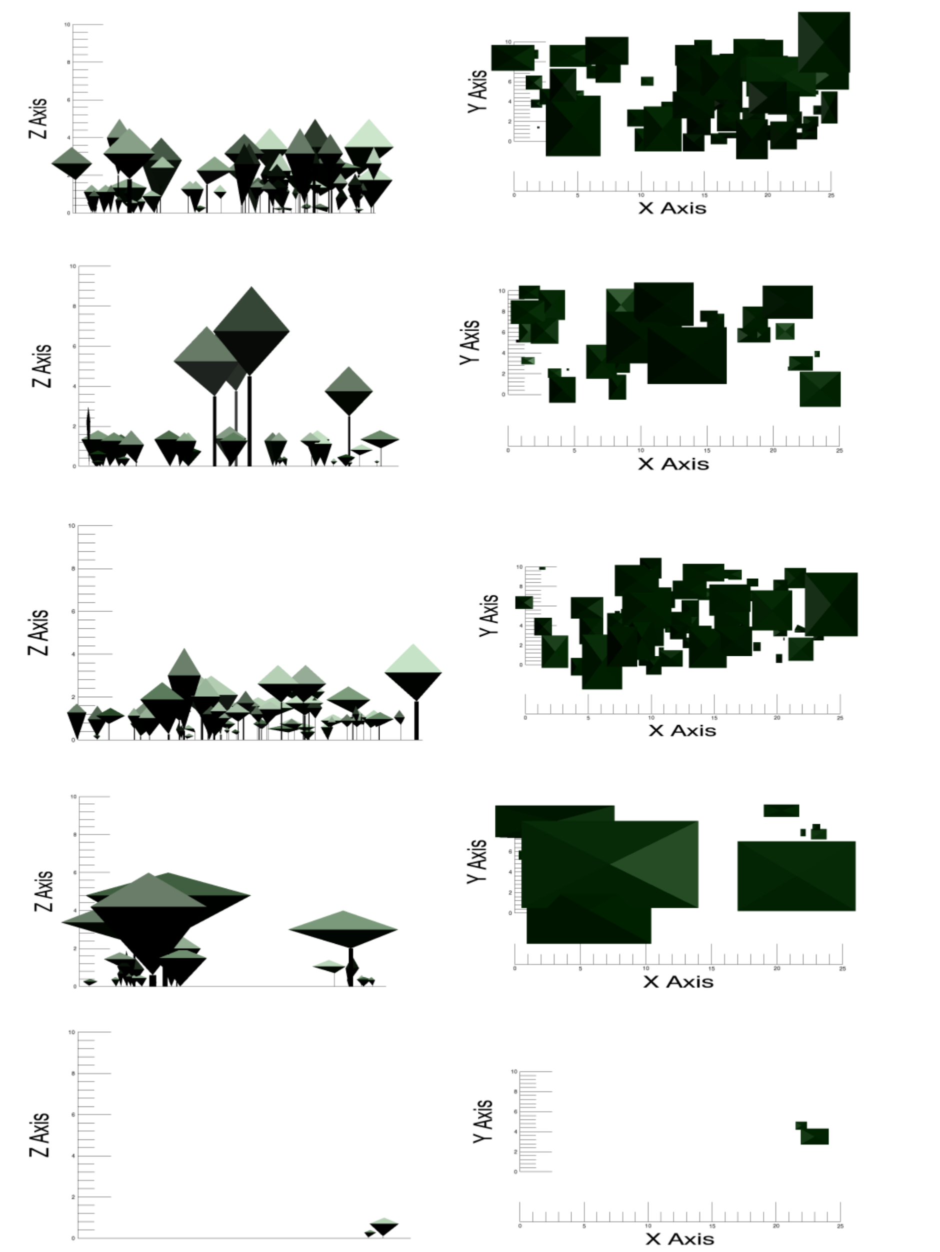

Illustration 3: Structural heterogeneity within object-based land-cover classes (continued).

Openly treed open shrubland

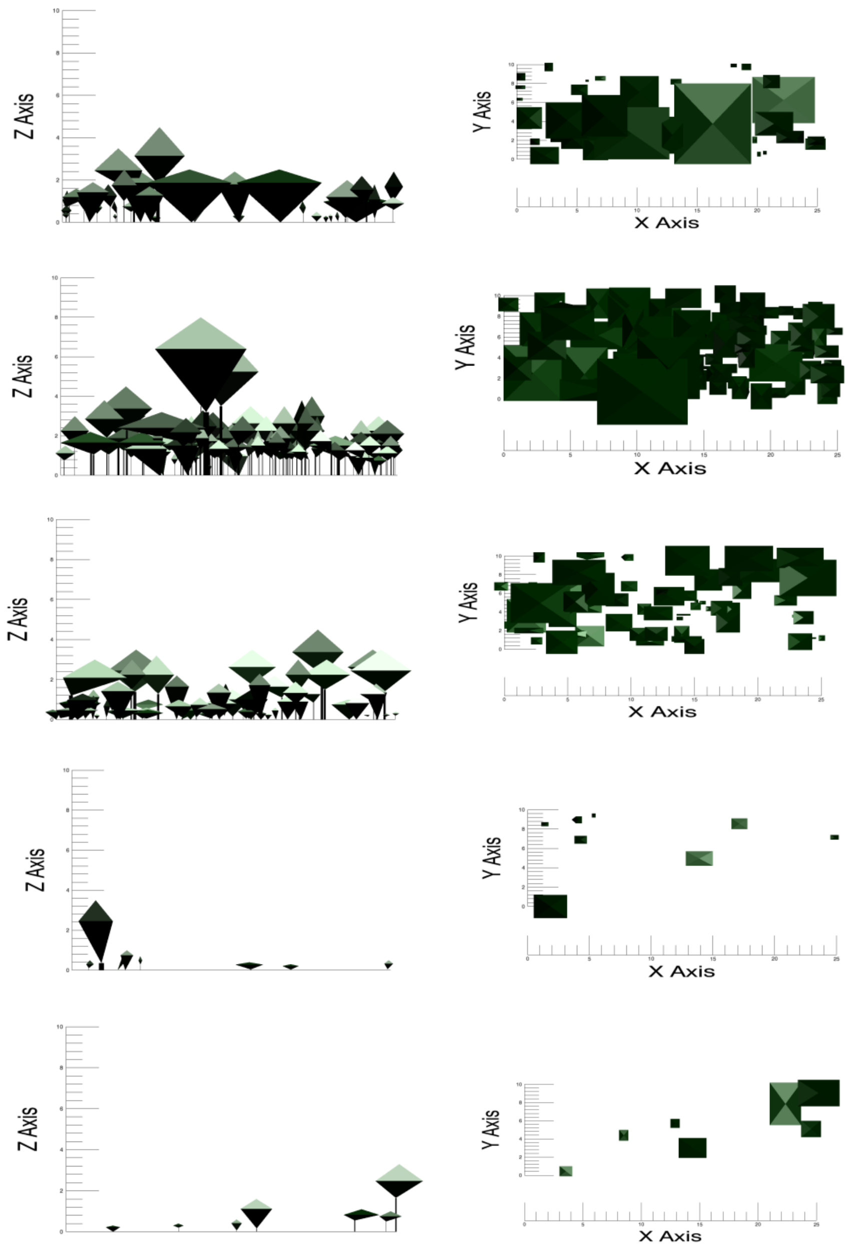

Illustration 3: Structural heterogeneity within object-based land-cover classes (continued).

Openly treed open shrubland (continued)	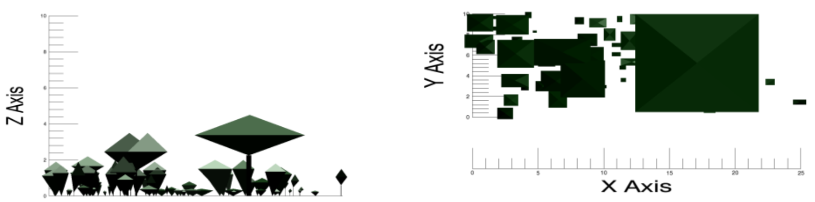
Sparsely treed dense shrubland	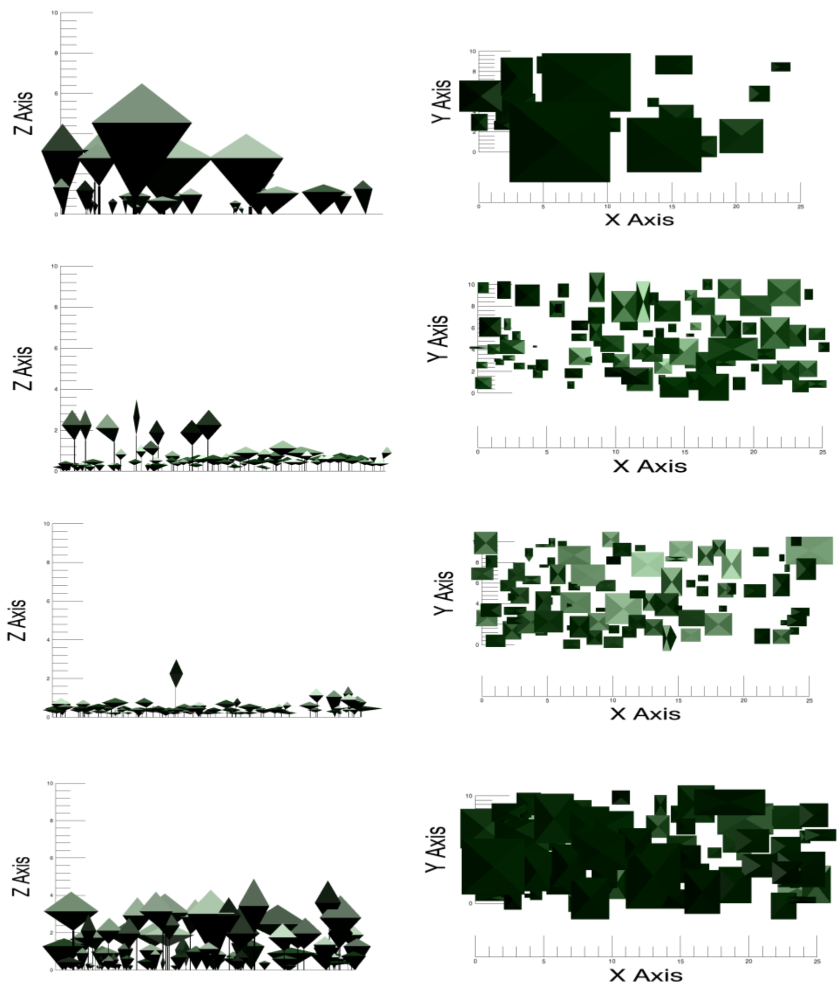

Illustration 3: Structural heterogeneity within object-based land-cover classes (continued).

Sparsely treed dense shrubland (continued)	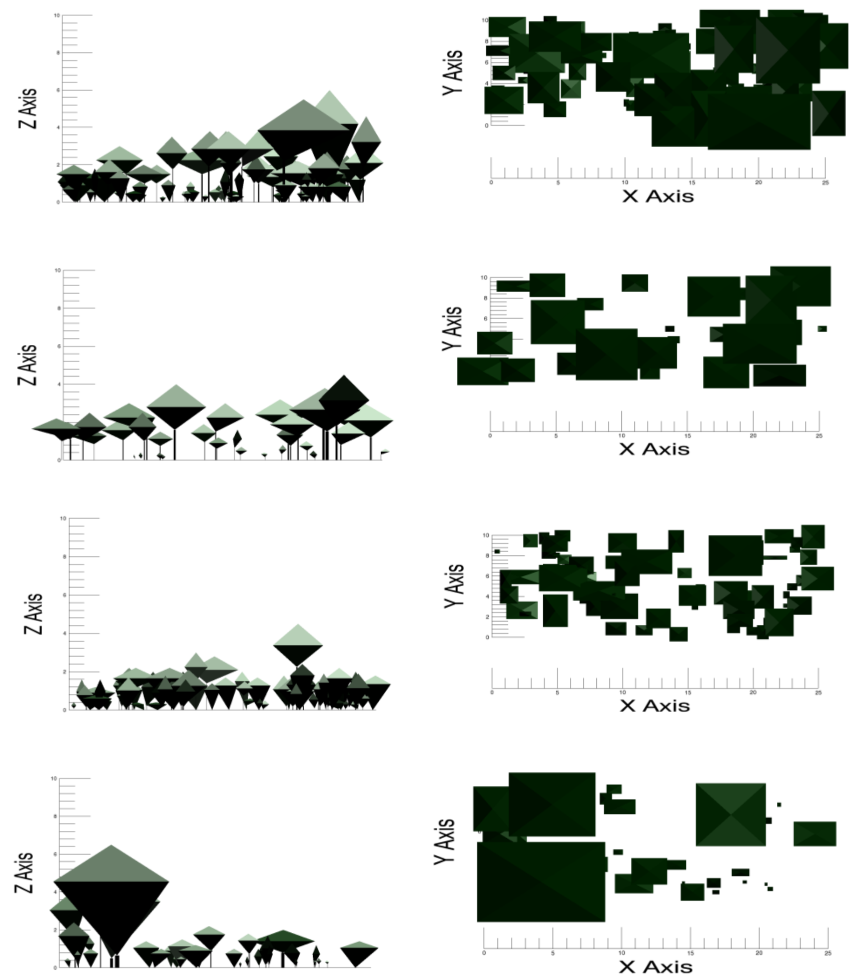
Sparsely treed open shrubland	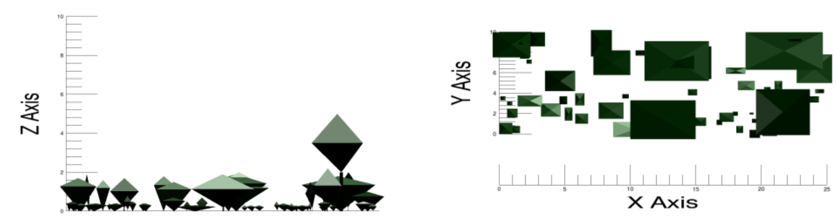

Illustration 3: Structural heterogeneity within object-based land-cover classes (continued).

Sparsely treed open shrubland (continued)	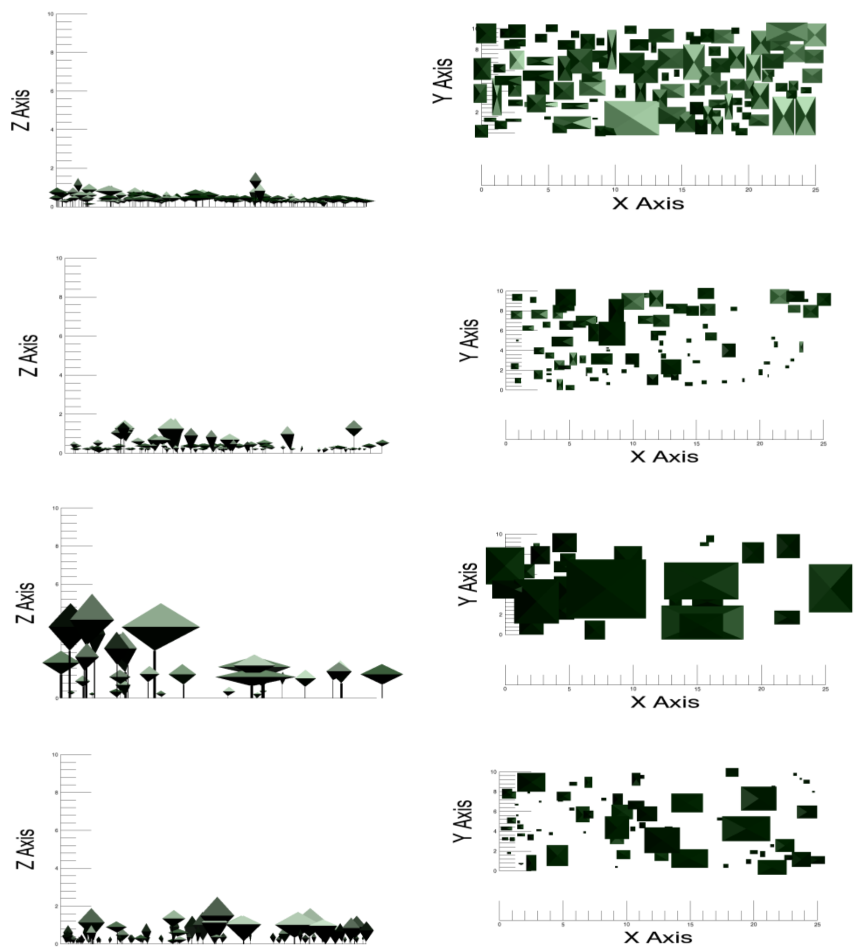

Illustration 3: Structural heterogeneity within object-based land-cover classes (continued).

4.3.1 Structural Vegetation Categories (SVCs)

Structural variables from plot data were used in a classification and regression tree (CART) to determine statistical splits in the data and create structural vegetation categories (SVCs) as a result. The CART analysis resulted in 10 structural categories with multiple structural variables; number of individuals, height category 1 (below 0.5

m), height category 2 (0.5 m to 2 m), height category 3 (above 2 m), stem category 3 (6 to 20 stems), and stem category 4 (20+ stems).

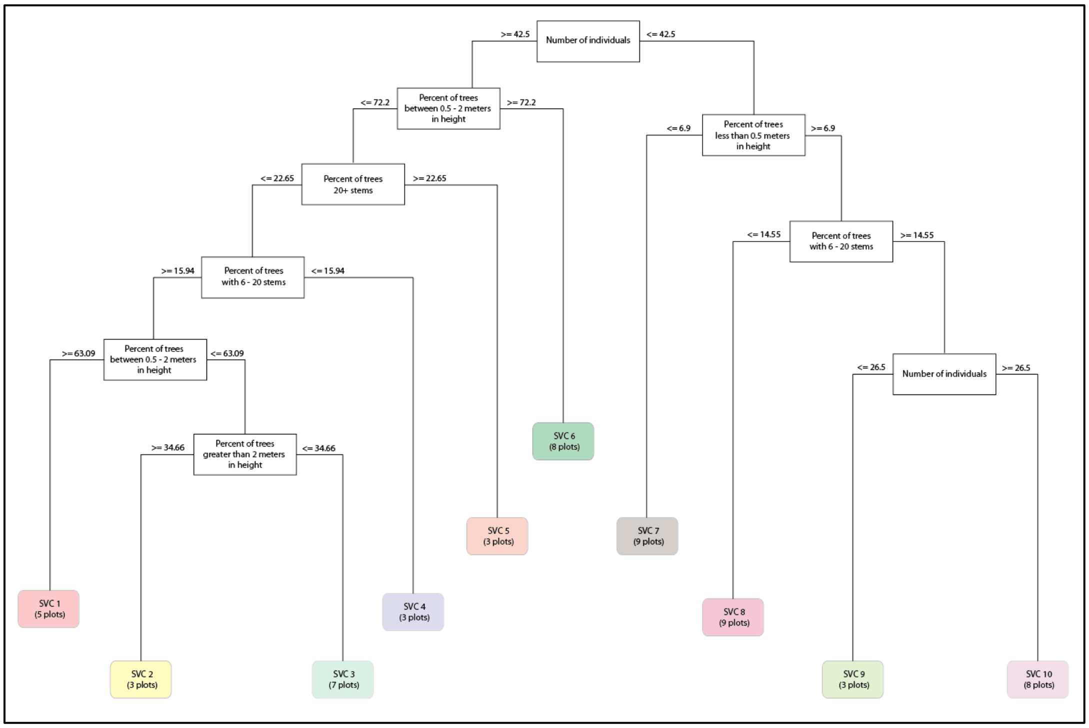

Figure 11: Classification and Regression Tree

The categories are summarized in the table 3 below. Each CART category (SVC) contains plots with unique structural characteristics. In addition, each SVC identified a relatively unique species composition thus confirming the strength of the CART method. Species do overlap between SVCs, but when inspected further through the IDL visualizations the morphological characteristics (e.g. height) of each species is significantly different in each SVC. This difference in structure of species between plots points to the ability of the CART method of detecting different successional stages (or various growth forms caused by disturbances) of individual species (such as

Colophospermum mopane in multi-stemmed shrub form in abandoned fields versus tall single stemmed structure in open woodland).

	Structural Characteristics	Plots within each SVC	Genus composition (over 10% listed)
CART Category 1	> 42 individuals 63 - 72% medium trees < 22% 20+ stems > 15 % 6-20 stems	t1p4, t1p6, t1p7, t2p3, t2p8	Colophospermum, Baphia
CART Category 2	> 42 individuals < 63% medium trees < 22% 20+ stems > 15 % 6-20 stems > 34% tall trees	t1p3, t1p9	Colophospermum, Dichrostachys
CART Category 3	> 42 individuals < 63% medium trees < 22% 20+ stems > 15 % 6-20 stems < 34 % tall trees	t3p2, t3p3, t3p6, t3p7, t4p2, t5p8, t7p3	Baphia, Combretum, Terminalia
CART Category 4	> 42 individuals < 72% medium trees < 22% 20+ stems < 15 % 6-20 stems	t5p2, t5p5, t6p7	Terminalia, Acacia, Grewia
CART Category 5	> 42 individuals < 72% medium trees > 22% 20+ stems	t3p9, t8p3, t8p4	Colophospermum, Baphia, Bauhinia
CART Category 6	> 42 individuals > 72% medium trees	t2p2, t5p6, t6p10, t6p11, t7p6, t8p8, t9p3	Mundulea, Grewia, Dichrostachys, Baphia, Lonchocarpus
CART Category 7	< 42 individuals < 7 % small trees	t1p5, t2p5, t3p8, t6p5, t7p9	Baphia, Grewia, Colophospermum
CART Category 8	< 42 individuals > 7 % small trees < 14 % trees with 6-20 stems	t2p4, t4p6, t5p12, t6p3, t6p6, t9p2	Terminalia, Mundulea, Combretum, Acacia
CART Category 9	< 26. 5 individuals > 7 % small trees > 14 % trees with 6-20 stems	t6p4, t8p2	Grewia, Gymnosporia, Acacia
CART Category 10	27 - 42 individuals > 7 % small trees > 14 % trees with 6-20 stems	t6p9, t8p5, t8p6, t9p4, t9p5, t9p6, t9p7, t9p8	Grewia, Acacia, Baphia, Combretum

Table 3: Characteristics and composition of CART SVCs.

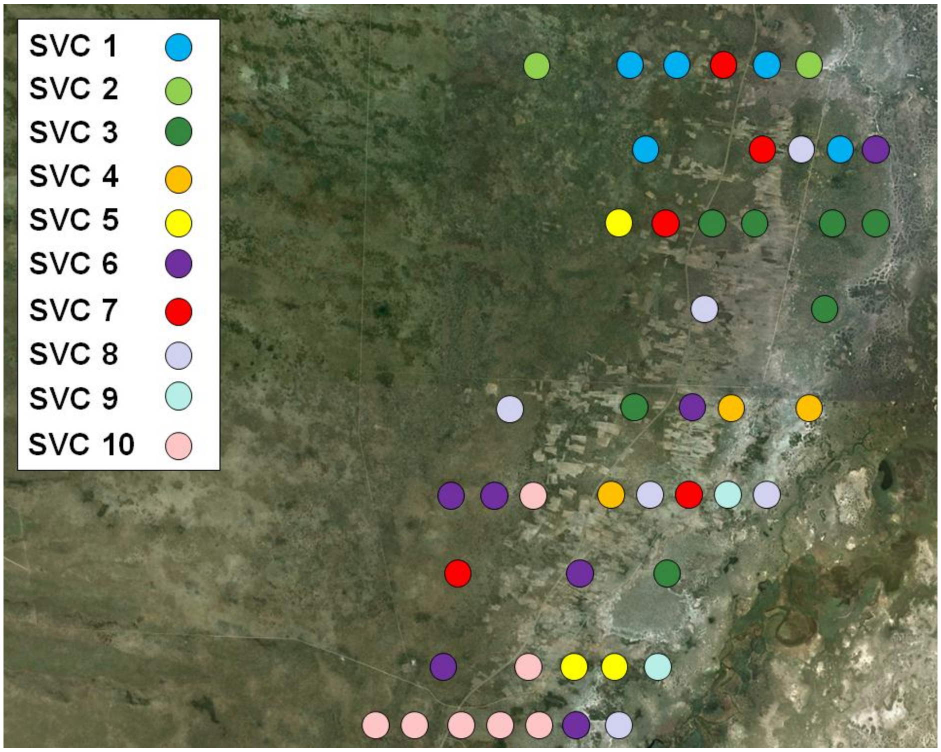

Figure 12: Spatial locations of structural vegetation categories.

Note that several SVCs are found throughout the study area (such as SVC 6 and SVC 7), while others are exclusively found towards the North (such as SVC 1 and SVC 2) and others towards the South (such as SVC 10).

4.3.2 Structural Heterogeneity within SVCs

Plots within each SVC were compared in terms of vegetation structure using IDL visualizations in the illustration below (illustration 4). Note that the plots are now grouped based on statistical similarities in regards to structural variables and are not necessarily close to each other spatially. The structural heterogeneity is therefore minimized when compared to illustrations 2 and 3.

Structural Vegetation Category	**Plots within each SVC (side and top view)**
SVC 1	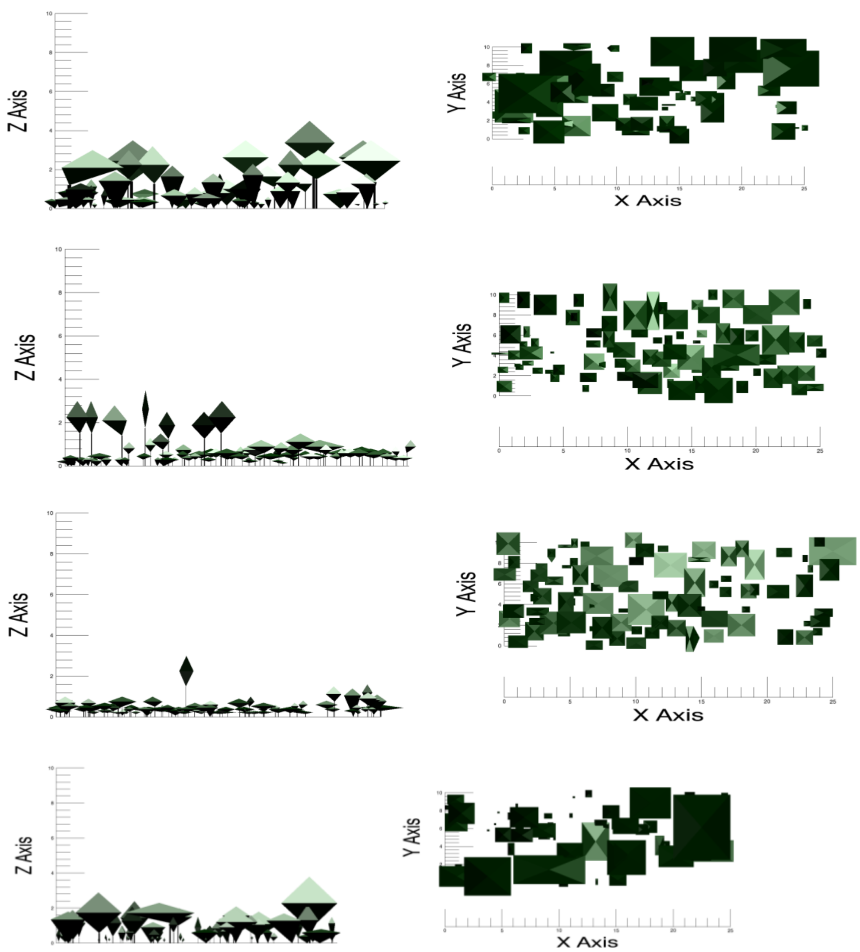

Illustration 4: Structural heterogeneity within structural vegetation categories (SVCs).

SVC 1 (continued)	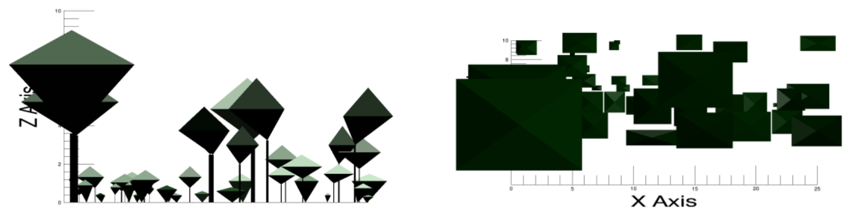
SVC 2	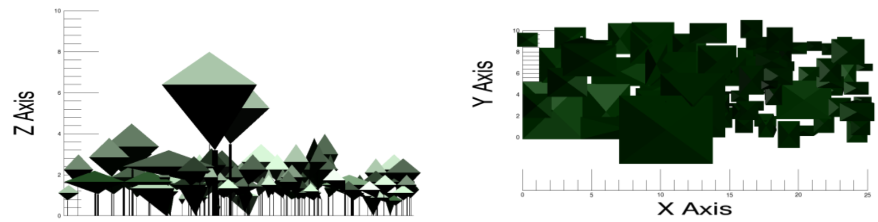 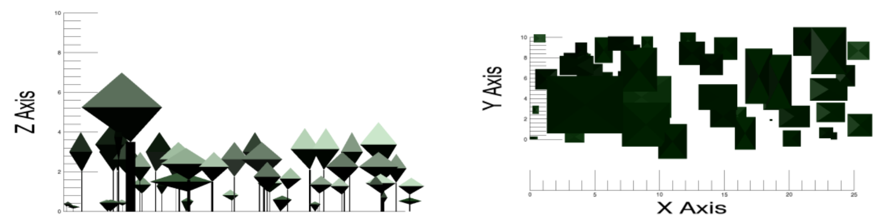
SVC 3	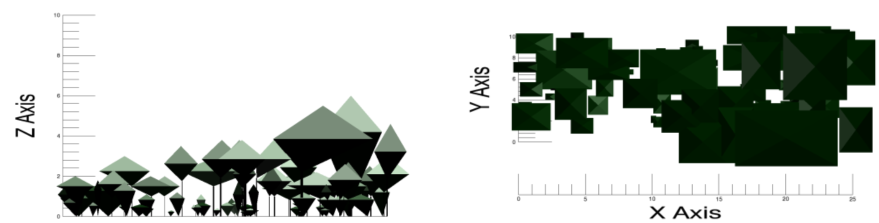 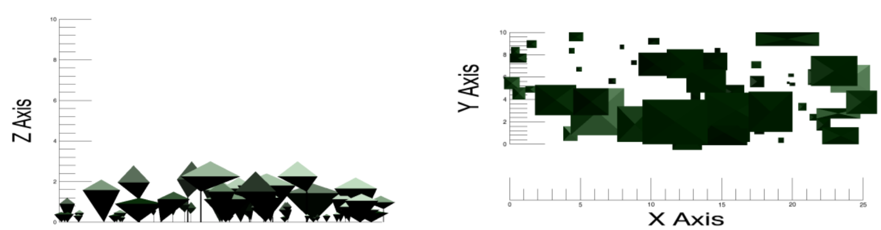

Illustration 4: Structural heterogeneity within structural vegetation categories (SVCs) (continued).

SVC 3 (continued)	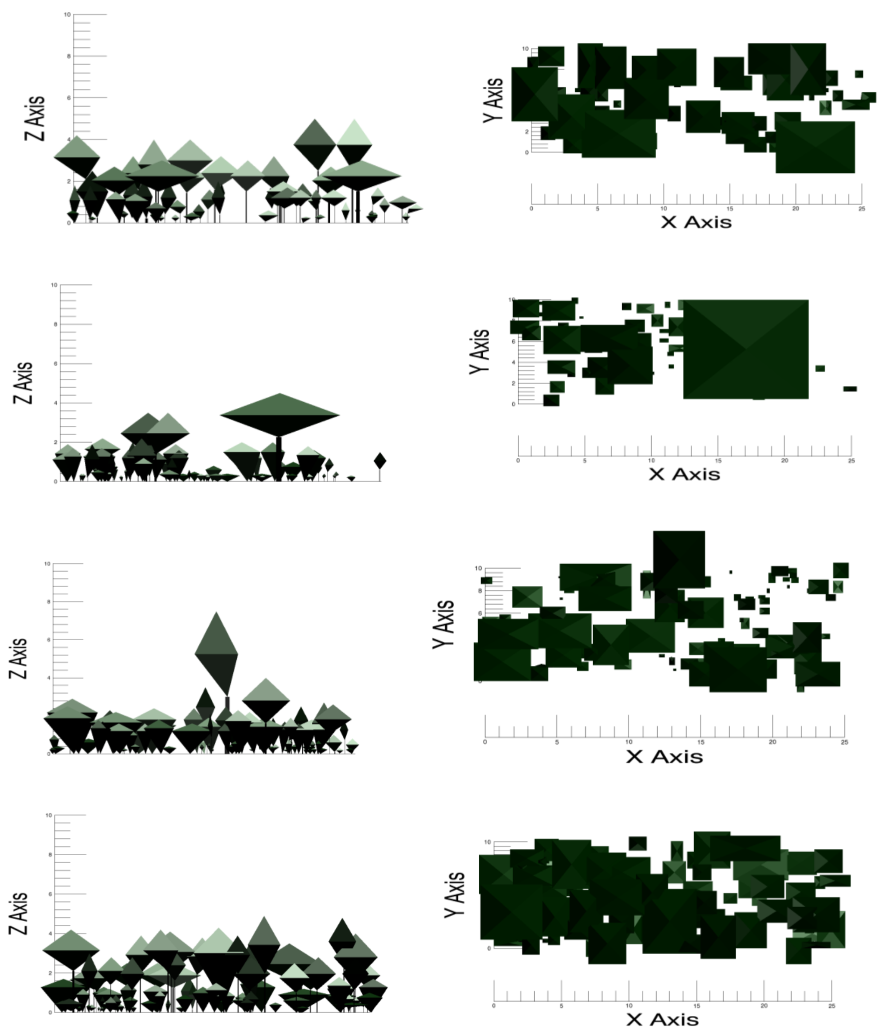
SVC 4	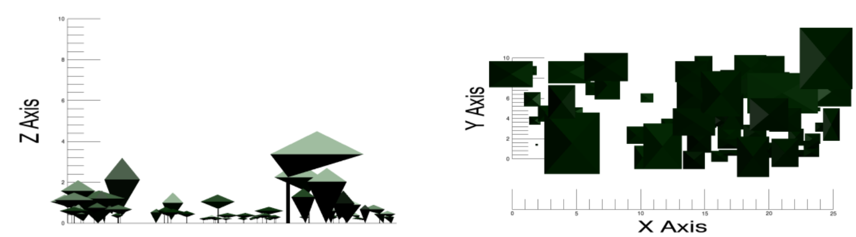

Illustration 4: Structural heterogeneity within structural vegetation categories (SVCs) (continued).

SVC 4 (continued)	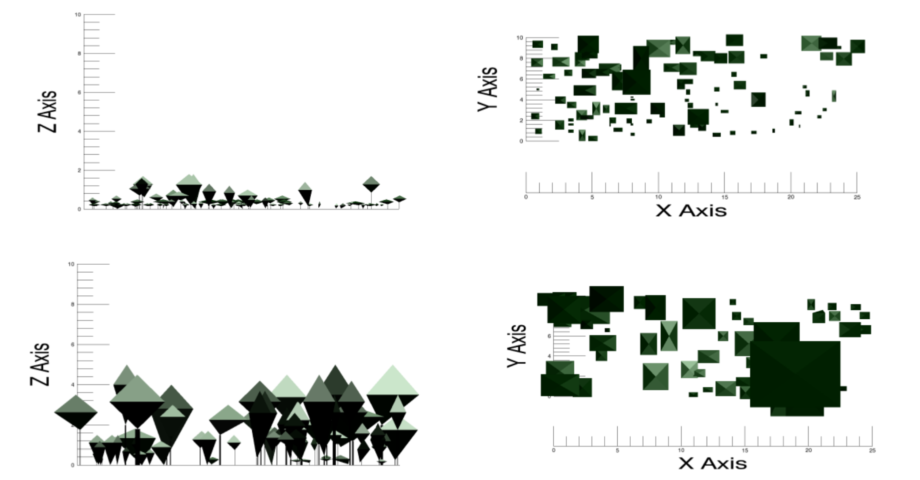
SVC 5	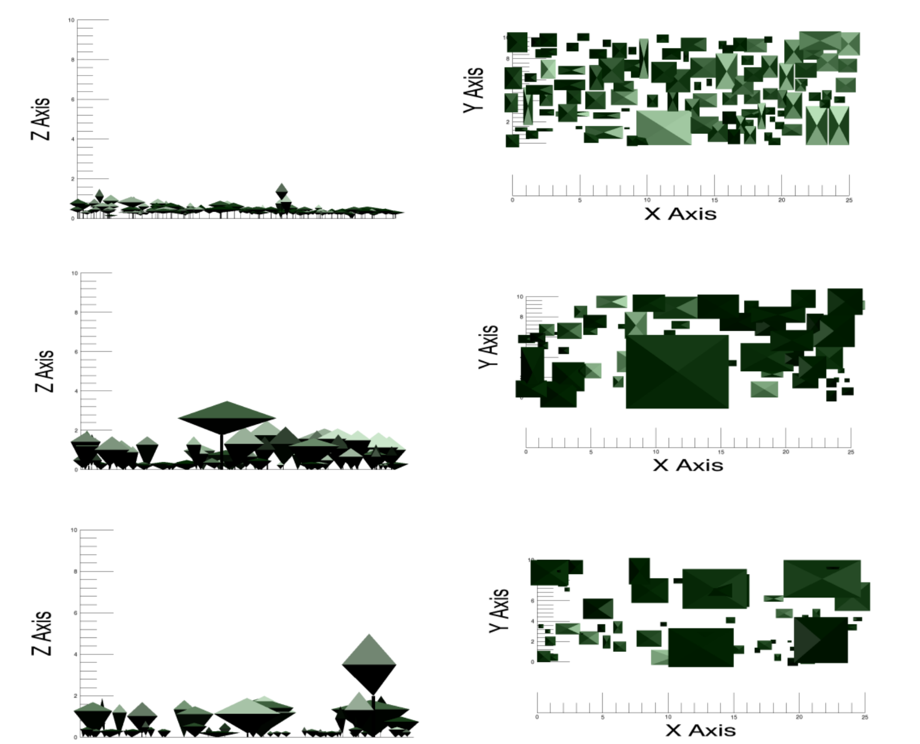

Illustration 4: Structural heterogeneity within structural vegetation categories (SVCs) (continued).

SVC 6

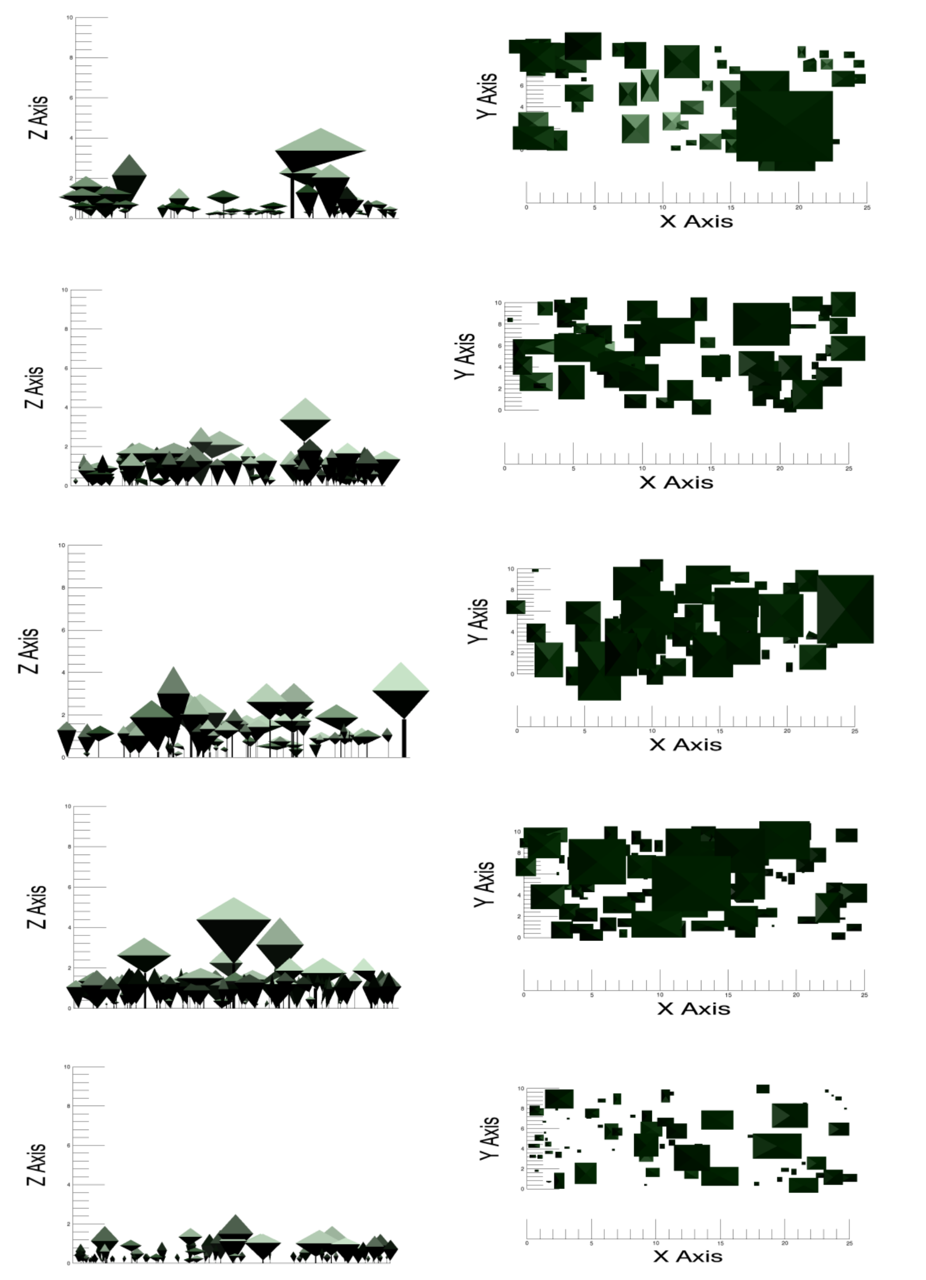

Illustration 4: Structural heterogeneity within structural vegetation categories (SVCs) (continued).

<table>
<tr>
<td>SVC 6

(continued)</td>
<td>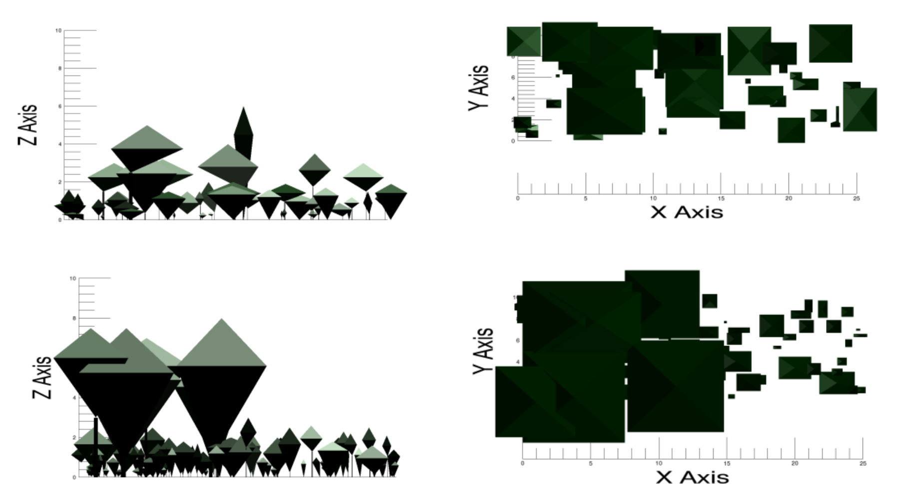
</td>
</tr>
<tr>
<td>SVC 7</td>
<td>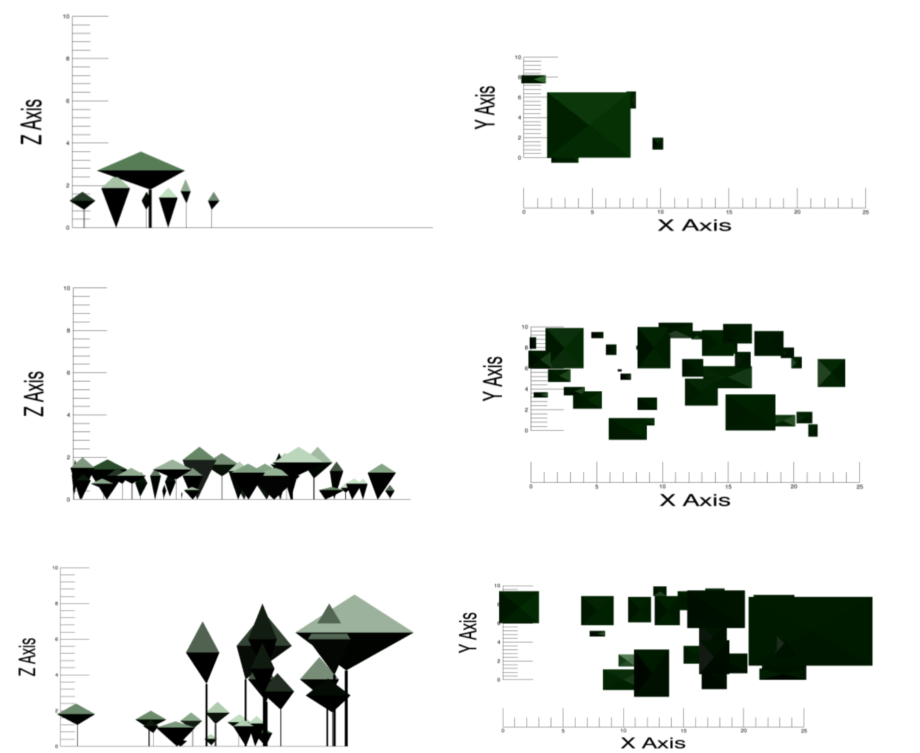
</td>
</tr>
</table>

Illustration 4: Structural heterogeneity within structural vegetation categories (SVCs) (continued).

SVC 7

(continued)

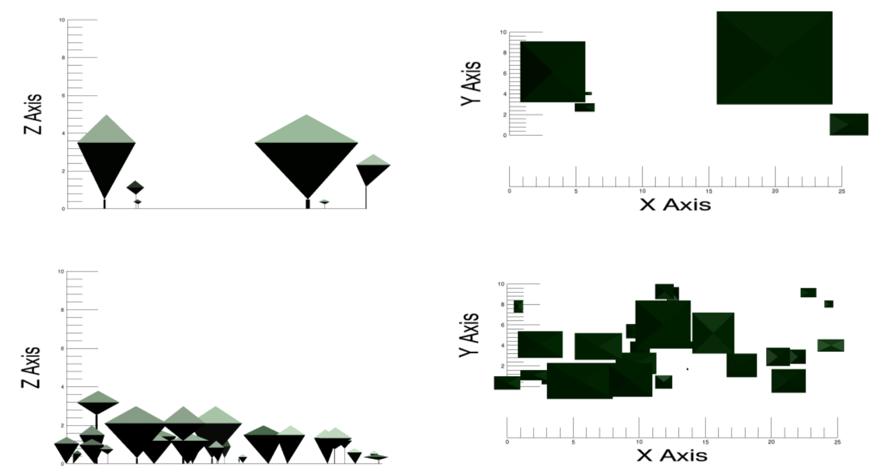

SVC 8

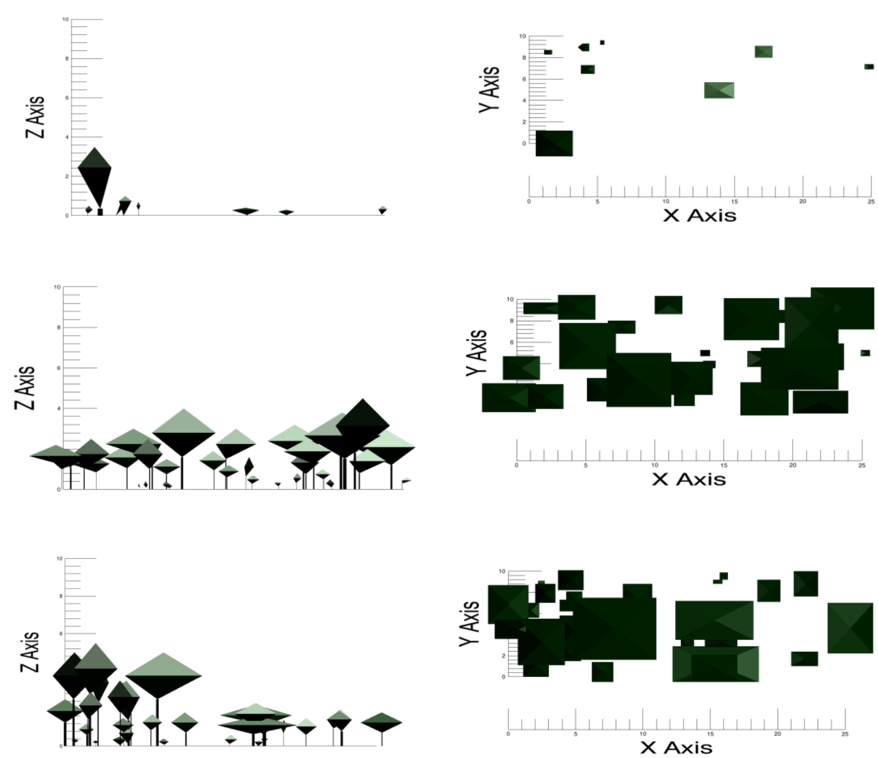

Illustration 4: Structural heterogeneity within structural vegetation categories (SVCs) (continued).

SVC 8 (continued)	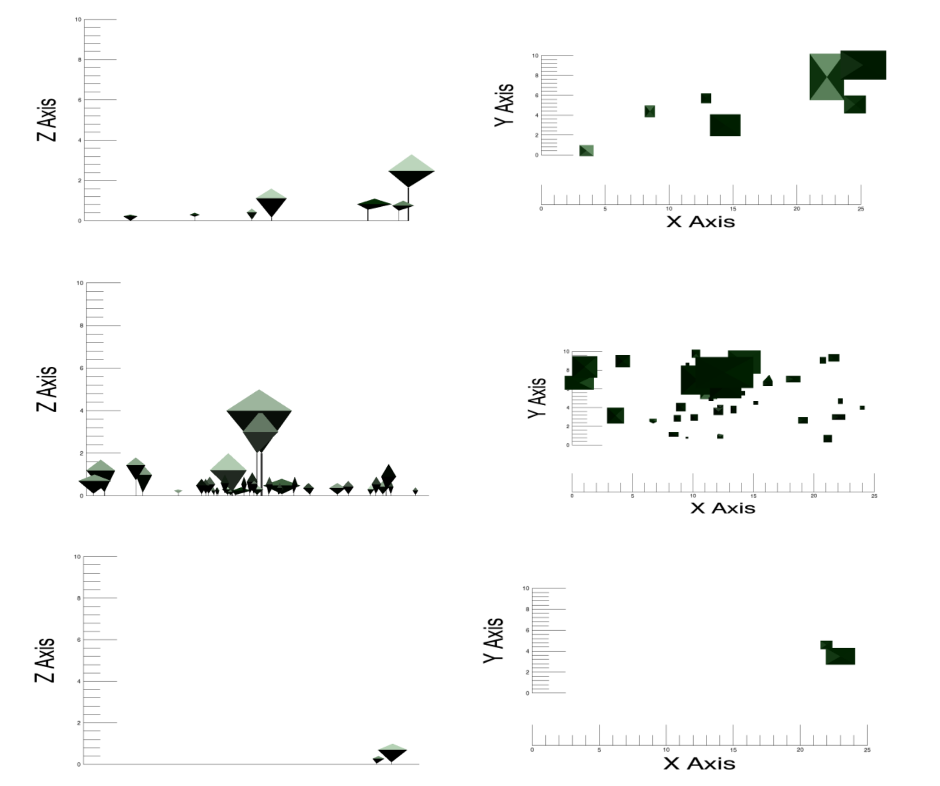
SVC 9	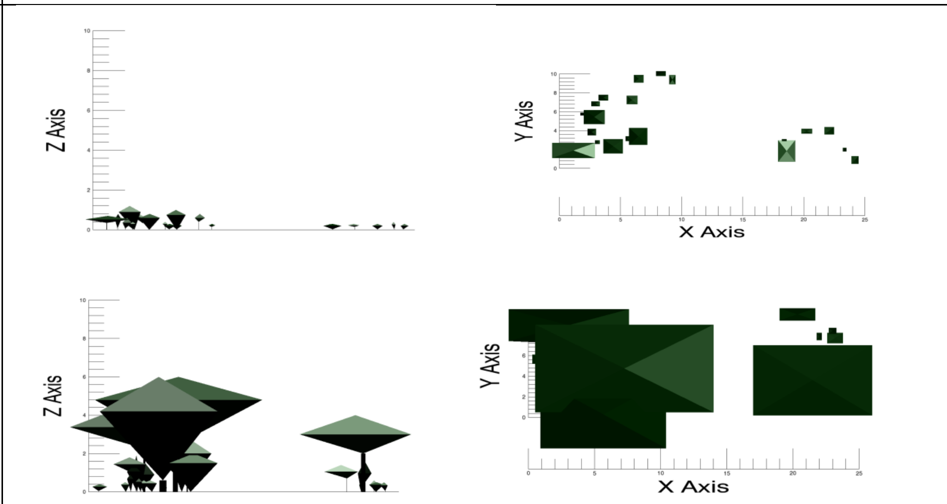

Illustration 4: Structural heterogeneity within structural vegetation categories (SVCs) (continued).

SVC 10	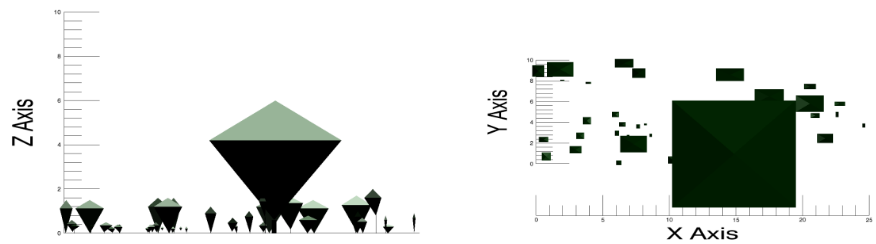

Illustration 4: Structural heterogeneity within structural vegetation categories (SVCs) (continued).

4.4 ACCURACY ASSESSMENT OF CLASSIFICATION METHODS

Accuracy assessment was conducted for each plot based on its IDL visualization, pixel-based land-cover class, and object-based land-cover class. The pixel- and object-based land-cover class was given an accuracy ranking per plot based on their ability to describe the vegetation structure in the IDL visualization for that plot, using the thematic linguistic system ranking system in Table 4, modified from Gopal and Woodcock (1994) and Woodcock and Gopal (2000) in order to better account for uncertainty in both the classification and accuracy assessment processes (Woodcock 2002).

Rank	Description
2	The land-cover class best describes the observed vegetation structure
1	The land-cover class could be understood as describing the observed vegetation structure
-1	The land-cover class does not describe the observed vegetation structure
-2	The land-cover class absolutely does not describe the observed vegetation structure

Table 4: Accuracy assessment ranking system (modified from Gopal and Woodcock 1994 and Woodcock and Gopal 2000)

The sum of the classification scores of each plot for each method then served as a proxy for classification accuracy. The pixel-based classification method had a total classification score of 24 while the object-based classification method had a total classification score of 32 (see appendix 1).

The relative and absolute accuracy for each classification was assessed in order to gain insight into when each land-cover classification performed well. The relative agreement of the ranking between the pixel- and object-based land-cover classifications tested whether the two land-cover classifications agreed when describing the vegetation structure (irrelevant if a classification is accurate when compared to the ground truth). The agreement assessment was split into five categories: (1) when the pixel-based classification describes the vegetation as woodland, (2) when the object-based classification describes the vegetation as woodland, (3) when the pixel-based classification describes the vegetation as shrubland, (4) when the object-based classification describes the vegetation as shrubland, and (5) assessment for all classes over both methods. The correlation factors were then calculated between the classification ranking scores of plots within each category (see table 5 below).

When described as woodland, both the pixel- and object-based classification ranking scores were slightly negatively correlated (-0.18 and -0.13 respectively), which means that the two classification types tended to disagree in woodland environments. This disagreement is likely due to classifying trees as shrubs or vice versa, which for example can lead to classifying a dense woodland as a dense shrubland. When described as shrubland, both the pixel- and object-based classification ranking scores were strongly positively correlated (0.54 and 0.64 respectively), which means that the two classification types tend to agree in shrubland environments.

Comparison→ Classified ↓	W_{PB}	W_{OB}	S_{PB}	S_{OB}
W_{PB}	*1.00*	-0.18	---	---
W_{OB}	-0.13	*1.00*	---	---
S_{PB}	---	---	*1.00*	0.54
S_{OB}	---	---	0.64	*1.00*
	C*, Overall (all classes, both methods)			**0.40**

Table 5: Relative agreement between the pixel- and object-based classifications.

(PB = pixel-based, OB = object-based, W = woodland, S = shrubland, W_{PB} = Woodland, pixel-based, W_{OB} = Woodland, object-based, S_{PB} = Shrubland, pixel-based, S_{OB} = Shrubland, object-based, C_* = All classes, both methods).

Second, the absolute agreement of the ranking between the pixel- and object-based land-cover classifications was assessed. This ranking tests how accurately each type of land-cover classification classified vegetation structure (using IDL visualizations as ground truth). It also identifies how correlated the ranking scores of the object-based classification was when the pixel-based classification was correct, and vice versa. The object-based classification outperformed the pixel-based classification (70.83% versus 64.58% accuracy respectively) when tested across all plots. The object-based classification tended to agree with the pixel-based when the pixel-based classification was correct. The pixel-based tended to disagree with the object-based when the object-based classification was correct. For woodland areas, the pixel-based classification outperformed the object-based classification (90.91% versus 76.47% accuracy respectively). However, the object-based classification had a larger percentage of ranking scores of 2 (versus ranking scores of 1) than the pixel-based classification, which indicates that the object-based described the vegetation structure better when the classification is correct.

The pixel-based and object-based classifications were both expected to perform well in woodland environments. The pixel-based classification should perform well as woodlands are both spatially and spectrally clustered. The object-based classification should perform well as it should be able to identify woodland areas easily as object due to their spectra and texture characteristics. However, the object-based classification classified 13 out of 17 plots correctly as woodland. The four misclassified plots exhibited two primary mistakes. First, shrubs were misidentified as trees and the plot was therefore classified as woodland. Second, plots having relatively low number of trees but with extremely large canopies led to their classification as woodland. Another parameter to further explore is the level of segmentation, which for this work was relatively high. I hypothesize that the object-based classification would perform better at finer segmentation scales as it would allow the classification to detect more detailed changes in canopy cover.

The object-based classification outperformed the pixel-based classification (67.74% versus 56.76% accuracy respectively) in shrubland areas. This matches the expected result, although both of these numbers were lower than anticipated. The spatial heterogeneity of shrublands, in combination with the relative coarse nature of the land-cover classifications (30 x 30 meter), were likely problematic for both land-cover classifications. Again, increasing the segmentation level for the object-based classification is likely to increase its accuracy. Spatial heterogeneity may particularly cause problems for pixel-based classification as variation can be larger within classes than among classes. When incorrect, the object-based classification exhibited three main mistakes. First, trees were misidentified as shrubs and the plot was therefore classified as shrubland. Second, sparse plots were classified as dense and vice versa- third, dense plots were classified as sparse. These last two mistakes could be due to spatial and structural heterogeneity caused by the placement of plots in openings within otherwise denser vegetation (or vice versa).

Method	**Accuracy**
W_{PB}	90.91
W_{OB}	76.47
S_{PB}	56.76
S_{OB}	67.74
$C_{C,PB}$	64.58
$C_{C,OB}$	70.83

Table 6: Accuracy percentage of each method.

(PB = pixel-based, OB = object-based, W = woodland, S = shrubland, W_{PB} = Woodland, pixel-based, W_{OB} = Woodland, object-based, S_{PB} = Shrubland, pixel-based, S_{OB} = Shrubland, object-based, $C_{C,PB}$ = All classes correct, pixel-based, $C_{C,OB}$ = All classes correct, object-based, C_* = All classes, both methods).

The absolute agreement assessment further identifies how correlated the ranking scores of the object-based classification were with the pixel-based classification ranking scores when the pixel-based classification was correct (and vice versa). When the pixel-based classification correctly classified plots as woodland, the object-based classification tended to disagree slightly (correlation factor of -0.14). When the object-based classification correctly classified plots as woodland, the pixel-based classification tended to strongly disagree (correlation factor of -0.5). When the pixel-based classification correctly classified plots as shrubland, the object-based classification tended to agree relatively strongly (correlation factor of 0.37). When the object-based classification correctly classified plots as shrubland, the pixel-based classification tended to agree (correlation factor of 0.13). When the pixel-based classification correctly classified plots in either environment, the object-based classification tends to agree (correlation factor of 0.14). However, when the object-based classification correctly classified plots in either environment, the pixel-based classification tends to moderately disagree (correlation factor of -0.22). This is reflected in the higher overall accuracy of the object-based classification, as it classified correctly when (and therefore disagreed with) the pixel-based classification misclassified.

Comparison → Correct ↓	W_{PB}	W_{OB}	S_{PB}	S_{OB}	$C_{C,PB}$	$C_{C,OB}$
W_{PB}	*1.00*	-0.14	---	---	---	---
W_{OB}	-0.50	*1.00*	---	---	---	---
S_{PB}	---	---	*1.00*	0.37	---	---
S_{OB}	---	---	0.13	*1.00*	---	---
$C_{C,PB}$	---	---	---	---	*1.00*	0.14
$C_{C,OB}$	---	---	---	---	-0.22	*1.00*
		C_*, Overall (all classes, both methods)				**0.40**

Table 7: Absolute agreement between the pixel- and object-based classifications.

(PB = pixel-based, OB = object-based, W = woodland, S = shrubland, W_{PB} = Woodland, pixel-based, W_{OB} = Woodland, object-based, S_{PB} = Shrubland, pixel-based, S_{OB} = Shrubland, object-based, $C_{C,PB}$ = All classes correct, pixel-based, $C_{C,OB}$ = All classes correct, object-based, C_* = All classes, both methods).

4.5.1 Linking Land-cover with Structural Vegetation Categories

The land-cover classifications were related spatially with the SVCs in order to attribute the broader area in terms of quantifiable vegetation structure. Ideally, plots with the same SVC would all fall within the same land-cover class. The locations of SVCs were compared to both the pixel-based and object-based land cover classifications. As shown in table 8 below, multiple SVCs fall within each pixel-based land-cover class (e.g., seven SVCs fall within the open treed shrubland land-cover class). No plots fall within the sparse treed shrubland and open shrubland land-cover classes.

Pixel-based land-cover classification	Plot	Structural vegetation category
Dense shrubbed woodland	T1P6	1
	T2P8	1
	T1P3	2
	T3P7	3
	T2P2	6
	T3P8	7
	T8P5	10
Dense treed shrubland	T1P7	1
	T2P3	1
	T3P2	3
	T3P3	3
	T3P6	3
	T4P2	3
	T5P8	3
	T7P3	3
	T8P4	5
	T5P6	6
	T6P10	6
	T6P11	6
	T2P5	7
	T6P9	10
	T8P6	10
	T9P5	10
	T9P6	10
Dense woodland	T9P3	6
Open shrubbed woodland	T1P4	1
	T9P7	10
	T9P8	10
Open treed shrubland	T1P9	2
	T5P2	4
	T5P5	4
	T6P7	4
	T7P6	6
	T8P8	6
	T1P5	7
	T6P5	7
	T7P9	7
	T2P4	8
	T4P6	8
	T5P12	8
	T6P3	8
	T6P6	8
	T9P2	8
	T6P4	9
	T8P2	9
	T9P4	10
Sparse shrubland	T3P9	5
	T8P3	5

Table 8: Ability of linking pixel-based land-cover classes with SVCs.

A majority type attribution could be used to assign a single SVC to each land cover (see table 9). This process, however, ignores the structural heterogeneity found within each land-cover class and thus simplifies the vegetation structure for the broader area. Such simplification misrepresents niche differences, abiotic factors (which determine structure), and available resources.

Pixel-based land-cover classification	**Dominant structural vegetation category**
Dense shrubbed woodland	SVC 1
Dense shrubbed shrubland	SVC 3
Dense woodland	SVC 6
Open shrubbed woodland	SVC 10
Open treed shrubland	SVC 8
Sparse shrubland	SVC 5

Table 9: Majority-rule SVC to land-cover attribution.

As shown in table 10 below, multiple SVCs fall within each object-based land-cover class (e.g., five SVCs fall within the openly shrubbed dense woodland land-cover class). As before, land-cover classes and SVCs are not mutually exclusive. The overlap, however, is smaller than when using a pixel-based classification.

Object-based land-cover classification	Plot	Structural vegetation category
Openly shrubbed closed woodland	T5P8	3
	T2P2	6
Openly shrubbed dense woodland	T1P9	2
	T8P3	5
	T6P11	6
	T8P8	6
	T9P3	6
	T2P5	7
	T3P8	7
	T7P9	7
	T8P5	10
	T9P7	10
	T9P8	10
Openly shrubbed open woodland	T5P2	4
Openly treed dense shrubland	T2P3	1
	T2P8	1
	T3P2	3
	T3P3	3
	T4P2	3
	T6P7	4
	T6P10	6
	T9P2	8
	T6P4	9
	T8P2	9
	T6P9	10
	T9P4	10

Object-based land-cover classification	Plot	Structural vegetation category
Open treed open shrubland	T1P4	1
	T1P3	2
	T7P3	3
	T2P4	8
	T6P3	8
	T8P6	10
Sparsely shrubbed dense woodland	T1P5	7
Sparsely shrubbed dense woodland	T6P5	7
	T6P6	8
Sparsely treed dense shrubland	T1P6	1
	T1P7	1
	T3P6	3
	T3P7	3
	T5P6	6
	T4P6	8
	T9P5	10
	T9P6	10
Sparsely treed open shrubland	T5P5	4
	T3P9	5
	T8P4	5
	T7P6	6
	T5P12	8

Table 10: Ability of linking object-based land-cover classes with SVCs.

Chapter 5: Conclusion and Future Directions

This thesis proposed a protocol to 1) assess the structural heterogeneity within pixel- and object-based land-cover classifications using three-dimensional IDL vegetation visualizations, 2) leveraging field data, IDL visualizations, and CART results 3) to generate structural vegetation categories, and 4) to discern the ability of detecting structural vegetation categories through land-cover classifications, both pixel- and object-based, for non-sampled areas.

A pixel-based land-cover classification was performed on a Landsat TM 5 image based on the classification scheme presented by Grunblatt et al. (1989) resulting in 9 land-cover types over the Etsha region (approximately 1125 km2). The classification identified dense woodlands across longitudinal dunes in the backcountry (EbR) and agricultural fields were primarily classified as sparse shrublands. An object-based land-cover classification was performed on a subset of the same image (as high-resolution IKONOS imagery was not available for the entire ExR area, which was used as a reference in the classification) using a modified classification scheme to describe both trees and shrubs in terms of percent cover resulting in 16 land-cover classes. The classification was able to detect highly accurate representations of agricultural fields and village settlement areas, a necessity within the context of social-ecological systems. It must be noted that the Landsat TM 5 (April 27th, 2009) and IKONOS (October 17th, 2011) imagery were neither from the same season nor year. This difference could negatively affect the object-based classification results since the IKONOS image was used in the classification of the Landsat TM 5 image. The field work campaigns were conducted in June and July 2011 and 2012 further adding to the inconsistency. Future work will include acquiring additional imagery for the field work campaign dates and running the classification on those images. Accuracy assessment of methods must also be performed for non-sampled areas.

The generated three-dimensional visualizations of the vegetation structure of each field plot allow the verification of field measurements (due to notation error in the field or through data entry) and enables structural comparisons within and between plots. Locations of field plots were used as accuracy assessment for the two land-cover classifications by comparing the land-cover class to the three-dimensional visualizations of plot vegetation structure. For the pixel-based classification, woodland areas had a classification accuracy of 90.91%, shrubland areas had a classification accuracy of 56.76%, and the overall classification accuracy was 64.58% across all plots. For the object-based classification, woodland areas had a classification accuracy of 76.47%, shrubland areas had a classification accuracy of 67.58%, and the overall classification accuracy was 70.83% across all plots.

Structural vegetation categories (total of 10 categories) were created based on morphological characteristics of field plots using CART analysis. While this method was successful in classifying field plots based on vegetation structure, the aim of using this method for disturbance detection is currently unclear. Future work will involve the creation of a consistent (since the CART analysis is dependent on the input variables) manual classification tree in order to track both pixels and objects (or patches) through time (after Crews-Meyer 2001, 2002) and thus enable the detection of changes from one SVC to another through time, better facilitating causal assessment such as different types, magnitudes, or frequencies of disturbances.

The structural heterogeneity across plots within the same land-cover (for both pixel- and object-based classifications) class was assessed visually using the three-dimensional visualizations of the vegetation structure. The object-based classification showed significantly lower structural heterogeneity than the pixel-based classification, as was hypothesized. However, some plots within the same object-based land-cover class (particularly for shrubland areas) were misclassified, resulting in the accuracy percentages mentioned above. The SVCs were successful in categorizing vegetation structure as they showed the lowest structural heterogeneity (compared to the land-cover classification) when assessed in the same fashion. However, the SVCs were not mutually exclusive to land-cover classes, which means additional efforts are required to link SVCs with land-cover classes in order to be able to derive quantifiable structural information from land-cover classifications.

In order to place this work fully within the context of social-ecological systems it needs to be related to human land-use explicitly. During the field campaigns, semi-structured interviews were also conducted across the Etsha settlements. These interviews currently under analysis (see Shinn et al. 2014) will hopefully reveal insights into how people in this region use their environment to sustain their livelihoods, seasonality of livelihoods, and livelihood strategies to cope with environmental uncertainty (e.g. years of low rainfall or high flood level). These data must be compared to land-cover classification and (CART and manually based) structural vegetation categories, particularly with regards to reports of which and what percentage livelihoods are based on veld products and which veld products are most commonly collected and from where. In addition, considerations must be made for developing a new land-use land-cover classification scheme designed specifically for use within the context of social-ecological system studies. Results will then be able to inform future sampling designs and method protocols in spatio-temporally heterogeneous landscapes.

Appendices

APPENDIX 1: CLASSIFICATION SCORES FOR THE PIXEL- AND OBJECT-BASED CLASSIFICATIONS

Plot	Pixel-based land-cover	Classification score	Object-based land-cover	Classification score
t1p3	Dense Shrubbed Woodland	2	Openly treed open shrubland	-2
t1p4	Open Shrubbed Woodland	-1	Openly treed open shrubland	1
t1p5	Open Treed Shrubland	-1	Sparsely shrubbed dense woodland	-2
t1p6	Dense Shrubbed Woodland	1	Sparsely treed dense shrubland	2
t1p7	Dense Treed Shrubland	2	Sparsely treed dense shrubland	2
t1p9	Open Treed Shrubland	-2	Openly shrubbed dense woodland	2
t2p2	Dense Shrubbed Woodland	2	Openly shrubbed closed woodland	1
t2p3	Dense Treed Shrubland	1	Openly treed dense shrubland	2
t2p4	Open Treed Shrubland	-1	Openly treed open shrubland	-2
t2p5	Dense Treed Shrubland	1	Openly shrubbed dense woodland	1
t2p8	Dense Shrubbed Woodland	2	Openly treed dense shrubland	1
t3p2	Dense Treed Shrubland	2	Openly treed dense shrubland	2
t3p3	Dense Treed Shrubland	-2	Openly treed dense shrubland	-1
t3p6	Dense Treed Shrubland	-2	Sparsely treed dense shrubland	-2
t3p7	Dense Shrubbed Woodland	2	Sparsely treed dense shrubland	-1
t3p8	Dense Shrubbed Woodland	1	Openly shrubbed dense woodland	1
t3p9	Sparse Shrubland	-2	Sparsely treed open shrubland	-1
t4p2	Dense Treed Shrubland	2	Openly treed dense shrubland	1
t4p6	Open Treed Shrubland	1	Sparsely treed dense shrubland	1
t5p12	Open Treed Shrubland	1	Sparsely treed open shrubland	1
t5p2	Open Treed Shrubland	1	Openly shrubbed open woodland	2
t5p5	Open Treed Shrubland	1	Sparsely treed open shrubland	1
t5p6	Dense Treed Shrubland	2	Sparsely treed dense shrubland	2
t5p8	Dense Treed Shrubland	-1	Openly shrubbed closed woodland	2
t6p10	Dense Treed Shrubland	2	Openly treed dense shrubland	1
t6p11	Dense Treed Shrubland	2	Openly shrubbed dense woodland	1
t6p3	Open Treed Shrubland	-1	Openly treed open shrubland	-1
t6p4	Open Treed Shrubland	-2	Openly treed dense shrubland	-2
t6p5	Open Treed Shrubland	-1	Sparsely shrubbed open woodland	2
t6p6	Open Treed Shrubland	2	Sparsely shrubbed open woodland	2
t6p7	Open Treed Shrubland	-2	Openly treed dense shrubland	-1
t6p9	Dense Treed Shrubland	2	Openly treed dense shrubland	2
t7p3	Dense Treed Shrubland	2	Openly treed open shrubland	2
t7p6	Open Treed Shrubland	-1	Sparsely treed open shrubland	2
t7p9	Open Treed Shrubland	1	Openly shrubbed dense woodland	-1
t8p2	Open Treed Shrubland	-1	Openly treed dense shrubland	1
t8p3	Sparse Shrubland	-2	Openly shrubbed dense woodland	2
t8p4	Dense Treed Shrubland	2	Sparsely treed open shrubland	2
t8p5	Dense Shrubbed Woodland	2	Openly shrubbed dense woodland	2
t8p6	Dense Treed Shrubland	2	Openly treed open shrubland	1
t8p8	Open Treed Shrubland	-1	Openly shrubbed dense woodland	2
t9p2	Open Treed Shrubland	-2	Openly treed dense shrubland	-2
t9p3	Dense Woodland	1	Openly shrubbed dense woodland	2
t9p4	Open Treed Shrubland	1	Openly treed dense shrubland	1
t9p5	Dense Treed Shrubland	2	Sparsely treed dense shrubland	1
t9p6	Dense Treed Shrubland	2	Sparsely treed dense shrubland	1
t9p7	Open Shrubbed Woodland	1	Openly shrubbed dense woodland	-1
t9p8	Open Shrubbed Woodland	1	Openly shrubbed dense woodland	-1
Total		**24**		**32**

APPENDIX 2: OBLIQUE, HIGH OBLIQUE, AND NADIR VISUALIZATIONS OF ALL PLOTS

Plot	Oblique (Angled) View	High Oblique (Side) View	Nadir (Top) View
T1P1	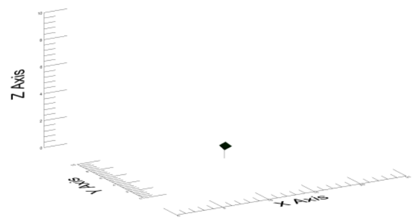		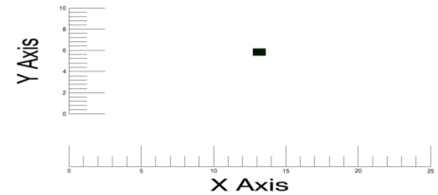
T1P3	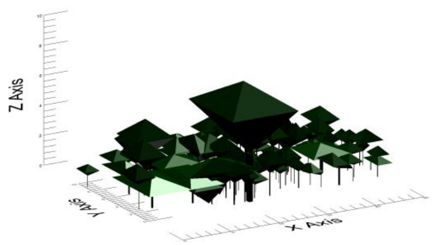	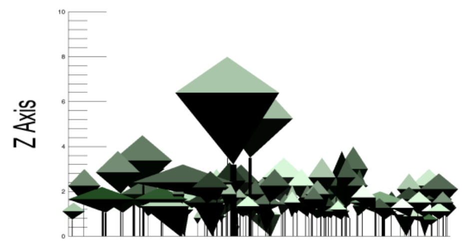	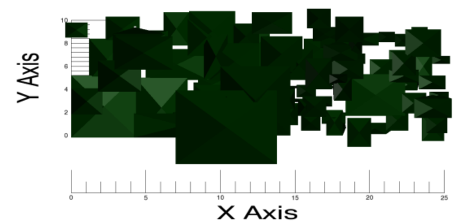

T1P4	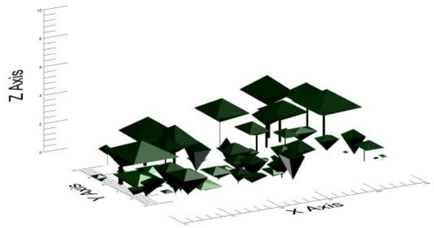	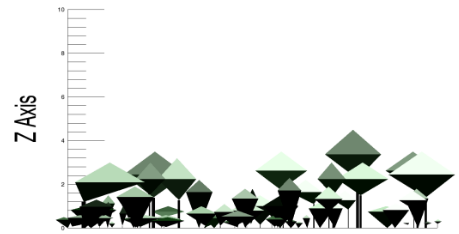	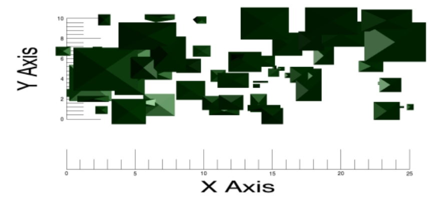
T1P5	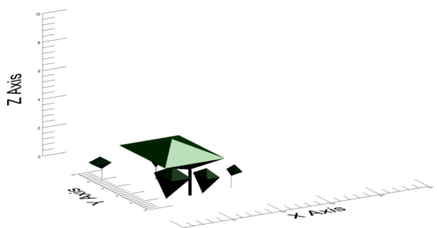	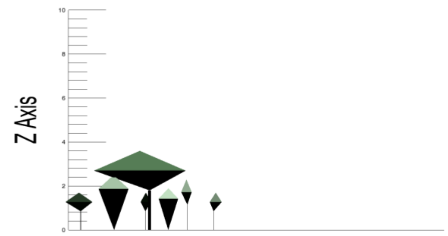	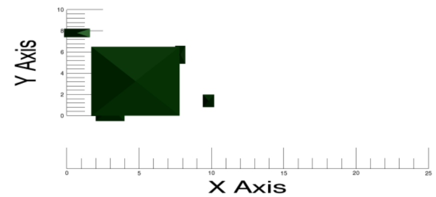
T1P6	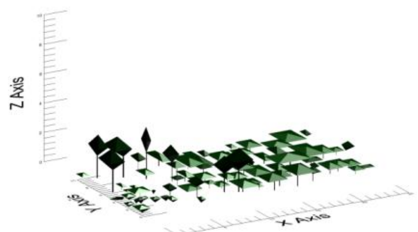	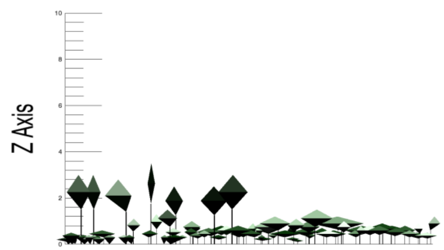	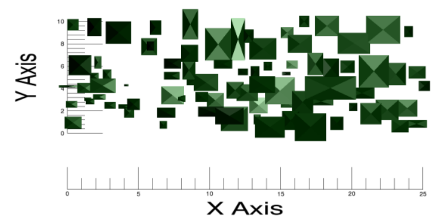

Appendix 2: Oblique, high oblique, and nadir visualizations of all plots (continued).

T1P7	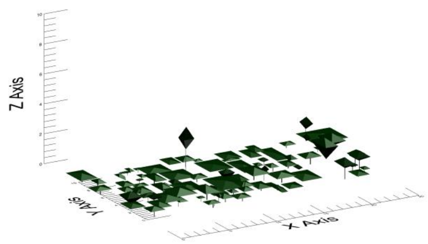	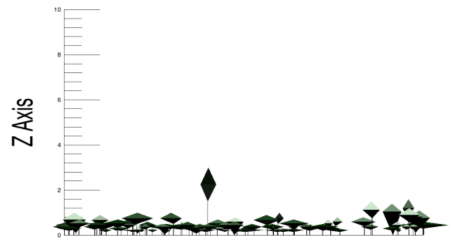	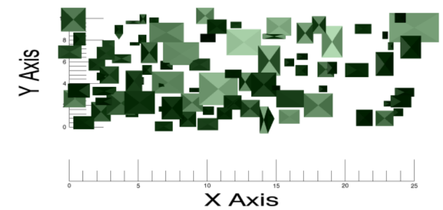
T1P9	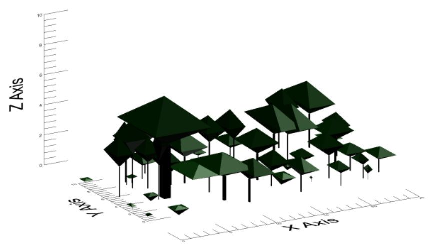	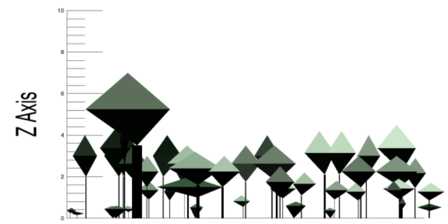	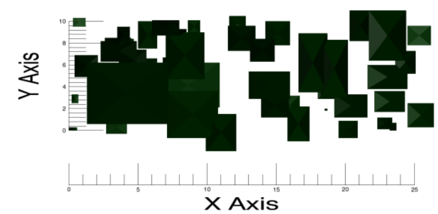
T2P1	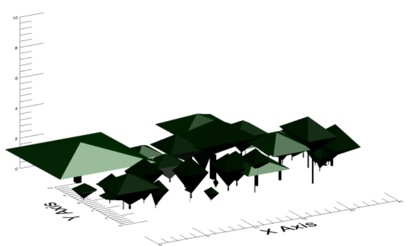	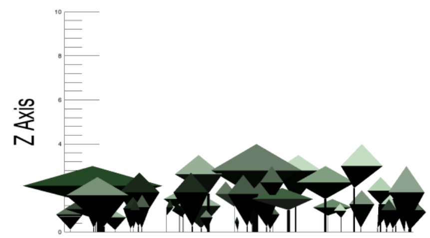	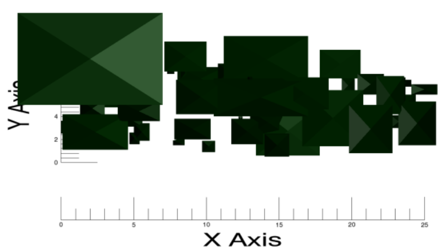

Appendix 2: Oblique, high oblique, and nadir visualizations of all plots (continued).

T2P2	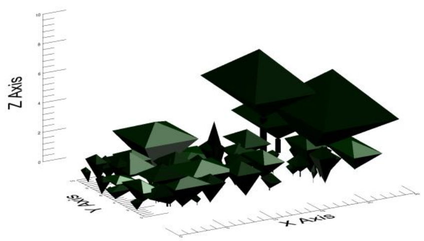	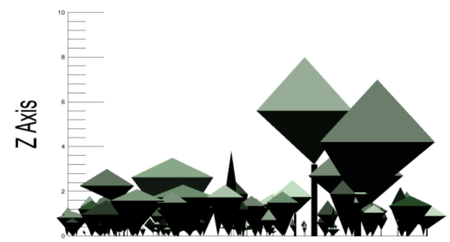	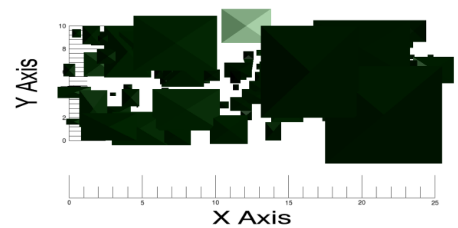
T2P3	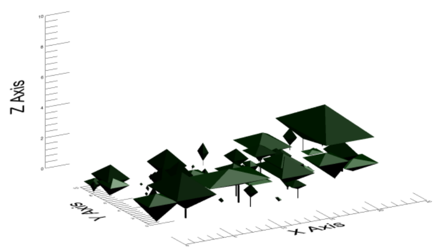	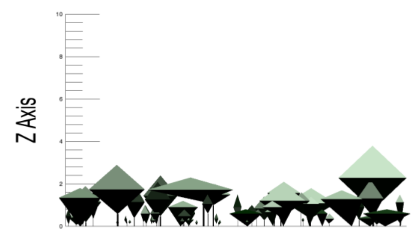	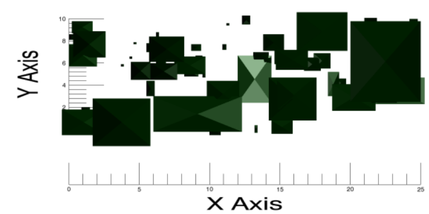
T2P4	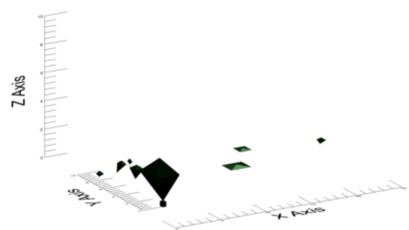	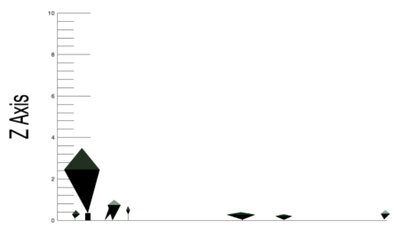	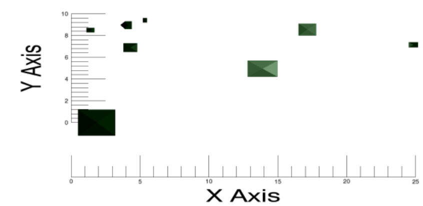

Appendix 2: Oblique, high oblique, and nadir visualizations of all plots (continued).

T2P5	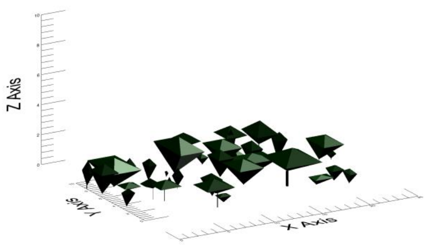	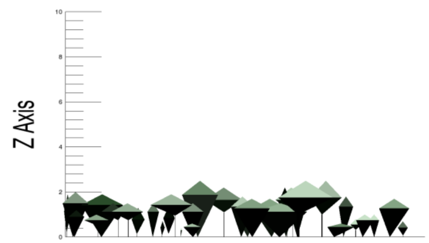	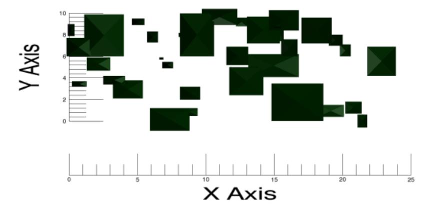
T2P8	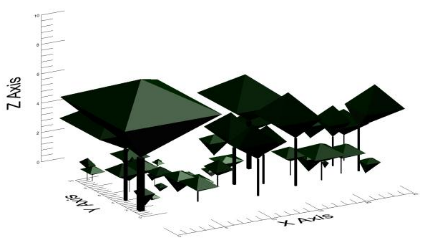	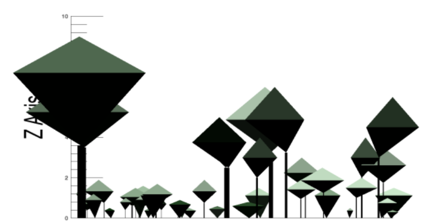	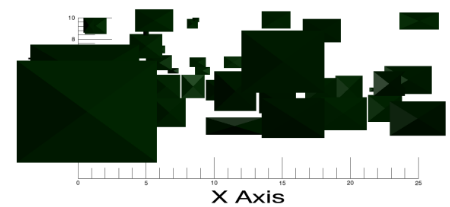
T3P1	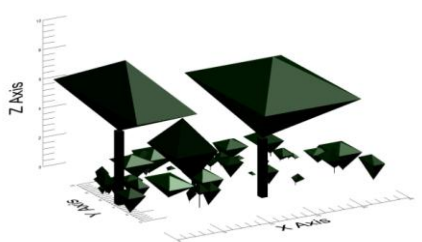	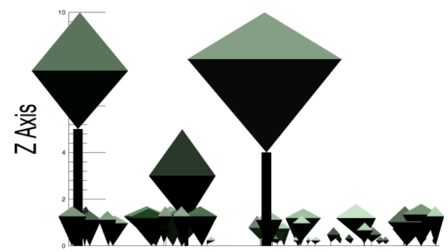	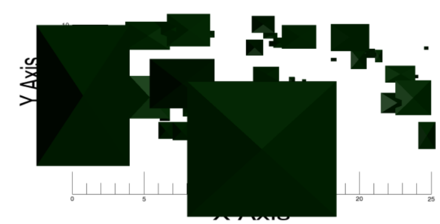

Appendix 2: Oblique, high oblique, and nadir visualizations of all plots (continued).

T3P2	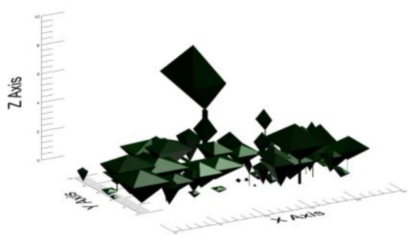	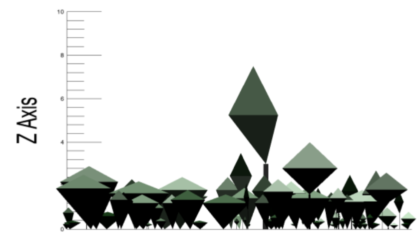	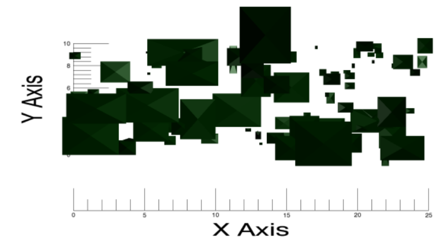
T3P3	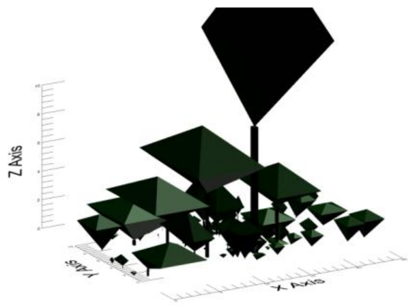	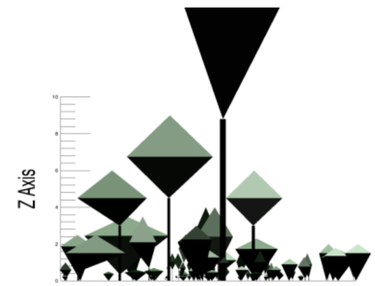	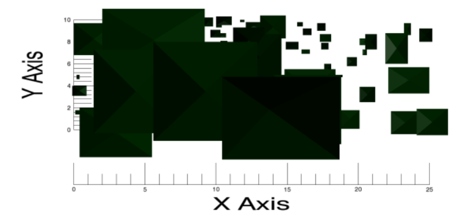

Appendix 2: Oblique, high oblique, and nadir visualizations of all plots (continued).

T3P6

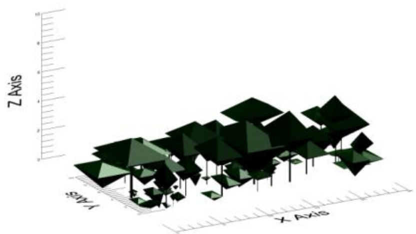

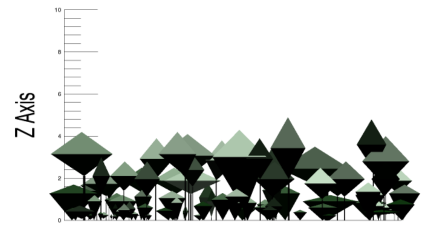

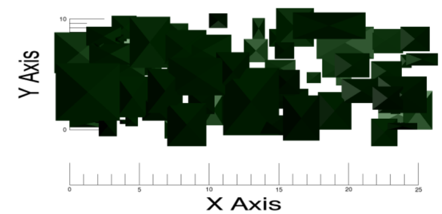

T3P7

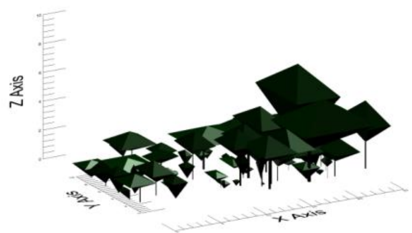

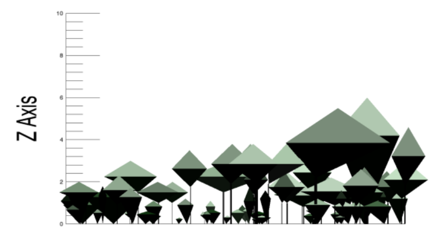

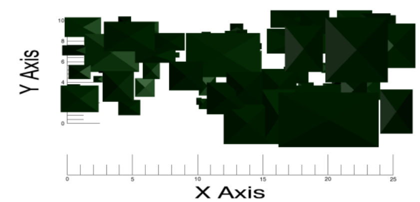

T3P8

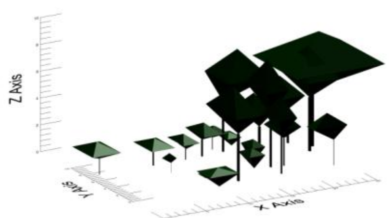

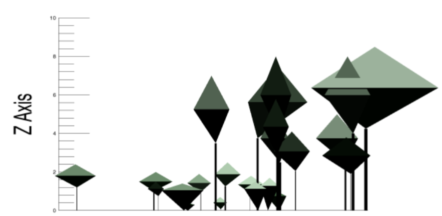

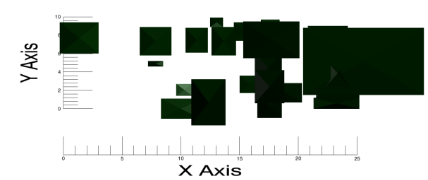

Appendix 2: Oblique, high oblique, and nadir visualizations of all plots (continued).

T3P9

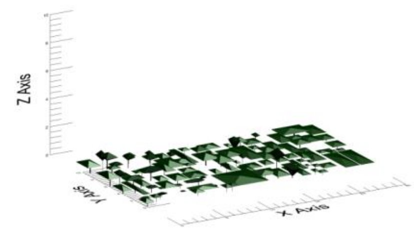

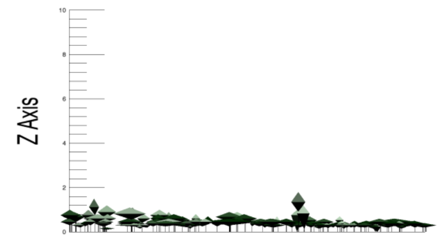

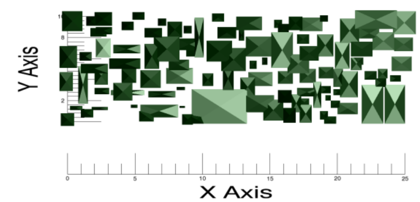

T4P1

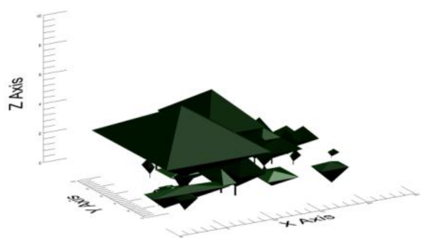

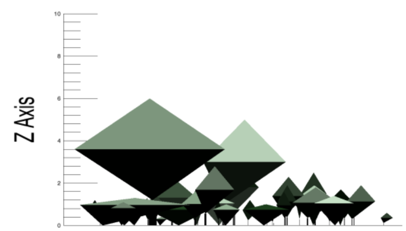

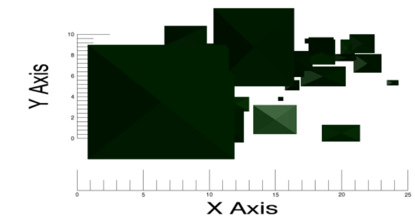

T4P2

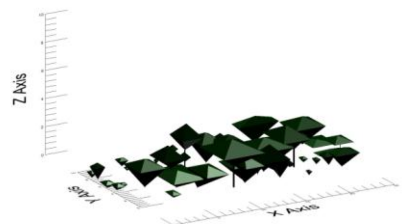

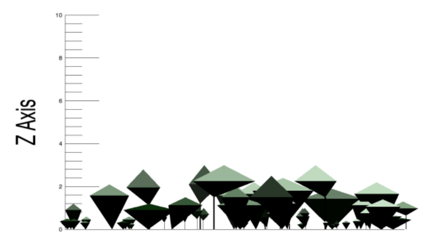

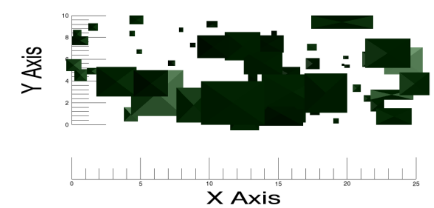

Appendix 2: Oblique, high oblique, and nadir visualizations of all plots (continued).

T4P6	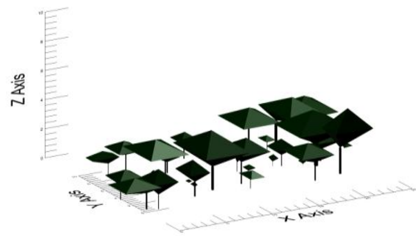	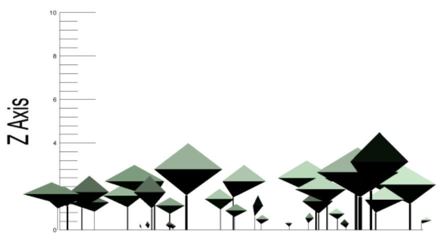	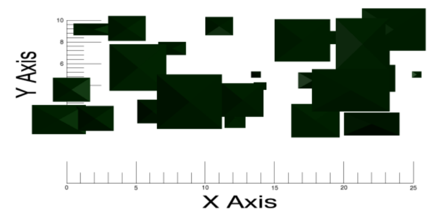
T5P1	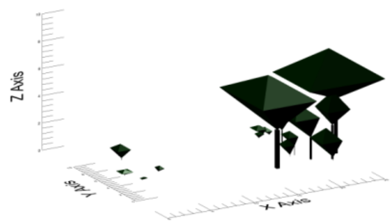	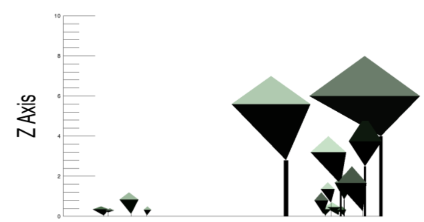	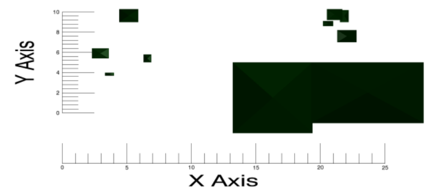
T5P2	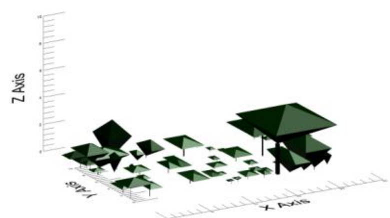	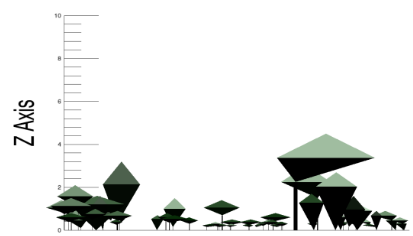	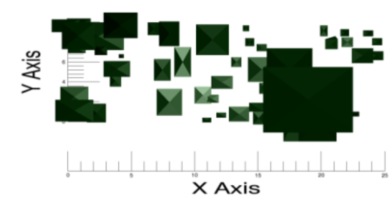

Appendix 2: Oblique, high oblique, and nadir visualizations of all plots (continued).

T5P5	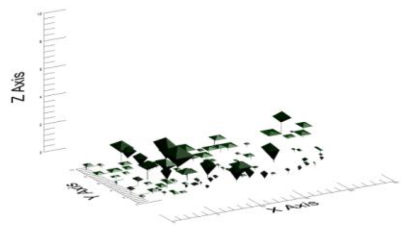	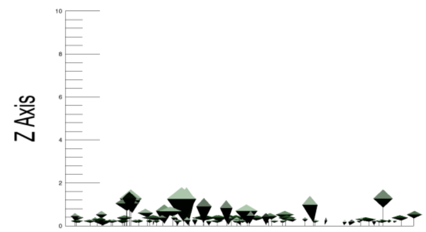	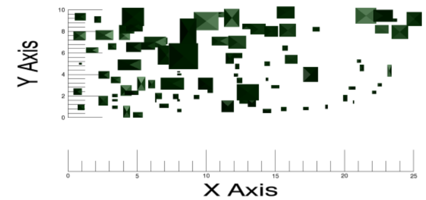
T5P6	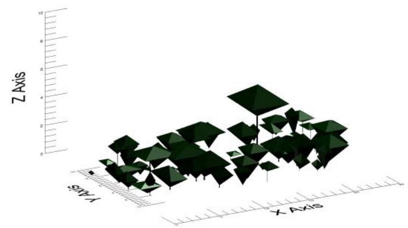	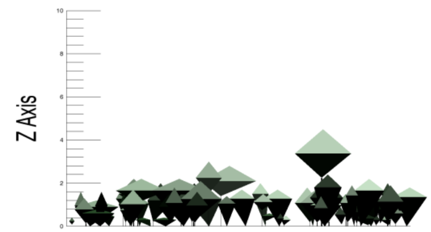	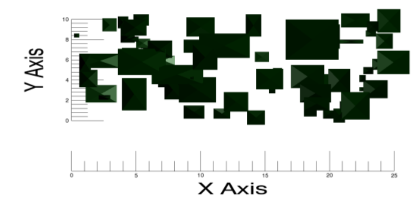
T5P8	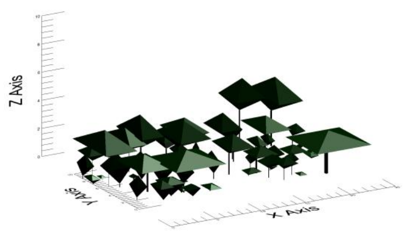	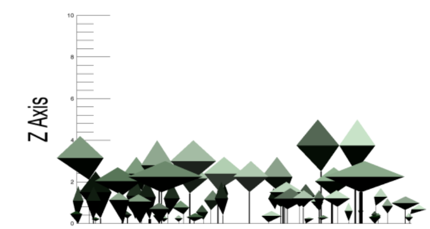	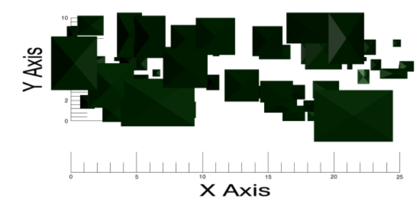

Appendix 2: Oblique, high oblique, and nadir visualizations of all plots (continued).

T5P12	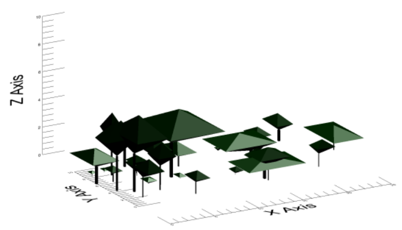	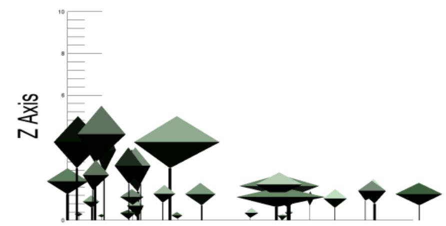	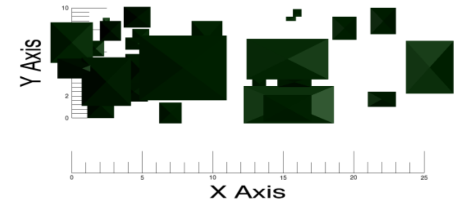
T6P1	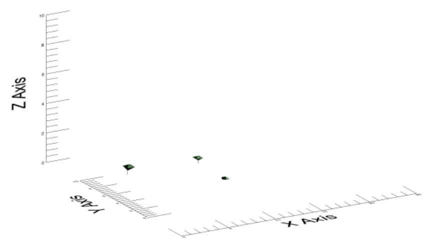	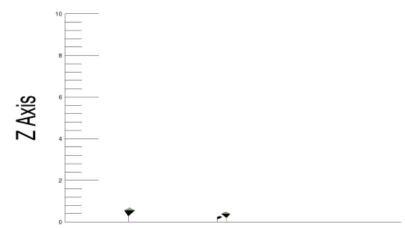	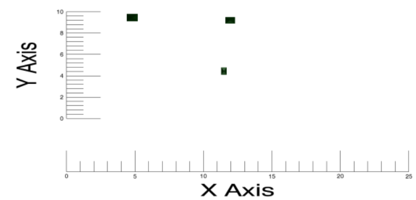
T6P2	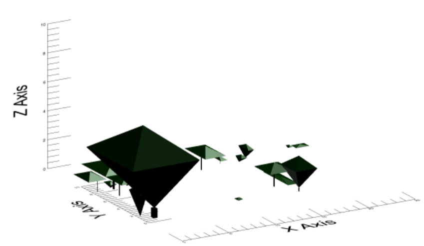	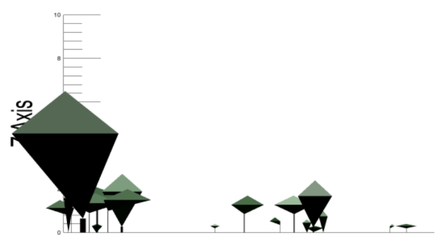	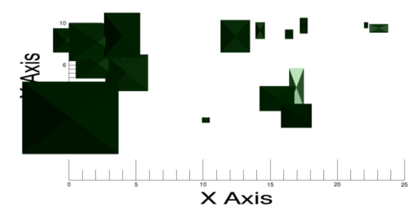

Appendix 2: Oblique, high oblique, and nadir visualizations of all plots (continued).

T6P3	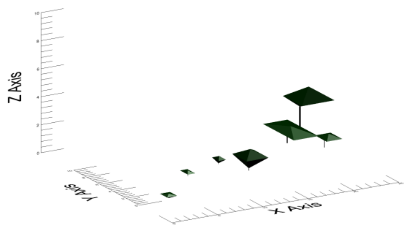	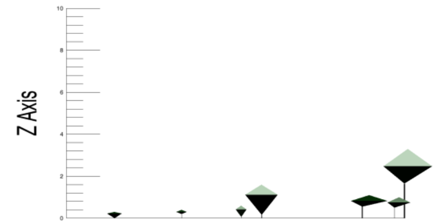	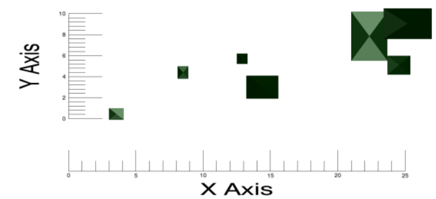
T6P4	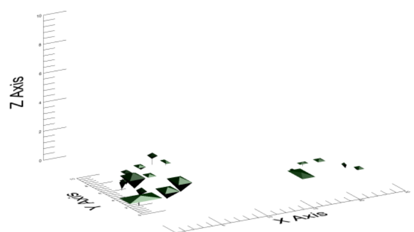	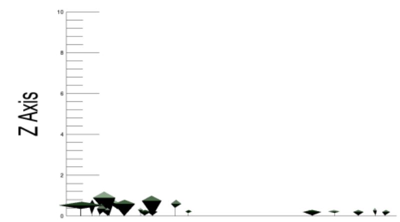	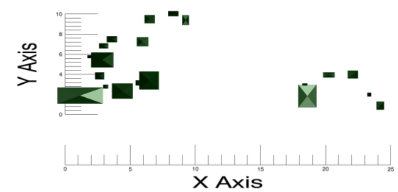
T6P5	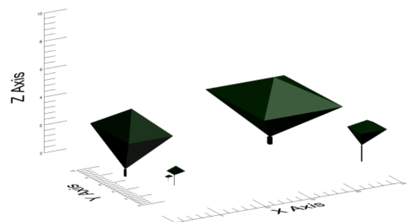	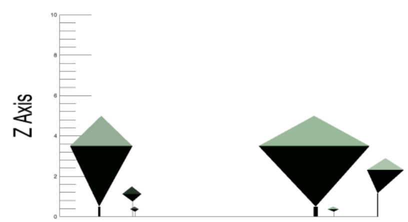	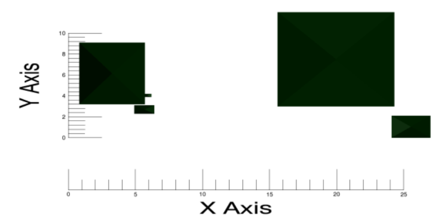

Appendix 2: Oblique, high oblique, and nadir visualizations of all plots (continued).

T6P6	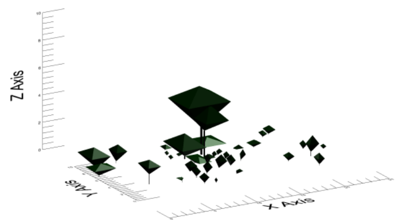	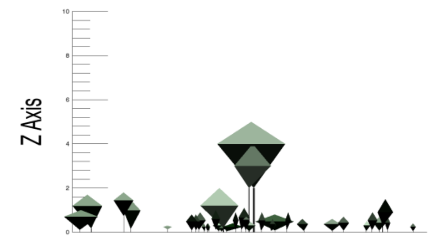	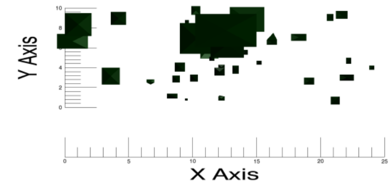
T6P7	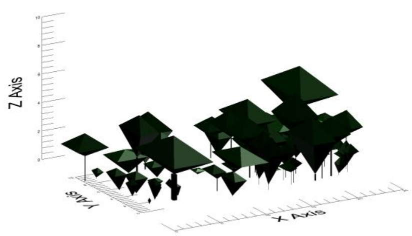	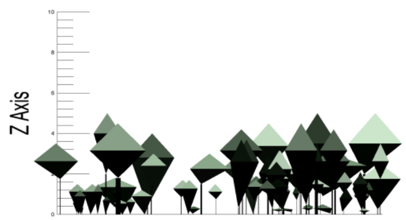	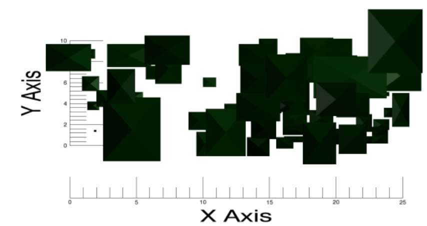
T6P9	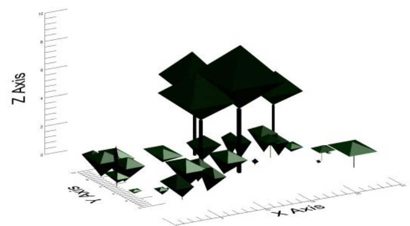	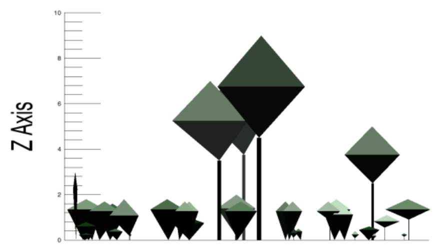	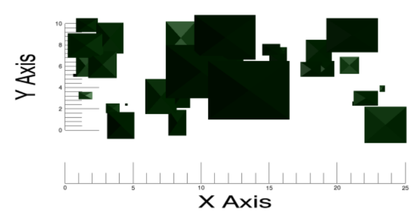

Appendix 2: Oblique, high oblique, and nadir visualizations of all plots (continued).

T6P10	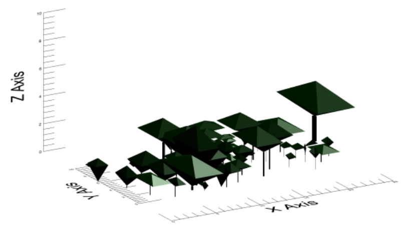	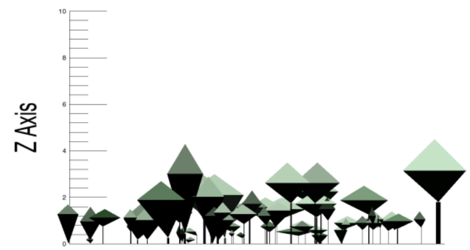	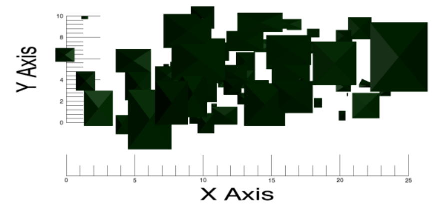
T6P11	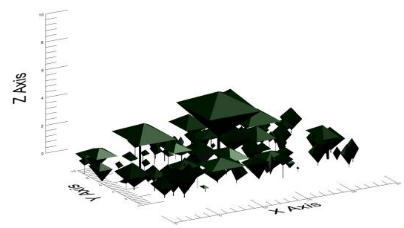	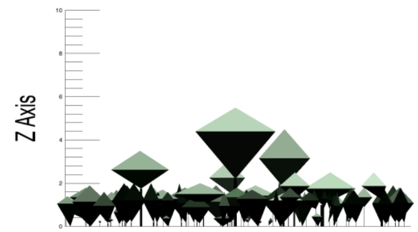	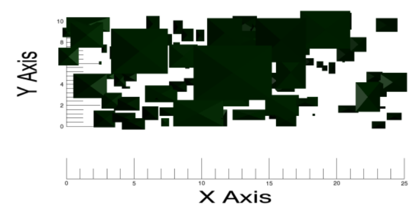
T7P1	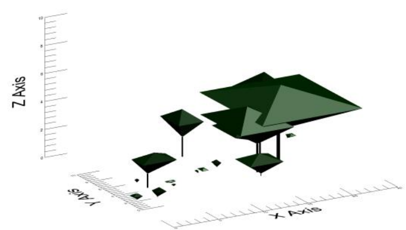	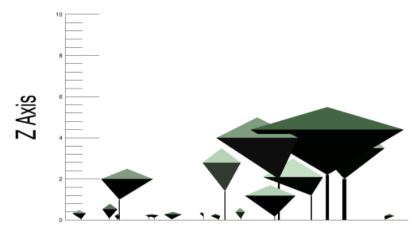	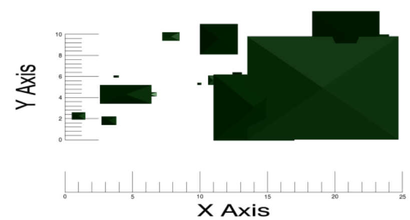

Appendix 2: Oblique, high oblique, and nadir visualizations of all plots (continued).

T7P2	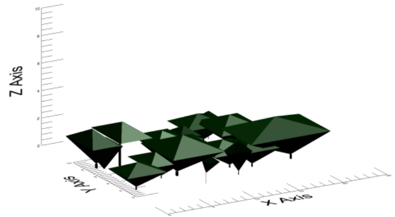	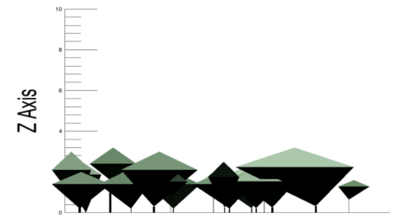	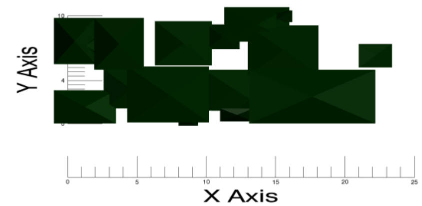
T7P3	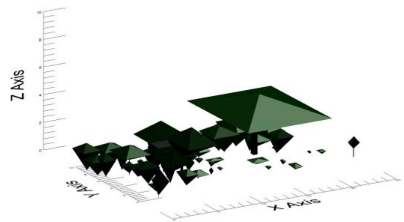	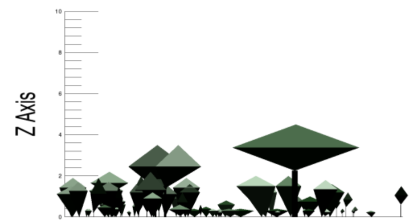	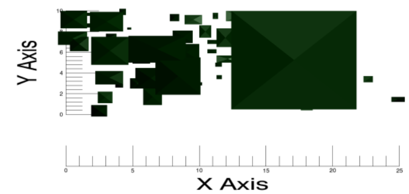
T7P6	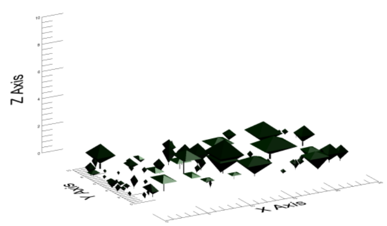	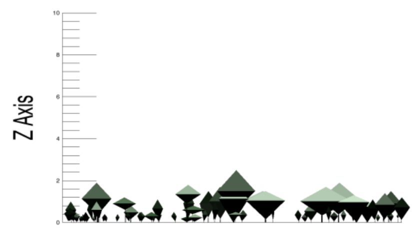	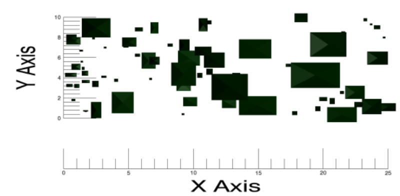

Appendix 2: Oblique, high oblique, and nadir visualizations of all plots (continued).

T7P9	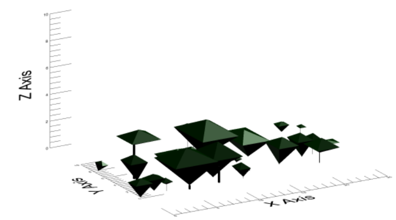	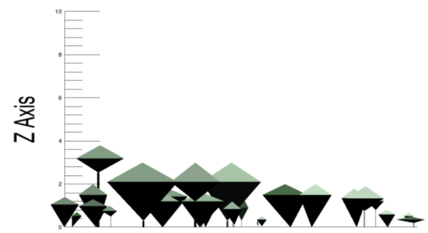	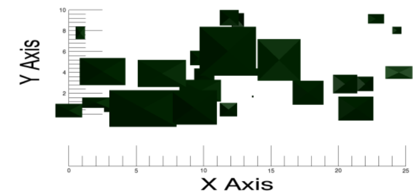
T8P2	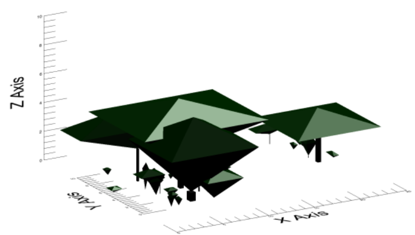	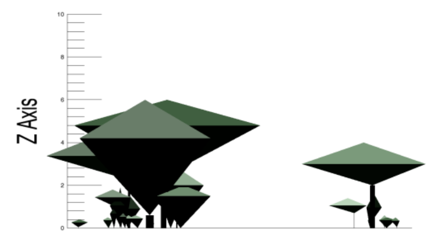	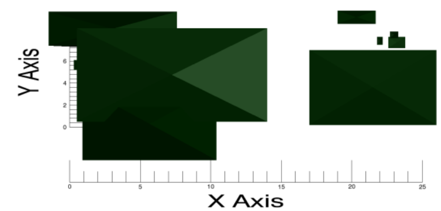
T8P3	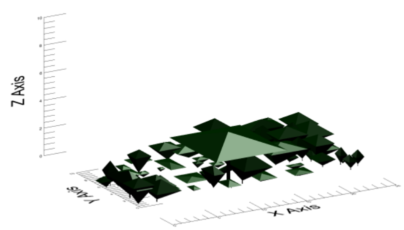	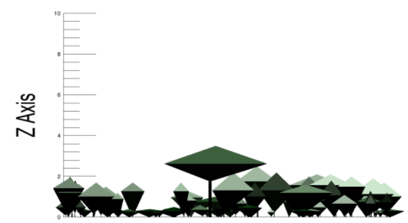	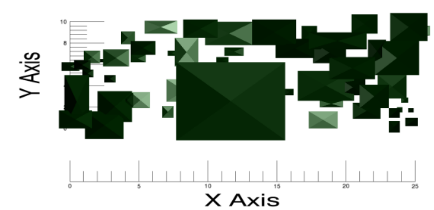

Appendix 2: Oblique, high oblique, and nadir visualizations of all plots (continued).

T8P4	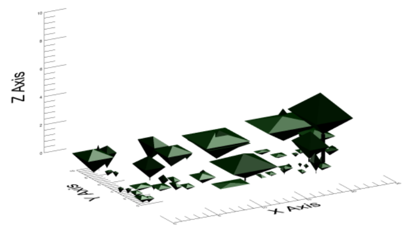	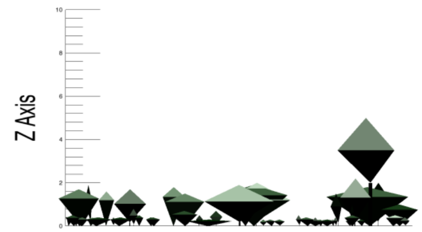	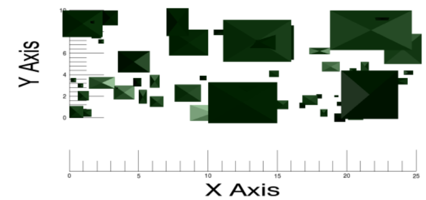
T8P5	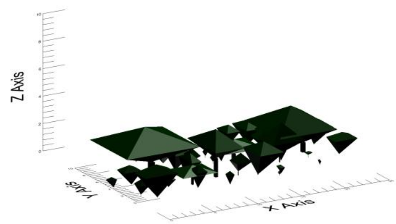	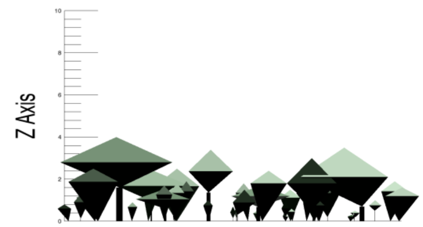	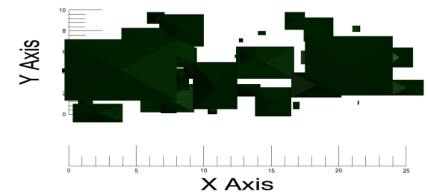
T8P6	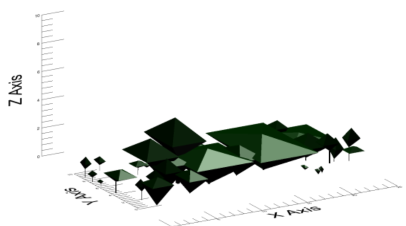	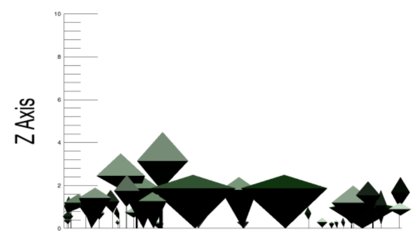	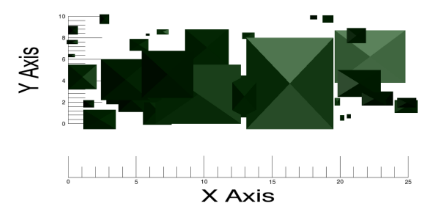

Appendix 2: Oblique, high oblique, and nadir visualizations of all plots (continued).

T8P8	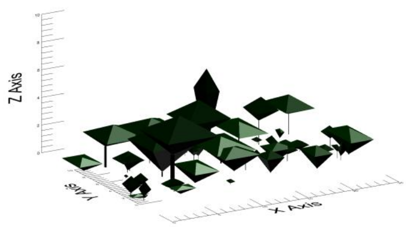	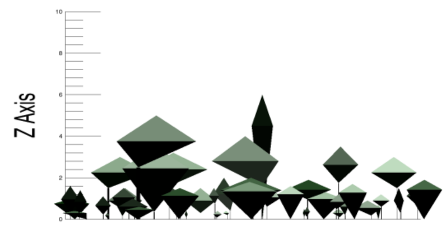	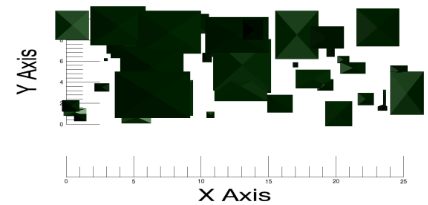
T9P1	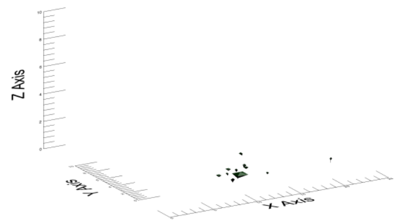		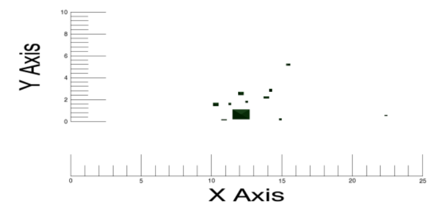
T9P2	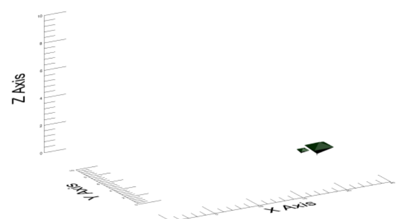	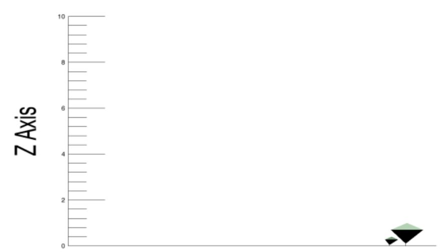	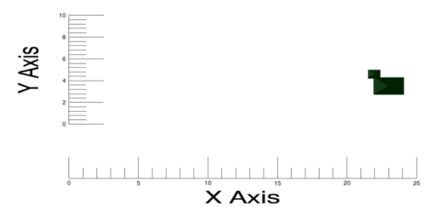

Appendix 2: Oblique, high oblique, and nadir visualizations of all plots (continued).

T9P3

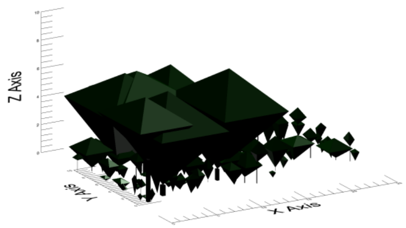

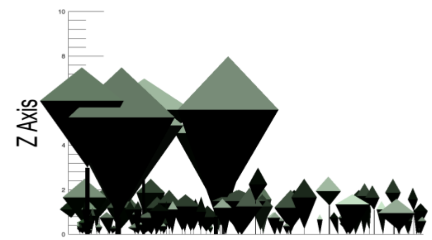

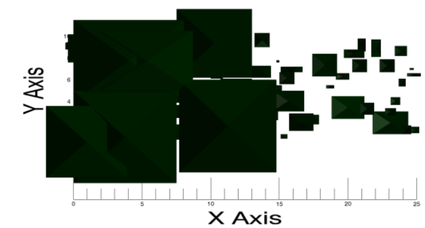

T9P4

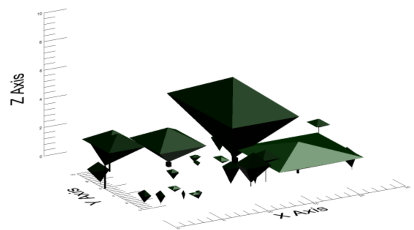

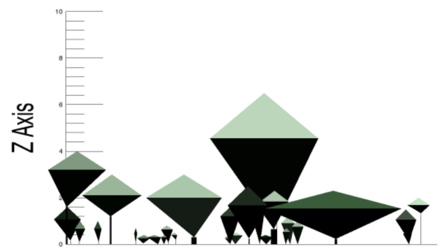

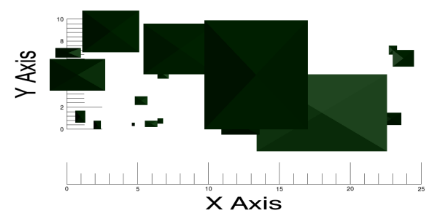

T9P5

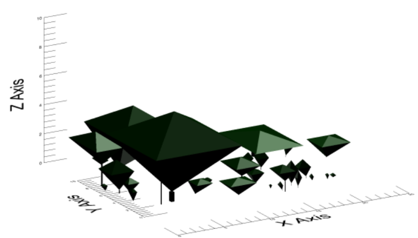

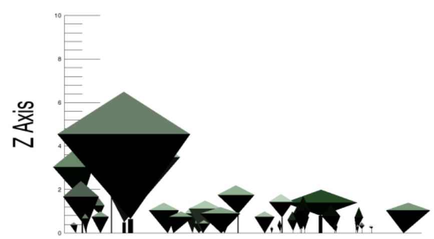

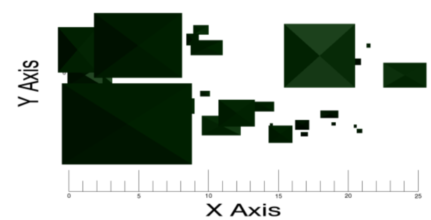

Appendix 2: Oblique, high oblique, and nadir visualizations of all plots (continued).

<table>
<tr><td>T9P6</td><td>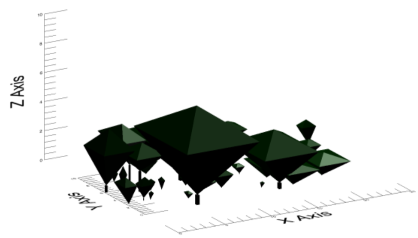
</td><td>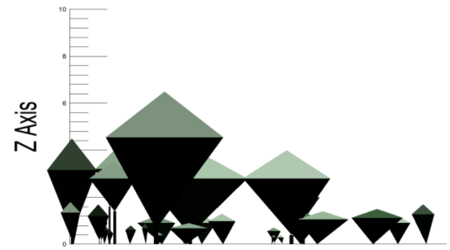
</td><td>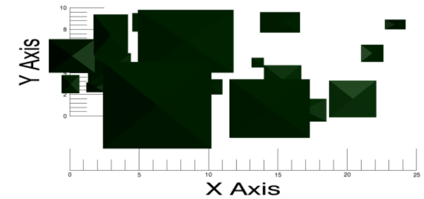
</td></tr>
<tr><td>T9P7</td><td>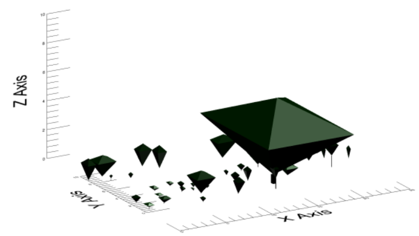
</td><td>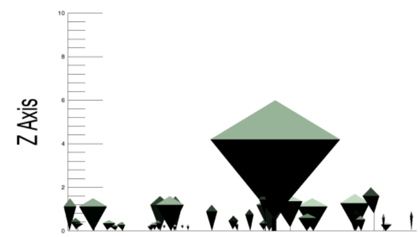
</td><td>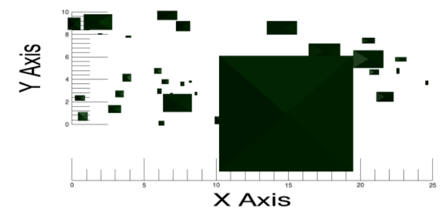
</td></tr>
<tr><td>T9P8</td><td>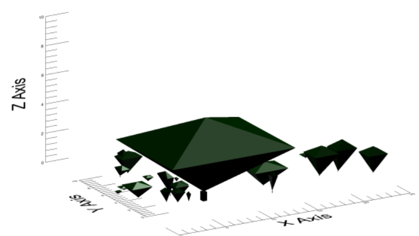
</td><td>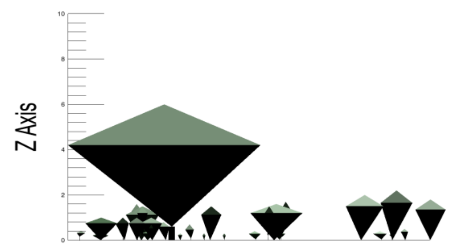
</td><td>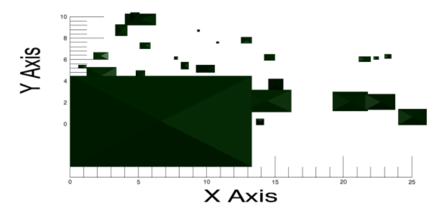
</td></tr>
</table>

Appendix 2: Oblique, high oblique, and nadir visualizations of all plots (continued).

References

ADRC, A. D. R. C. 2001. A Report on the Socio-Ecological Survey of the Okavango Basin. In *Kalahari Conservation Society*. Gaborone.

Anderson, J. R. 1976. *A land use and land cover classification system for use with remote sensor data*. US Government Printing Office.

Archer, S., D. S. Schimel & E. A. Holland (1995) Mechanisms of shrubland expansion: land use, climate or CO2? *Climatic Change,* 29**,** 91-99.

Augustine, D. J., S. J. McNaughton & D. A. Frank (2003) Feedbacks between soil nutrients and large herbivores in a managed savanna ecosystem. *Ecological Applications,* 13**,** 1325-1337.

Beerling, D. J. & C. P. Osborne (2006) The origin of the savanna biome. *Global Change Biology,* 12**,** 2023-2031.

Bond, W. J. & B. W. van Wilgen. 1996. Introduction. In *Fire and Plants,* 1-15. Springer.

Cash, D. W. & S. C. Moser (2000) Linking global and local scales: designing dynamic assessment and management processes. *Global environmental change,* 10**,** 109-120.

Cole, M. M. 1986. *The savannas, biogeography and geobotany*. Academic Press.

Crews-Meyer, K.A. 2001. Assessing Landscape Change and Population-Environment Interactions via Panel Analysis in Geocarto International, 16(4): 69-79.

Crews-Meyer, K.A. 2002. Characterizing Landscape Dynamism via Paneled-Pattern Metrics in Photogrammetric Engineering and Remote Sensing, 68(10): 1031-1040.

D'Odorico, P., K. Caylor, G. S. Okin & T. M. Scanlon (2007) On soil moisture–vegetation feedbacks and their possible effects on the dynamics of dryland ecosystems. *Journal of Geophysical Research: Biogeosciences (2005–2012),* 112.

D'Odorico, P. & A. Porporato. 2006. Ecohydrology of arid and semiarid ecosystems: an introduction. In *Dryland Ecohydrology,* 1-10. Springer.

Edwards, D. (1983) broad-scale structural classification of vegetation for practical purposes. *Bothalia*.

Ellis, F. (2000) The determinants of rural livelihood diversification in developing countries. *Journal of Agricultural Economics,* 51**,** 289-302.

Fernandez-Illescas, C. P. & I. Rodriguez-Iturbe (2003) Hydrologically driven hierarchical competition-colonization models: the impact of interannual climate fluctuations. *Ecological Monographs,* 73**,** 207-222.

Frost, P., E. Medina & J. Menaut (1986) Solbrig 0, Swift M, Walker BH (1986) Responses of savannas to stress and disturbance. *Biol Int (Special Issue),* 10**,** 1-82.

Gibson, C. C., E. Ostrom & T.-K. Ahn (2000) The concept of scale and the human dimensions of global change: a survey. *Ecological economics,* 32**,** 217-239.

Gopal, S. & C. Woodcock (1994) Theory and methods for accuracy assessment of thematic maps using fuzzy sets. *Photogrammetric Engineering and Remote Sensing;(United States),* 60.

Grunblatt, J., W. Ottichilo & R. Sinange (1989) A hierarchical approach to vegetation classification in Kenya. *African Journal of Ecology,* 27**,** 45-51.

Higgins, S. I., W. J. Bond & W. S. Trollope (2000) Fire, resprouting and variability: a recipe for grass–tree coexistence in savanna. *Journal of Ecology,* 88**,** 213-229.

Hochberg, M. E., J. C. Menaut & J. Gignoux (1994) The influences of tree biology and fire in the spatial structure of the West African savannah. *Journal of Ecology***,** 217-226.

Hopcraft, J. G. C., H. Olff & A. Sinclair (2010) Herbivores, resources and risks: alternating regulation along primary environmental gradients in savannas. *Trends in Ecology & Evolution,* 25**,** 119-128.

House, J. I., S. Archer, D. D. Breshears & R. J. Scholes (2003) Conundrums in mixed woody–herbaceous plant systems. *Journal of biogeography,* 30**,** 1763-1777.

IPCC. 2013. Climate Change 2013: The Physical Science Basis. Contribution of Working Group I to the Fifth Assessment Report of the Intergovernmental

Panel on Climate Change eds. T. F. Stocker, D. Qin, G.-K. Plattner, M. Tignor, S.K. Allen, J. Boschung, A. Nauels, Y. Xia, V. Bex and P.M. Midgley & (eds.), 1535 pp.: Cambridge University Press, Cambridge, United Kingdom and New York, NY, USA, .

Jeltsch, F., S. J. Milton, W. Dean & N. van Rooyen (1996) Tree spacing and coexistence in semiarid savannas. *Journal of Ecology***,** 583-595.

Jeltsch, F., G. E. Weber & V. Grimm (2000) Ecological buffering mechanisms in savannas: a unifying theory of long-term tree-grass coexistence. *Plant Ecology,* 150**,** 161-171.

Jensen, J. R. 1996. *Introductory digital image processing: a remote sensing perspective*. Prentice-Hall Inc.

Jensen, J. R. 2009. *Remote Sensing of the Environment: An Earth Resource Perspective 2/e*. Pearson Education India.

Joffre, R. & S. Rambal (1993) How tree cover influences the water balance of Mediterranean rangelands. *Ecology***,** 570-582.

Jung, M., K. Henkel, M. Herold & G. Churkina (2006) Exploiting synergies of global land cover products for carbon cycle modeling. *Remote Sensing of Environment,* 101**,** 534-553.

Kates, R. W., W. C. Clark, R. Corell, J. M. Hall, C. C. Jaeger, I. Lowe, J. J. McCarthy, H. J. Schellnhuber, B. Bolin & N. M. Dickson (2001) 1. Sustainability Science of Local Communities. *Science,* 641**,** 642.

Kgathi, D., H. Bendsen, P. Blaikie, J. Mbaiwa, B. Ngwenya & J. Wilk (2004) Rural livelihoods, indigenous knowledge systems, and political economy of access to natural resources in the Okavango delta, Botswana. *Report to the EU-WERRD Project. Web-published.*

Lambin, E. F., B. L. Turner, H. J. Geist, S. B. Agbola, A. Angelsen, J. W. Bruce, O. T. Coomes, R. Dirzo, G. Fischer & C. Folke (2001) The causes of land-use and land-cover change: moving beyond the myths. *Global environmental change,* 11**,** 261-269.

Liu, J., T. Dietz, S. R. Carpenter, M. Alberti, C. Folke, E. Moran, A. N. Pell, P. Deadman, T. Kratz & J. Lubchenco (2007) Complexity of coupled human and natural systems. *Science,* 317**,** 1513-1516.

Liverman, D., E. F. Moran, R. R. Rindfuss & P. C. Stern (1998) People and pixels: linking remote sensing and social science.

Mbaiwa, J. E. & O. I. Mbaiwa (2006) The effects of veterinary fences on wildlife populations in Okavango Delta, Botswana. *International Journal of Wilderness,* 12.

McCarthy, J. M., T. Gumbricht, T. McCarthy, P. Frost, K. Wessels & F. Seidel (2003) Flooding patterns of the Okavango wetland in Botswana between 1972 and 2000. *AMBIO: A Journal of the Human Environment,* 32**,** 453-457.

MEA. 2005. *Millennium ecosystem assessment synthesis report*. Millennium Ecosystem Assessment.

Mendelsohn, J., C. Vanderpost, L. Ramberg, M. Murray-Hudson, P. Wolski & K. Mosepele. 2010. *Okavango Delta: floods of life*. Raison Windhoek Namibia.

Messina, J. P., K. A. Crews-Meyer & S. J. Walsh. 2000. Scale dependent pattern metrics and panel data analysis as applied in a multiphase hybrid landcover classification scheme. In *Proc. 2000 ASPRS Conf*.

Meyer, T. 2014. Multi-scale quantification of woody biomass in heterogeneous landscapes: Leveraging traditional field sampling, spectral unmixing, and allometric modeling in Kalahari savanna ecosystems. In *Department of Environmental Sciences*. Charlottesville: University of Virginia.

Meyer, T., L. Cassidy, S. Ringrose, C. Vanderpost, D. Kgathi, B. Ngwenya, H. Bendsen, W. Matheson & T. Kemosidile. 2011. *An Assessment Of Plant Based Natural Resources in The Okavango Region, Botswana Using Satellite Imagery* Nova Press.

Mishra, N. B. and Young, K. R. 2014. 'Savannas and Grasslands', invited encyclopedia entry in Encyclopedia of Natural Resources (Ed Y.Q. Wang), Taylor and Francis

Ostrom, E. (2007) A diagnostic approach for going beyond panaceas. *Proceedings of the National Academy of Sciences,* 104**,** 15181-15187.

Ostrom, E. (2008) Frameworks and theories of environmental change. *Global environmental change,* 18**,** 249-252.

Ostrom, E. (2009) A general framework for analyzing sustainability of social-ecological systems. *Science,* 325**,** 419.

Pearce, D. W. & R. K. Turner. 1990. *Economics of natural resources and the environment*. JHU Press.

Perkins, J. & S. Ringrose (1996) Development Co-operation's Objectives and the Beef Protocol: The Case of Botswana, A Study of

Livestock/Wildlife/Tourism/Degradation Linkages. *Contract B-7-504094. University of Botswana, Gaborone*.

Pringle, R. M., T. P. Young, D. I. Rubenstein & D. J. McCauley (2007) Herbivore-initiated interaction cascades and their modulation by productivity in an African savanna. *Proceedings of the National Academy of Sciences,* 104**,** 193-197.

Ramberg, L., P. Hancock, M. Lindholm, T. Meyer, S. Ringrose, J. Sliva, J. Van As & C. Vander Post (2006) Species diversity of the Okavango Delta, Botswana. *Aquatic sciences,* 68**,** 310-337.

Reid, K. D., B. P. Wilcox, D. D. Breshears & L. MacDonald (1999) Runoff and erosion in a piñon–juniper woodland influence of vegetation patches. *Soil Science Society of America Journal,* 63**,** 1869-1879.

Rietkerk, M. & J. Van de Koppel (1997) Alternate stable states and threshold effects in semi-arid grazing systems. *Oikos***,** 69-76.

Roy, D. P., L. Boschetti, L. Giglio, M. Hill & N. Hanan (2011) Remote Sensing of Global Savanna Fire Occurence, Extent and Properties. *Ecosystem Function in Savannas: Measurement and Modeling at Landscape to Global Scales*.

Sala, O., W. Lauenroth & R. Golluscio (1997) Plant functional types in temperate semi-arid regions.

Sankaran, M., N. P. Hanan, R. J. Scholes, J. Ratnam, D. J. Augustine, B. S. Cade, J. Gignoux, S. I. Higgins, X. Le Roux & F. Ludwig, et al. (2005) Determinants of woody cover in African savannas. *Nature,* 438**,** 846-849.

Schlesinger, W. H., J. A. Raikes, A. E. Hartley & A. F. Cross (1996) On the spatial pattern of soil nutrients in desert ecosystems. *Ecology,* 77**,** 364-374.

Scholes, R. & S. Archer (1997) Tree-grass interactions in savannas 1. *Annual Review of Ecology and Systematics,* 28**,** 517-544.

Scholes, R., P. Dowty, K. Caylor, D. Parsons, P. Frost & H. Shugart (2002) Trends in savanna structure and composition along an aridity gradient in the Kalahari. *Journal of Vegetation Science,* 13**,** 419-428.

Scholes, R. J. & B. H. Walker. 1993. *An African savanna: synthesis of the Nylsvley study*. Cambridge University Press.

Shinn, J. E., B. King, K. R. Young & K. A. Crews (2014) Variable adaptations: Micro-politics of environmental displacement in the Okavango Delta, Botswana. *Geoforum,* 57**,** 21-29.

Shugart, H., S. Macko, P. Lesolle, T. Szuba, M. Mukelabai, P. Dowty & R. Swap (2004) The SAFARI 2000–Kalahari transect wet season campaign of year 2000. *Global Change Biology,* 10**,** 273-280.

Sinclair, A. (1995) Equilibria in plant-herbivore interactions. *Serengeti II: dynamics, management, and conservation of an ecosystem. University of Chicago Press, Chicago***,** 91-113.

Skarpe, C. (1992) Dynamics of savanna ecosystems. *Journal of Vegetation Science,* 3**,** 293-300.

Smith, N. D., T. S. McCarthy, W. Ellery, C. L. Merry & H. Rüther (1997) Avulsion and anastomosis in the panhandle region of the Okavango Fan, Botswana. *Geomorphology,* 20**,** 49-65.

Solbrig, O. T. 1996. The diversity of the savanna ecosystem. In *Biodiversity and savanna ecosystem processes*, 1-27. Springer.

Tedder, M., K. Kirkman, C. Morris & R. Fynn (2014) Tree–grass competition along a catenal gradient in a mesic grassland, South Africa. *Grassland Science,* 60**,** 1-8.

Thomas, D. S. & P. A. Shaw. 1991. *The Kalahari Environment*. Cambridge University Press.

Thompson, M. (1996) Standard land-cover classification scheme for remote-sensing applications in South Africa. *South African Journal of Science,* 92.

Trodd, N. & A. Dougill (1998) Monitoring vegetation dynamics in semi-arid African rangelands: use and limitations of earth observation data to characterize vegetation structure. *Applied Geography,* 18**,** 315-330.

Trollope, W., L. Trollope, H. Biggs, D. Pienaar & A. Potgieter (1998) Long-term changes in the woody vegetation of the Kruger National Park, with special reference to the effects of elephants and fire. *Koedoe,* 41**,** 103-112.

Tucker, C. J. & S. E. Nicholson (1999) Variations in the size of the Sahara Desert from 1980 to 1997. *Ambio***,** 587-591.

Van Langevelde, F., C. A. Van De Vijver, L. Kumar, J. Van De Koppel, N. De Ridder, J. Van Andel, A. K. Skidmore, J. W. Hearne, L. Stroosnijder & W. J. Bond (2003) Effects of fire and herbivory on the stability of savanna ecosystems. *Ecology,* 84**,** 337-350.

van Wijk, M. T. & I. Rodriguez-Iturbe (2002) Tree-grass competition in space and time: Insights from a simple cellular automata model based on ecohydrological dynamics. *Water Resources Research,* 38**,** 18-1-18-15.

Van Wilgen, B., N. Govender, H. Biggs, D. Ntsala & X. Funda (2004) Response of savanna fire regimes to changing fire-management policies in a large African national park. *Conservation biology,* 18**,** 1533-1540.

Walker, B. H., D. Ludwig, C. S. Holling & R. M. Peterman (1981) Stability of semi-arid savanna grazing systems. *The Journal of Ecology***,** 473-498.

Walker, B. H. & I. Noy-Meir. 1982. Aspects of the stability and resilience of savanna ecosystems. In *Ecology of tropical savannas*, 556-590. Springer.

Walter, H. & D. Mueller-Dombois. 1971. *Ecology of tropical and subtropical vegetation*. Edinburgh, UK, Oliver & Boyd.

Woodcock, C. E. (2002) Uncertainty in remote sensing. *Uncertainty in remote sensing and GIS***,** 19-24.

Woodcock, C. E. & S. Gopal (2000) Fuzzy set theory and thematic maps: accuracy assessment and area estimation. *International Journal of Geographical Information Science,* 14**,** 153-172.

Vita

My research revolves within landscape ecology, disturbance ecology, savanna ecology, biogeography, GIS & remote sensing. Research topic include: (1) linking field based structural measurements and satellite derived products within semi-arid savanna systems, (2) the development of improved disturbance quantification and detection within the context of social-ecological systems, and (3) assessing the impact of fire regime, precipitation, and land management on vegetation structure, composition, and distribution. Upon completion of this thesis, I will begin my dissertation work at the Department of Geography and the Environment at the University of Texas at Austin with expected graduation in 2019. Please contact me personally if you have any questions regarding this thesis work.

Permanent address: 2203 Sharon Drive, Cedar Park, Texas 78613

Email: t.brandt8@gmail.com

This thesis was typed by Thomas Brandt Christiansen.